Quantifying the Spatiotemporal $PM_{2.5}$, Black Carbon, and Ultrafine Particle Concentrations Aboard Public Buses in Brazil: A Comparison of Three Cities

by

Ellen Patrick

Submitted in partial fulfillment of the requirements
for the degree of Master of Applied Science

at

Dalhousie University
Halifax, Nova Scotia
March 2018

Table of Contents

List of Tables

List of Figures

Abstract

The transportation environment contributes disproportionately to air pollution exposure, despite the short amount of time spent in this microenvironment. Elevated concentrations of air pollution within bus passenger cabins are often observed. Buses stop frequently at bus stops for passengers to get on and off, as well as typically travel down main roads with high traffic characteristics. These events will facilitate the entry of outdoor air pollution into the bus passenger cabin, resulting in pollutant spikes. There are many negative health effects associated with exposure to $PM_{2.5}$, black carbon (BC), and ultrafine particles (UFP); three components of air pollution related to vehicle exhaust emissions. This work quantifies the $PM_{2.5}$, BC, and UFP concentrations aboard buses in three different sized cities in Brazil where transportation air pollution studies are in their infancy. It was found that traffic characteristics contributed to fluctuations in on-board particulate air pollution concentrations.

List of Abbreviations Used

ATN	Attenuation
BC	Black Carbon
BRT	Bus Rapid Transit
CET	Traffic Engineering Company of São Paulo
CETESB	Environmental Company of the State of São Paulo
Cl	Chloride
EC	Elemental Carbon
GIS	Geographic Information System
GPS	Global Positioning System
HDV	Heavy Duty Vehicle
IPPUC	Institute of Research and Urban Planning of Curitiba
IQR	Interquartile Range
LDV	Light Duty Vehicle
LOD	Limit Of Detection
Lpm	Liters per minute
n	Number of data values
NO	Nitrogen oxide
NO_3	Nitrate
OC	Organic Carbon
PM	Particulate Matter
PM_{10}	Particulate matter with an aerodynamic diameter ≤ 10 µm
$PM_{2.5}$	Particulate matter with an aerodynamic diameter ≤ 2.5 µm
PNC	Particle Number Concentration

PROCONVE	Brazilian Motor Vehicle Air Pollution Control Program
SEM	Scanning Electron Microscope
SIMEPAR	Meteorological System of Paraná
SO_4	Sulphate
SPARTAN	Surface PARTiculate mAtter Network
TSP	Total Suspended Particles
UFP	Ultrafine Particulate Matter
UHI	Urban Heat Island
UTFPR	Federal University of Technology - Paraná
VOC	Volatile Organic Compound
WHO	World Health Organization

Acknowledgements

Firstly, I would like to thank Mitacs and the Globalink Internship program, without which this project would not have been possible. Secondly, a huge thank you goes out to Dr. Admir Targino and his invaluable expertise in the field of traffic related air pollution as well as his coordination and supervision of this project. Dr. Targino, Dr. Krecl, and their Atmospher research group welcomed me so warmly to Brazil and I thank all of them for their contribution to my success. In particular, thank you to Julián Segura and Thiago Landi for assisting in field work and Marcos Rodrigues for always being there to help with ArcGIS. Thirdly, thank you to Dr. Mark Gibson for providing supervision on this project here in Canada, for providing some of the instruments with which to conduct the study, and his expertise on the topic of air pollution exposure. Thank you to the whole Atmospheric Forensics Research Group for their support throughout this entire process, and particular thanks go to Codey Barnett and Kelsey Tunney for helping out with lab work. Lastly, many thanks are due to my friends and family for their continued support and guidance throughout this degree.

Chapter 1 Introduction

Despite the small amount of time spent by the average person in the transport environment, a disproportionately large amount of air particulates is inhaled as a result of motor vehicle emissions (de Nazelle *et al.*, 2012; Dons *et al.*, 2012; Targino *et al.*, 2018). Air particulates are referred to as particulate matter (PM) and are composed of many different toxic and non-toxic materials. When comparing different modes of transportation, bus commutes often observe the highest concentrations of in-cabin PM (Dons *et al*., 2012; Onat & Stakeeva, 2013; Targino *et al.*, 2018). Bus passengers are unable to control many of the variables that can influence the PM intake into the bus including air ventilation settings, open windows, and frequency of bus stops. It is common in areas with warmer climates for the windows to be open to increase air circulation and improve passenger comfort, however, this also facilitates the direct entry of roadway pollution into the bus (Hill *et al.*, 2005). Li *et al.* (2015) observed that open windows lead to higher black carbon (BC) exposure in the bus than in the street. The infiltration of PM is highly dependent on in-cabin pressurization and the pressure differential between the interior and exterior environments (Lee, 2013).

Motor vehicles like buses and cars tend to be older in South America relative to other more developed parts of the world. This results in the production of a higher amount of air pollution when compared to newer vehicles with improved emissions control technology (Andrade *et al.*, 2017). The Andean Development Corporation quantified personal vehicle traffic in Latin America and South America as making up 69 % of the total PM emissions from vehicle traffic, and public transit representing the other 31 %, despite there being significantly more personal vehicles on the road than public transit vehicles (CAF, 2009). In Brazil, diesel powered vehicles are primarily trucks and buses. However, the emissions standards for heavy duty vehicles (HDVs) lag behind those in Europe and buses are not equipped with diesel particle filters or oxidation catalysts resulting in higher PM emissions (ICCT, 2017).

Three components of PM known to be associated with traffic related air pollution were investigated in this thesis work: (i) particulate matter with a median aerodynamic diameter less than 2.5 μm ($PM_{2.5}$); (ii) particulate matter with a median aerodynamic diameter less than 0.1 μm, referred to as ultrafine particulate matter (UFP); and (iii) BC. These three pollutants were chosen for this study based on their direct link to vehicle emissions and their known impacts on human health (Cyrys *et al.*, 2003; Geller *et al.*, 2006*)*. $PM_{2.5}$ has been well documented to be linked with cardiovascular disease (Brook *et al.,* 2004; Dockery & Stone, 2007). While UFP, due to their small size, are capable of penetrating deep into lung tissue and entering the bloodstream thus allowing the distribution of these particles throughout the human body (Oberdörster *et al.*, 2005). More recently however, BC has been a pollutant of interest due to its relationship with cancer occurrences (Silverman *et al.,* 2011).

The objective of this thesis is to quantify the $PM_{2.5}$, BC, and UFP concentrations during bus passenger trips in Brazil and determine what variables influence these concentrations. For comparison purposes, three cities of different size classifications were measured: a mid-sized city, a large city and a mega city. Time series and maps were made to explore both the temporal and spatial trends. Air pollution data was then separated from bus stops and traffic lights to observe the influence of these events on PM concentrations. Data was also separated riding the bus from waiting for the bus for comparison. Lastly, the relationship between speed and pollutant concentrations was examined. Through these different methods of data analysis, conclusions can be drawn as to what factors are influencing fluctuations in PM concentrations on-board buses in Brazil.

Chapter 2 Background

2.1 Air Pollutants of Interest

Air pollution is a heterogeneous mixture of gases, liquids, and solid particles with many sources, e.g. anthropogenic, geogenic, and biogenic emissions into the atmosphere. One important criteria air pollutant is PM, also referred to as aerosols (Hinds, 1999; Gibson et al., 2009, 2013, and 2015). Criteria air pollutants are regulated in the United States National Ambient Air Quality Standards as selected by the United States Environmental Protection Agency due to their impact on health. The primary components of PM include sulphate (SO_4), nitrate (NO_3), chloride (Cl), elemental carbon (EC), organic carbon (OC) and crustal minerals (Harrison *et al.*, 2003). SO_4 and NO_3 are both major secondary components of particulate air pollution. SO_4 is often found in the atmosphere as ammonium sulphate ($(NH_4)_2SO_4$), where NO_3 exists as both ammonium nitrate and sodium nitrate in the atmosphere (Harrison *et al.,* 2003). Cl will be found in the atmosphere as sodium chloride, or salt, as a result of marine aerosols (Harrison *et al.*, 2003; Gibson *et al.,* 2009). However, in urban environments, acidic aerosols convert $Cl_{(s)}$ to $HCl_{(g)}$ and it is lost from the particulate phase (Gibson *et al.*, 2009). EC is a primary source pollutant, forming through the incomplete combustion of fuel, particularly vehicle emissions in an urban site (Castro *et al.,* 1999). EC is also commonly referred to as BC which is discussed in more detail in further sections. OC includes primary emissions from vehicle emissions, as well as secondary emissions from gas to particle conversion of volatile organic compounds (VOCs). OC is a mixture of hydrocarbons and oxygenates (Castro *et al.*, 1999). Lastly, crustal minerals will be present in PM as a result of soil, road dust, and construction and demolition dust resuspension (Gibson *et al.*, 2009). Iron (Fe), aluminum (Al), silicon (Si), and calcium (Ca) are common tracer elements of this PM source (Harrison *et al.*, 2003). The three pollutants measured in this study are described below along with their associated health impacts.

2.1.1 Particle Mass Size Distribution and the Importance of $PM_{2.5}$

Size fractions of PM were first devised by Whitby *et al.* (1972) and Whitby (1978) upon observation of two curves in the particle size distribution of observed air quality measurements, representing coarse and fine sized PM. This definition has since been revised and refined to size fractions that are accepted and regulated worldwide. These size fractions can be seen below in Figure 2-1. The fine and coarse particles differ not only in size, but also in source, composition, and formation mechanisms, amongst other properties. There is an overlap in the 1 to 3 µm range between coarse and fine particulate resulting in what is referred to as intermodal PM in this size range (Geller *et al.,* 2004). $PM_{2.5}$ is defined as PM with an aerodynamic diameter less than or equal to 2.5 µm and is chosen as a measurement of fine particulate mass concentrations worldwide. $PM_{2.5}$ is composed of solid particles and liquid droplets and is commonly used as this size fraction reflects gas-to-particle generated aerosols, combustion associated particles, and importantly is the size fraction that can penetrate deep into the human lung. However, for the reasons stated above, $PM_{2.5}$ is only an approximation of fine particulate mass (Wilson & Suh, 1997).

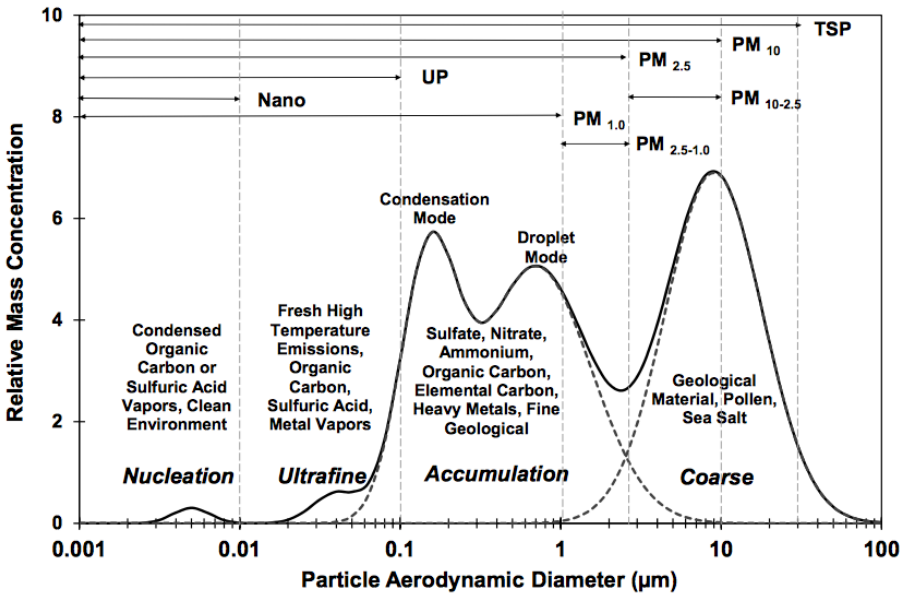

Figure 2-1: Size fractions of different particulate matter. Taken with permission from Cao et al., 2013.

Different size fractions of PM are associated with different sources. Generally, coarse PM is derived from dust, soil, and pollen (Gibson *et al*., 2009). Fine PM is observed to be largely from gaseous emissions and smoke, resulting in a higher toxicity (Hinds, 1999; Gibson *et al.,* 2015). In an urban environment, PM is primarily composed of combustion particles from vehicle emissions, secondary particles, and soil and road surface dust (Harrison, 2000; Gibson *et al*., 2013). In a study by Keuken *et al.* (2013) based in Rotterdam, Netherlands it was determined that people living in street canyons are exposed to elevated levels of PM derived from exhaust, brake and tire wear, and resuspended road dust. A study in São Paulo by de Miranda *et al.* (2017) observed PM containing elevated levels of resuspended road dust, exhaust emissions, secondary aerosols, and marine aerosol.

The Surface PARTiculate mAtter Network (SPARTAN) characterizes $PM_{2.5}$ from twelve sites distributed globally, with results presented in Snider *et al.* (2016). The South American site is represented by Buenos Aires, located on the Atlantic coast. Figure 2-2 shows that Buenos Aires experiences a large sea salt contribution to $PM_{2.5}$ mass when compared to most of the other sampling sites due to its proximity to the ocean. The average $PM_{2.5}$ mass concentration, located in the centre of the pie chart, at the Buenos Aires site was found to be lower overall than most other cities (represented by the values in the centre of the $PM_{2.5}$ pie charts), likely due to the clean oceanic air. BC, referred to as equivalent BC in this case due to measurements taken with optical absorption methods, made a high contribution to Buenos Aires $PM_{2.5}$ due to what was assumed to be diesel vehicle emissions.

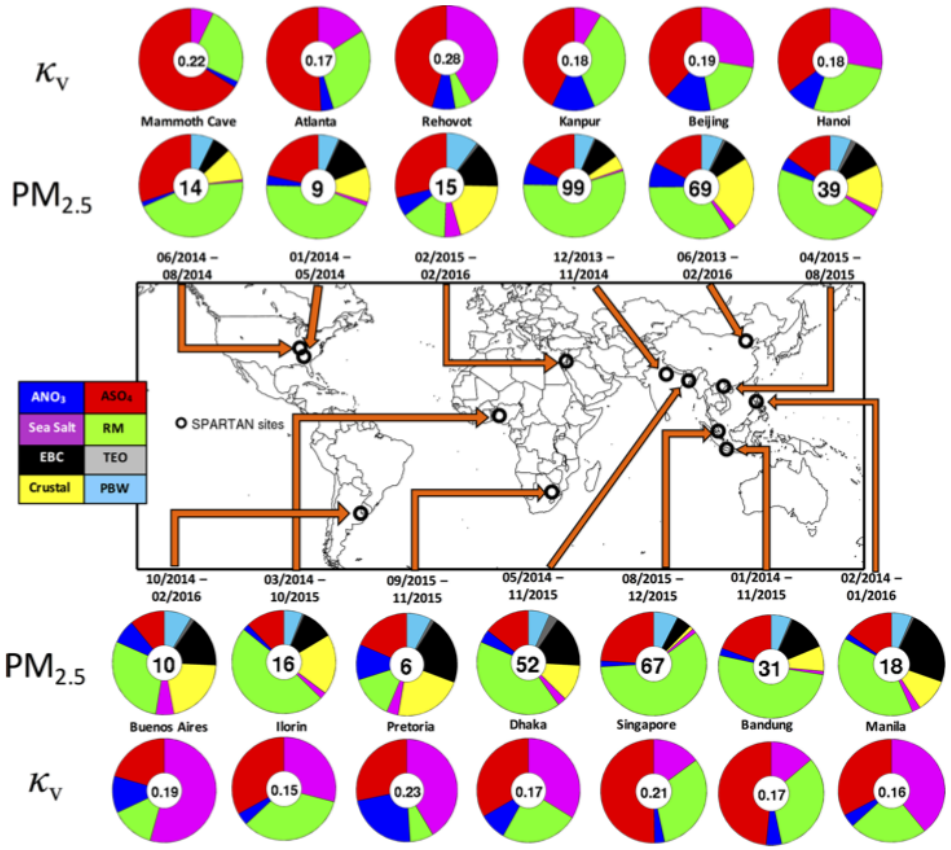

Figure 2-2: $PM_{2.5}$ composition from twelve locations around the world (Snider et al., 2016).

2.1.2 Ultrafine Particulate Matter

UFP are defined as particles with a median aerodynamic diameter less than, or equal to, 0.1 µm. Concentrations of UFP are typically expressed in particle number concentration (PNC) due to representing a very small fraction of the total mass, but a very large number concentration (Kittelson, 1998; Fuzzi *et al.*, 2015). PNC across Europe range from hundreds up to 50,000 particles/cm^3 (Fuzzi *et al.*, 2015). For example, Krecl *et al.* (2015) reported a peak concentration of 38,000 particles/cm^3 within a street canyon in Stockholm, Sweden during peak traffic flow. Sources of UFP include anthropogenic emissions, particularly vehicle emissions in urban environments (Kumar *et al.*, 2014). UFP emissions from vehicles along the side of heavily trafficked roads contribute up to 90% of the total PNC with UFP concentrations decreasing rapidly with increasing

distance away from the road (Kumar *et al.,* 2014). Indoor cooking can also generate a vast amount of UFP which can be expelled into city streets via kitchen exhaust fans (Wallace *et al*., 2004). Roadside cooking and restaurant ventilation can also generate UFP. Peaks in indoor UFP when cooking are well documented, however, Peters *et al.* (2014) noted a non-exhaust related UFP peak during outdoor measurements when passing by a restaurant due to cooking activities in Antwerp, Belgium. Brazil contains many sources of unregulated air pollution including bakeries, restaurants, pizzerias, and barbecues. São Paulo alone has 8,000 pizza shops, 80% of which are fueled by wood (Kumar *et al.*, 2016).

A fraction of the UFP is formed through nucleation from the gas phase through several different pathways, such as binary nucleation in which water vapour and sulphuric acid participate (Kulmala *et al.*, 2004). However, there is also strong evidence linking VOCs and growth into UFPs (Ehn *et al.*, 2014; O'Dowd *et al.*, 2002). UFPs have a relatively short lifetime in the atmosphere due to coagulation and accumulation into larger particles (Pope, 2000). There are currently no UFP regulations in place worldwide and therefore UFPs have not received much attention in studies globally. However, as negative health effects have recently become more widely associated with UFP, studies have become more frequent (Oberdörster *et al.,* 2005). It is noted however that PNC of UFP are elevated in Asia in comparison to Europe due to higher sulphur content in diesel, inferior vehicle emissions control technology, and densely built urban cities (Kumar *et al*., 2014).

In a study by Kumar *et al.* (2008), measurements of PNC within a street canyon showed that UFP concentrations were highest close to the road surface and decreased with vertical height. This is due to vehicle tailpipes being close to surface level and thus a well-mixed region results near surface-level due to vehicle induced turbulence (Kumar *et al.*, 2008). Wallace and Ott (2011) observed moderate levels of UFP PNC in-vehicle while driving (30,000 particles/cm^3) within the US states of Virginia and California. In a study by Fruin *et al.* (2008), high UFP concentrations were observed while on freeways in Los Angeles with one highway having a median value of 190,000 particles/cm^3. They

determined that a correlation existed between the quantity of diesel powered trucks and PNC. Measurements on arterial streets however observed much lower concentrations, about one third in comparison to freeways. Fruin *et al.* (2008) also observed high concentrations of UFP during hard accelerations, for example at traffic lights. Brace *et al.* (2014) used a P-Trak to monitor UFP in Halifax, Nova Scotia, Canada and observed PNC in the range of 7,902 – 14,105 particles/cm^3 during rooftop measurements in the city.

A study by Xu *et al.* (2016) measured UFP concentrations along a busy street in Montreal, Canada. Using their measured results, they built a model that assessed factors leading to increases in UFP concentrations. Xu *et al.* (2016) concluded that lower wind speeds resulted in higher PNC in the street and wind speeds parallel to the street decreased PNC. When wind speed is parallel to the street, this allows air pollutants to be flushed out of the street as opposed to a cross-wind which promotes the creation of a vortex within the street. The authors also noted that different built environments contributed significantly to UFP concentrations. When buildings are on both sides of the street, i.e. a street canyon, concentrations tend to be higher than other built environment conditions.

2.1.3 Black Carbon

BC is a component of $PM_{2.5}$ and UFP produced during fossil fuel combustion when the ratio of carbon to oxygen exceeds 0.5. The actual process of formation is through a complex series of steps outlined in Smith (1981). Spherules of BC are initially produced in the size range of 10 to 50 nm (Targino *et al*., 2018). These spherules rapidly coagulate together to produce particles containing chain-like structures (Bond *et al*., 2013). Figure 2-3 shows a scanning electron microscope (SEM) image of BC spherules forming these chain structures. The corresponding SEM-x-ray fluorescence wavelength spectra were associated with carbon and at a high intensity, providing further evidence that the SEM image was indeed BC (Gibson, 2004).

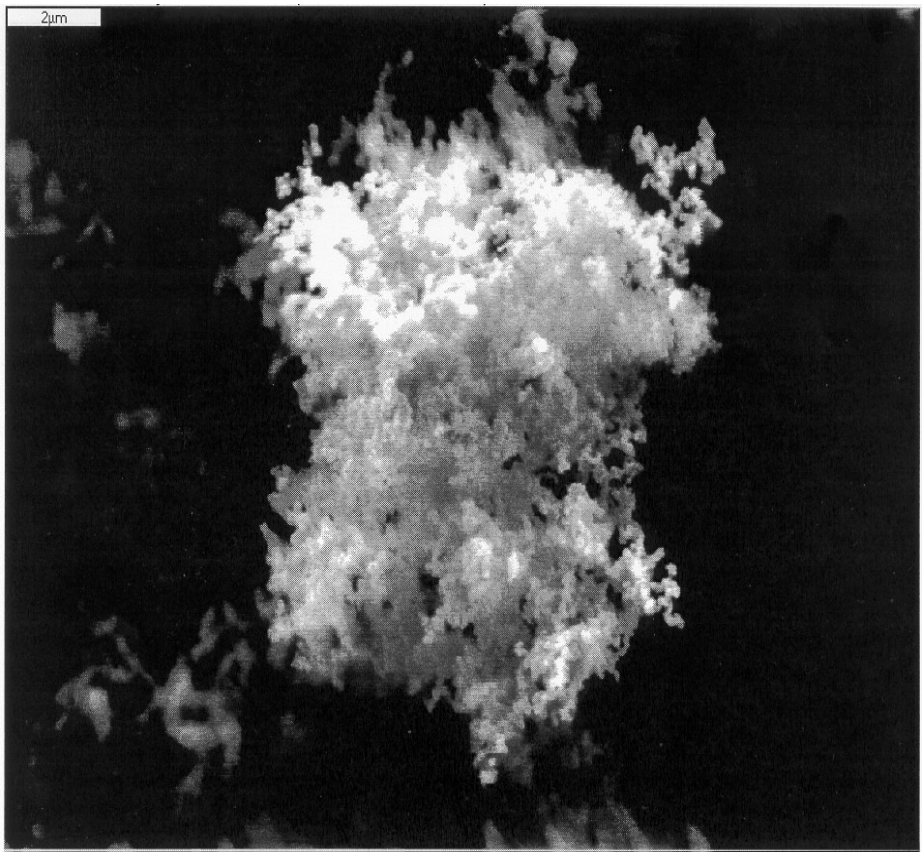

Figure 2-3:Scanning electron microscope image of BC spherules forming chain-like structures (Gibson, 2004).

BC is a known climate forcer contributing to an overall warming effect on the Earth (Ramanathan & Carmichael, 2008). Although radiative forcing by many aerosols has a net cooling effect on the Earth, the unique properties of BC cause it to positively increase radiative forcing. This is because BC absorbs radiation across the entire solar spectrum. Other carbonaceous materials co-emitted with BC, organic carbon and brown carbon, do not exhibit the same broadband absorption as BC, and so do not contribute as strongly as a climate forcer (Andreae & Gelencsér, 2006).

BC possesses many unique properties, including being characterized as a light-absorbing aerosol due to its significant absorption of light in the visible spectrum (Fuzzi *et al.*, 2015). Additionally, BC has a vaporization temperature of nearly 4000 K (Bond *et al.*,

2013). BC particles are insoluble and therefore are always distinctly separated from other material in an internally mixed particle (Jacobsen, 2001; Bond *et al*., 2013). Bare BC particles are hydrophobic (i.e. water repellant) when first emitted. Co-emitted aerosols are incapable of condensing when at hot ambient temperatures, however as the temperature of the emissions plume cools, these materials will condense onto available surfaces (Bond & Bergstrom, 2006). As can be seen in Figure 2-3, the irregular geometry and complex structure, consisting of many voids and pores, of BC particles makes them very attractive for the condensation of water and other species (Zhang *et al*., 2008). As the BC particle is coated, it becomes hydrophilic and therefore its atmospheric lifetime is decreased due to the increase in deposition potential (Bond *et al.*, 2013).

A large contributor of BC to the atmosphere is vehicle emissions (Gibson et al., 2015). Globally, approximately 9% of BC is produced from vehicle emissions, and of this, 98.7% is from diesel vehicle and freight emissions (Uherek *et al.*, 2010). Figure 2-4 below shows a global map of BC emissions from vehicle and freight traffic. It can be noted that along the coast of Brazil, the BC emission levels are elevated. This is associated with the major population centres along the coast and associated higher levels of vehicle traffic emissions. Values for this figure were adapted from Borken *et al.*'s (2007) global inventory of passenger and freight traffic. Emissions were calculated from national fuel sales, national energy balances, national vehicle stock data, estimates of annual vehicle mileage, and average vehicle fuel economy.

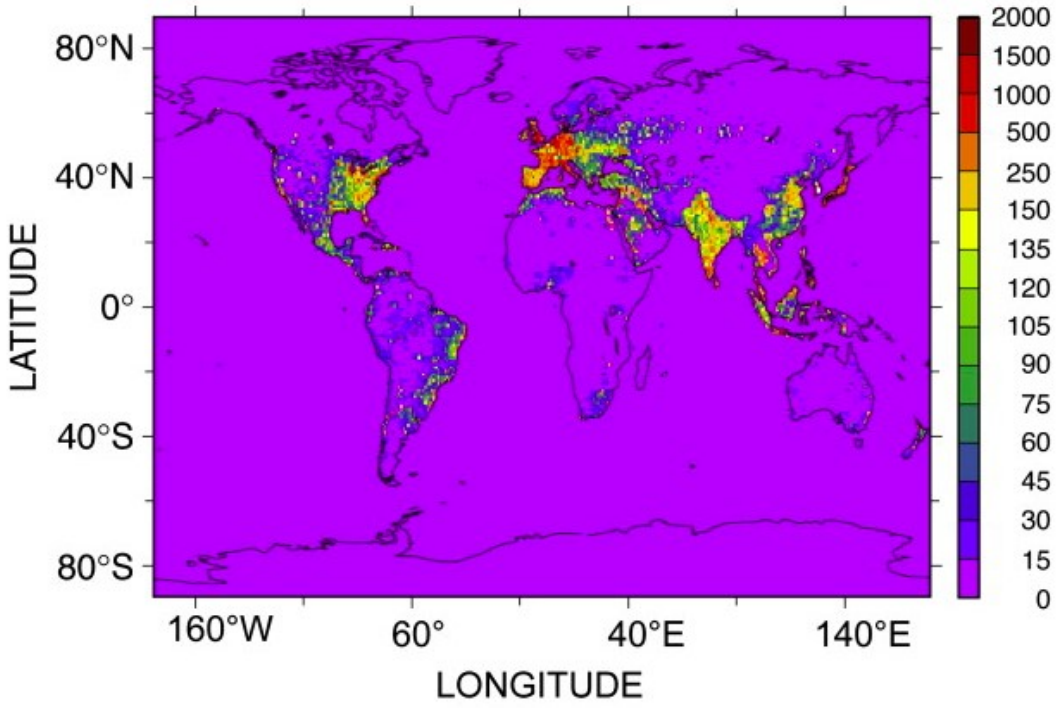

Figure 2-4: A map of the Earth showing BC vehicle and freight emissions in tonnes carbon per year. Taken with permission from Uherek et al., 2010.

Diesel engines produce higher amounts of BC than gasoline engines (Kupiainen & Klimont, 2007; Gibson *et al*., 2013). Unlike gasoline engines which have spark ignition engines, diesel engines are compression ignition. Carbon particles form during splitting of the hydrocarbon molecules during the diffusion-controlled combustion phase. These particles then combine to form the familiar chain-like structures of BC (Stone, 1992). Sulphur presence in diesel fuel is not involved in BC production, however it does increase particulate mass of exhaust by oxidising and attaching to BC particles (Mohankumar & Senthilkumar, 2017). Improvements in emission-controls of exhaust post-combustion, such as the addition of oxidation catalysts, have resulted in lower BC emission rates for newer diesel-powered vehicles in comparison to older vehicles with no emissions control. Low-sulphur diesel must be used in conjunction with a catalyst however, due to the formation of harmful sulphur by-products (Stone, 1992). Diesel particle filters are also available to remove PM using specialized filter media (Mohankumar & Senthilkumar, 2017). Table 2-1 contains BC emission factors for

gasoline- and diesel-powered vehicles that represent variable vehicle fleets across Europe (Kupiainen & Klimont, 2007). No controls indicate that no oxidation-catalysts are present. Diesel vehicles containing emission controls meeting EURO II standards are significantly lower than their no-control counterparts.

Table 2-1: BC emission factors for gasoline and diesel-powered engines with different types of exhaust treatment (Kupiainen & Klimont, 2007).

	BC Emission Factors (mg/MJ)
Heavy Duty Diesel with No Control	24-34
Heavy Duty Diesel with EURO II Control	6-9
Light Duty Diesel Vehicle with No Control	51-77
Light Duty Diesel with EURO II Control	17-25
Gasoline Vehicles (with and without control)	0.91-0.99

2.1.4 Associated Health Effects

The World Health Organization (WHO) identified air pollution to be the largest environmental risk to health and estimates 3 million premature deaths annually associated directly with outdoor air pollution (2016). One of the early studies on air pollution, commonly known as the Harvard six cities study, evaluated the long-term exposure to air pollution (Dockery *et al.,* 1993). Residents of six cities across the United States were evaluated and compared over a period of 14 to 16 years. It was determined that there were significant associations between inhalable particles, fine particles, and SO_4 particles with mortality. Additionally, the six-city study linked lung cancer and cardiopulmonary disease with $PM_{2.5}$ exposure (Dockery *at al.*, 1993). Another early study on $PM_{2.5}$ exposure addressed 151 metropolitan areas of the United States and used death certificate data retrieved from the American Cancer Society's Cancer Prevention Society. An association between air pollution and cardiopulmonary and lung cancer mortality was observed (Pope *et al.*, 2002).

Ambient $PM_{2.5}$ has varying composition and toxicity containing SO_4, NO_3, acids, metals, hydrocarbons, and various biological components, e.g. pollen, mold, bacteria, and viruses (Wilson and Brauer, 2006). It is also capable of permeating indoors from an outdoor environment more readily than coarse particles (MacNeill et al., 2014). Both acute and chronic exposures to $PM_{2.5}$ lead to negative health effects. Acute exposure studies observed increases in daily death counts during increased air pollution events while chronic exposure studies observed higher mortality rates and shorter lifespans associated with higher air pollution, particularly $PM_{2.5}$ and SO_4 particulates (Pope, 2000).

UFP, due to their smaller size, can access deeper lung tissue than larger particles. As can be seen in Figure 2-5, alveolar deposition increases with decreasing particle size. The respiratory tract does have several different clearance mechanisms to remove deposited PM from the system, however the human body does not have an effective method to remove UFP from the alveolar region (Chen *et al.,* 2016). Unlike larger particles, UFP are also able to gain access into the blood circulation system and therefore become distributed throughout the body (Oberdörster *et al.*, 2005). When UFP are deposited in the nasal cavity, there becomes potential for them to travel up into the brain through the olfactory system, however research into this is still in its infancy (Chen *et al.*, 2016).

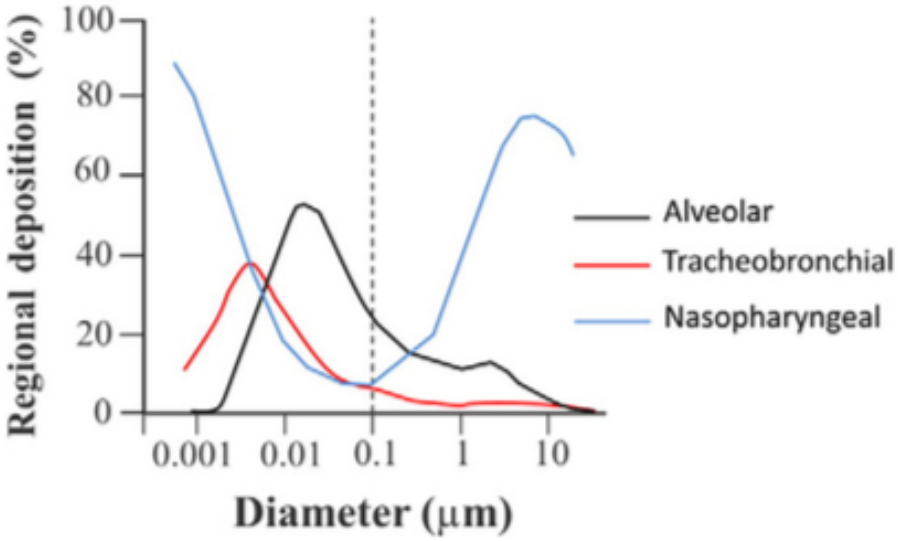

Figure 2-5: Deposition percentages in different locations of respiratory tract for varying particle sizes. Taken with permission from Chen et al., 2016.

There are five deposition mechanisms for PM: interception, inertial impaction, diffusion, gravitational settling, and electrostatic attraction. Within the respiratory system, only inertial impaction, diffusion, and gravitational settling are relevant. UFP have high deposition in the head airways due to their high diffusion coefficients. Larger particles on the other hand become deposited in large fractions in the head airways due to their large size resulting in settling or impaction on nose hairs. Particles deposit in the tracheobronchial region due to impaction and settling. These two regions serve to protect the more sensitive alveolar region from particulates. However, deposition into the alveolar region does occur when particles settle from the reserve air in the tracheobronchial region into the alveolar region (Hinds, 1999).

BC, a component of $PM_{2.5}$ and UFP, has been linked with lung cancer since early studies on the subject. A study by Silverman *et al.* (2011) explored a link between diesel exhaust exposure to underground mine workers and cancer. It was concluded that the workers had an increased risk of lung cancer, and exposure to higher levels of BC resulted in higher

risk levels of cancer. Residents of urban areas with high concentrations of BC could thus also be at risk of lung cancer. The health effects associated with a mass concentration increase of BC were substantially larger than for the same mass concentration increase in PM_{10} (PM with a median aerodynamic diameter < 10 μm). BC is a useful source identifier due to its direct relation with combustion-derived PM (Janssen *et al.*, 2011).

2.2 Air Quality Regulations in Brazil

Air quality measurements have taken place in São Paulo since the early 1960s however, national ambient air standards were not implemented in Brazil until 1990. These air quality standards have yet to be updated since their implementation. In comparison to other standards and guidelines around the world, the Brazilian standard levels typically have higher thresholds. It is up to individual states to regulate ambient air quality, and thus certain states have set their own regulatory levels including São Paulo state. Although there exists no national $PM_{2.5}$ standard, the São Paulo state standard regulates $PM_{2.5}$ concentrations (Andrade *et al.*, 2016). Smoke is also regulated in the national standard. Although smoke contains BC, it cannot be used as a proxy measurement. Smoke is measured by reflectance methods where BC is measured with absorption. The Brazilian national standards and São Paulo standards can be seen in Table 2-2 below for $PM_{2.5}$, PM_{10}, total suspended particles (TSP), and smoke. TSP accounts for the total particulate mass.

The Brazilian Motor Vehicle Air Pollution Control Program (PROCONVE) is a program implemented by the government to regulate vehicle emissions for the reduction of urban air pollution. The first phase was implemented in 1988 and new phases have been implemented every few years since adding further restrictions (Nogueira *et al.*, 2015). Initially only light duty vehicles (LDVs) were regulated, followed by HDVs in 1990 with no legal requirements for HDVs until the third released phase. These phases only apply to newly built vehicles, with older vehicles on the roads in Brazil not meeting the current PROCONVE standards (Andrade *et al.*, 2016).

Table 2-2: Brazil and São Paulo PM standards (Andrade et al., 2016).

		$PM_{2.5}$ *($\mu g/m^3$)*	**PM_{10}** *($\mu g/m^3$)*	**TSP** *($\mu g/m^3$)*	**Smoke** *($\mu g/m^3$)*
Brazil standard (CONAMA no. 03/90)	Short-term (24 hour)	-	150[a]	240[a]	150[a]
	Long-term (annual)	-	50[b]	80[c]	60[b]
São Paulo state standard	Short-term (24 hour)	60	120	240	120
	Long-term (annual)	20[b]	40[b]	80[b]	40[b]

[a] Not to be exceeded more than once annually

[b] Arithmetic mean

[c] Geometric mean

Lower sulphur diesel was required to meet recent phases for HDVs due to the formation of sulphur compounds in the combustion chamber affecting operation of the catalyst. Initially diesel in Brazil contained 13,000 ppm of sulphur and this was reduced gradually from the years 2005 through 2012 when 10 ppm diesel became available with the latest phase of PROCONVE in 2012. HDV standards in Brazil currently meet the EURO V European emission standards (Nogueira *et al.*, 2015). Although new diesel motors are regulated to run on 10 ppm sulphur diesel, older engines and buses are still permitted to use higher sulphur content diesel. Diesel fuel is also blended with a small fraction of biodiesel (Andrade *et al.*, 2016).

The results of emission reductions implemented through PROCONVE in São Paulo can be assessed by the results of tunnel studies conducted in 2004 and 2011. One tunnel was dominated by LDVs characterized by ethanol and gasohol (75% gasoline and 25%

ethanol) fuel types. The other tunnel was dominated by HDVs characterized by diesel and biodiesel fuelled vehicles. From the 2004 study, emission factors for the LDVs and HDVs were determined to be 92 mg $PM_{2.5}$/km and 588 mg $PM_{2.5}$/km, respectively (Sánchez-Ccoyllo *et al.*, 2009). From the 2011 study, emissions factors for the LDVs and HDVs were observed as 20 mg $PM_{2.5}$/km and 277 mg $PM_{2.5}$/km, respectively (Pérez-Martínez, 2013). The more recent study shows significantly lower emission factors as a result of recent reductions in vehicle emissions through PROCONVE.

2.3 Vehicle Share in Londrina, Curitiba, and São Paulo

Vehicle fleets in Brazil are composed of large quantities of passenger vehicles that run on either ethanol or a gasoline blend with 25 ± 1 % (v/v) anhydrous ethanol, called gasohol (Ré-Poppi et al., 2009). The total number of licensed vehicles from 2016 can be seen for the three cities of interest in this study below in Table 2-3. The breakdown of vehicle groups is included for comparison as well.

Table 2-3: Licensed vehicles for each city (DENATRAN, 2016)

	Londrina	**Curitiba**	**São Paulo**
Total Vehicles	**386,798**	**1,516,468**	**7,805,127**
Cars	232,108	1,048,938	5,442,775
Pick-up Trucks	29,206	107,160	461,384
SUVs	13,236	73,144	422,974
Trucks	11,614	50,336	152,324
Motorcycles/Mopeds	85,942	162,763	1,044,559
Buses	2,955	11,260	82,095
Utility Vans	2,950	19,722	107,781
Other	8,787	43,145	91,235

In São Paulo, the city mandates the removal of buses from its fleet after five years (Andrade *et al.*, 2016). Londrina however has an average bus fleet age of just over six years (C. R. Fabiano, personal communication, October 6, 2017) and Curitiba has an average bus fleet age of nearly eight years (URBS, 2017) indicating that the emissions from these older bus fleets may be more polluting than the newer fleet in São Paulo. Additionally, buses in Brazil are not equipped with diesel particle filters which can contribute to an increased level of particulate emissions (Targino *et al*., 2018). In Londrina, Curitiba, and São Paulo, the fleets consist primarily of buses meeting EURO III emissions standards (74 %, 89 %, and 70 % the total fleet size, respectively). Curitiba however, has a large component of its bus fleet meeting the earlier EURO II emissions standard (11 % the total fleet). Londrina and São Paulo on the other hand have large fractions of their bus fleets meeting the newer EURO V standard (26 % and 30 % the total fleet size, respectively).

2.4 Urban Effects on Air Quality

Urban centres have unique characteristics that lead to different air quality when compared to rural areas. The air exchange between the street level air and clean air above can be limited due to high building density and diverse meteorological conditions resulting in an accumulation of pollutants at surface level. Additionally, traffic emissions at street level tend to spread laterally as opposed to vertically (Kumar *et al.*, 2014). Complicated air flow patterns exist in a city due to buildings, streets, stagnant zones, and wakes. Due to the proximity of buildings, recirculation zones of air can develop with higher concentrations when compared to concentrations outside of the recirculation zone (Tiwary and Colls, 2010). Air pollution will also tend to accumulate along streets downwind from their emission zone (Buccolieri *et al.*, 2010).

Hotspots of air pollutants can be found within cities, especially within a street geometry known as a street canyon (Vardoulakis *et al.*, 2003). A street canyon refers to a narrow road with buildings continuously lining either side. A street canyon can be characterized by its aspect ratio (height of buildings divided by width of street) with a standard street

canyon having an aspect ratio of one (Vardoulakis *et al.*, 2003). As air skims the buildings above the street canyon, a wind vortex can be created within the canyon. This will lead to an accumulation of air pollutants on the sides of the street canyon. Additionally, when the above-canyon wind speed is low, the vortex may not occur and instead air will remain stagnant in the street canyon (Vardoulakis *et al.*, 2003). Krecl *et al.* (2016) evaluated the effects of a street canyon on BC and ozone concentrations in Londrina, Brazil. Higher pollution concentrations were observed inside the street canyon in comparison to the rooftop and background measuring sites. Diurnal patterns were observed related to traffic patterns and higher pollution levels were observed on the leeward (upwind) side of the street canyon, a common effect within street canyons due to the vortex morphology.

Many studies have also been conducted on the general location of air pollution within a city and the environmental injustice associated with it. People in lower socioeconomic positions are at greater risk to air pollution with disproportionate air pollution exposures affecting people with low socioeconomic positions and/or minority populations. The reasons for this disproportionate exposure include: housing market dynamics, racism, and class bias in land use decisions within an urban area (O'Neill *et al.*, 2003). It was observed that mean vehicle pollution was 1.5 – 2 times higher in low-income areas compared to areas with few low-income households in Christchurch, New Zealand (Kingham *et al.*, 2007). A study in Vancouver, British Columbia, Canada compared nitrogen oxide (NO) pollution to walkability and found that areas with high NO concentrations and high walkability corresponded to low-income neighbourhoods. Areas with low NO pollution and high walkability were almost entirely high-income neighbourhoods (Marshall *et al.*, 2009).

Although fixed monitoring sites are a common method of measuring air pollution distribution within a city, they commonly underestimate the air pollution concentrations resulting in a need for personal exposure monitoring. Kaur *et al.* (2005) conducted a study measuring the personal exposure to several pollutants through many modes of

transportation and comparing the values to kerbside and background fixed monitoring sites. The highest exposures were observed in car, taxi, and bus modes of transport with the lowest observed while walking. The fixed monitoring sites did not accurately reflect the air pollution concentrations observed by the personal monitors. Typically, air pollutants show an increasing concentration gradient as the measurements move from rural to urban to kerbside sites, respectively (Putaud *et al.*, 2010). Furthermore, particle number counts have been shown to decrease away from traffic resulting in the higher concentrations observed when measurements are taken closest to the emission source (Costabile *et al.*, 2009).

2.5 Review of Traffic Related Air Pollution Studies

Studies of commuter exposure to air pollution have been well documented worldwide comparing different methods of commuting including walking, cycling, driving, and taking public transit. Several studies have documented the highest exposure during bus transit modes of transportation (Chan *et al.*, 2002a; Gómez-Perales, 2007; Weichenthal *et al.*, 2008; Targino et al., 2018). This is due to a few different factors that will be discussed in the context of each study. A study by Gómez-Perales *et al.* (2007) in Mexico City measured $PM_{2.5}$ concentrations across different public transit modes including bus, minibus, and metro. It was determined that the bus and minibus air pollution concentrations were higher than in the metro. Gómez-Perales *et al.* (2007) concluded that this was due to traffic density, poor ventilation within the buses, and self-pollution of vehicle exhaust. Additionally, higher pollution values were observed in the morning associated with rush hour traffic and low combustion efficiency in the cold early mornings. As wind speeds increased across the city, $PM_{2.5}$ concentrations were shown to decrease indicating that higher wind speeds aid in dispersion of traffic emission pollution (Gibson, 2004; Gómez-Perales *et al.*, 2007).

A study by Chan *et al.* (2002a) in Hong Kong measured $PM_{2.5}$ concentrations across different modes of transport. The $PM_{2.5}$ concentrations were observed to be highest across roadway transport modes. Modes without air conditioning showed significantly

higher $PM_{2.5}$ concentrations. When air conditioning is used, the closed bus windows act as a barrier and the vehicle air filter can remove some PM. However, without air conditioning, pollutants can easily enter into the bus through open windows or from the ventilation system since the air intake is located near ground level. Passenger movement and opening of bus doors could cause increased concentrations of PM as well. Larger buses may help to disperse these pollutants once they enter the compartment due to a larger volume of passenger cabin and thus larger pollutant dilution (Chan *et al.*, 2002a).

Spinazzè *et al.* (2008) measured UFP concentrations in Como, Italy, across different modes of transportation including walking, cycling, driving, and traveling by bus. The highest PNC were observed on buses and walking/biking in heavy traffic. Although the buses used in the study were newer and had particulate filters, ventilation factors were key in the reduction of on-board air pollution. Higher PNC were also observed during morning rush hour and in the winter indicating that the UFP concentrations have diurnal and seasonal trends (Spinazzè *et al.*, 2015). Weichenthal *et al.* (2008) measured UFP concentrations in Montreal, Canada, comparing transport modes of walking, driving, and traveling by bus. The highest UFP values were observed in the automobile mode of transport, followed by buses, then walking. It was noted however that ventilation was not controlled across any mode of transport. As mentioned in Chan *et al.* (2002a), the use of air conditioning and recirculation mode in vehicles can have a drastic effect on in-vehicle air pollution concentrations. The UFP concentrations in Montreal were observed to be higher in the morning than evening rush hours during the measurement period (Weichenthal *et al.*, 2008).

A study by Dons *et al.* (2012) measured BC concentrations in Flanders, Belgium for 62 participants and the results were compared to assess exposure to BC across different transportation modes. The highest peaks of the participants' exposure throughout their daily activities were observed during transportation. The lowest BC concentrations during transportation were observed in rail transport, followed by walking/cycling. The highest BC concentrations were observed during driving, traveling by bus, and using light

rail/metro. However, overall, bus transportation showed the highest concentrations of BC when compared with other microenvironments. They concluded that although time in transportation modes may only consist of a small portion of daily activities, it contributes to a large portion of the inhaled dose of BC in a day. Targino *et al.* (2018) measured BC concentrations on buses in Londrina, Brazil. Simultaneous measurements were taken via cycling and walking along a portion of the measured bus route. Higher concentrations of BC were observed in-bus in comparison to the walking and cycling measurements. This could be due to self-pollution from the bus exhaust and in-bus accumulation of BC from air pollution penetration through the open windows and open doors at bus stops. Extreme BC values were observed to frequently occur at bus stops and traffic lights. Higher pollution levels were observed in the bus when traveling through the city core, which was attributed to heavier traffic and densely spaced tall buildings preventing dispersion of air pollutants. BC concentrations also were observed to decrease with speed due to the bus moving from congested, highly polluted areas of the city to less trafficked areas of the city (Targino *et al.*, 2018).

Air pollution across different modes of transport is heavily influenced by many factors including, but not limited to, vehicle ventilation settings, traffic density, proximity to traffic, time of day, and self-pollution. It was observed across many studies that buses tend to possess the highest concentrations of particulate air pollution on-board different modes of transport. Bus passengers are particularly at risk because they are unable to control ventilation settings and buses tend to travel through heavily trafficked areas unlike other personal modes of transportation where the operator can opt to travel through roads that contain less traffic. It is anticipated therefore that bus drivers and bus conductors (ticket agents) would be exposed to even greater concentrations of air pollution due to their occupation (Han *et al.*, 2010).

Chapter 3 Experimental Techniques and Instruments

3.1 Sampling Locations

We measured $PM_{2.5}$, BC, and UFP concentrations on urban buses in three Brazilian cities of different sizes: Londrina, Curitiba and São Paulo (Figure 3-1). Measurements in all cities were carried out at time periods different than peak congestion (i.e. rush hour) to prevent inflated pollution levels due to higher levels of vehicle traffic on the roads. It should be noted however that commuter exposure during rush hour could be different from those levels measured in this study due to the different traffic volumes. Detailed trip itineraries can be found in Appendix A.

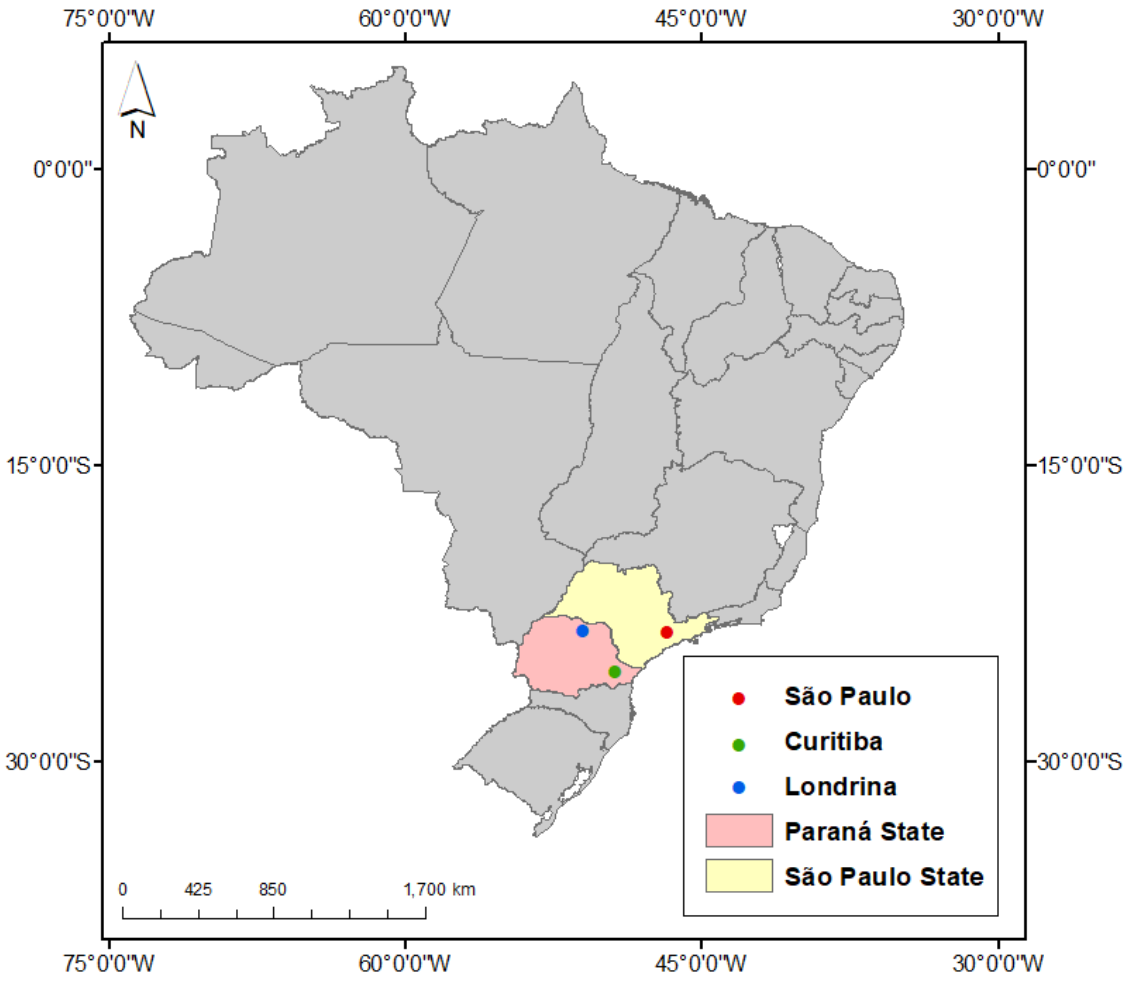

Figure 3-1: Map of Brazil highlighting the measured cities.

3.1.1 Londrina

Londrina is a mid-sized city of about 555,000 inhabitants (23° 18’ S, 51° 10’ W, elevation 610 m) in the southern state of Paraná (IBGE, 2017). Londrina was originally settled in the early 1900s by British colonists for the purposes of cotton farming, however, the enterprise failed due partially to low market prices. Londrina then went on to have many successful coffee plantations. Current economic activities in Londrina are dominated by the service sector (Krecl *et al.*, 2016). Measurements in Londrina were taken for a period of five days beginning on June 20, 2016 and starting at approximately 9:50 each morning (dependent on bus schedule and delays). The sampling route can be seen below in Figure 3-2. The sampling route commenced on bus #113 from the campus of the Federal University of Technology (UTFPR) to the Central Terminal in downtown Londrina. Samples were then collected on bus #217 to Acapulco Terminal. The route was reversed with sampling from Acapulco Terminal back to Central Terminal and returning to UTFPR.

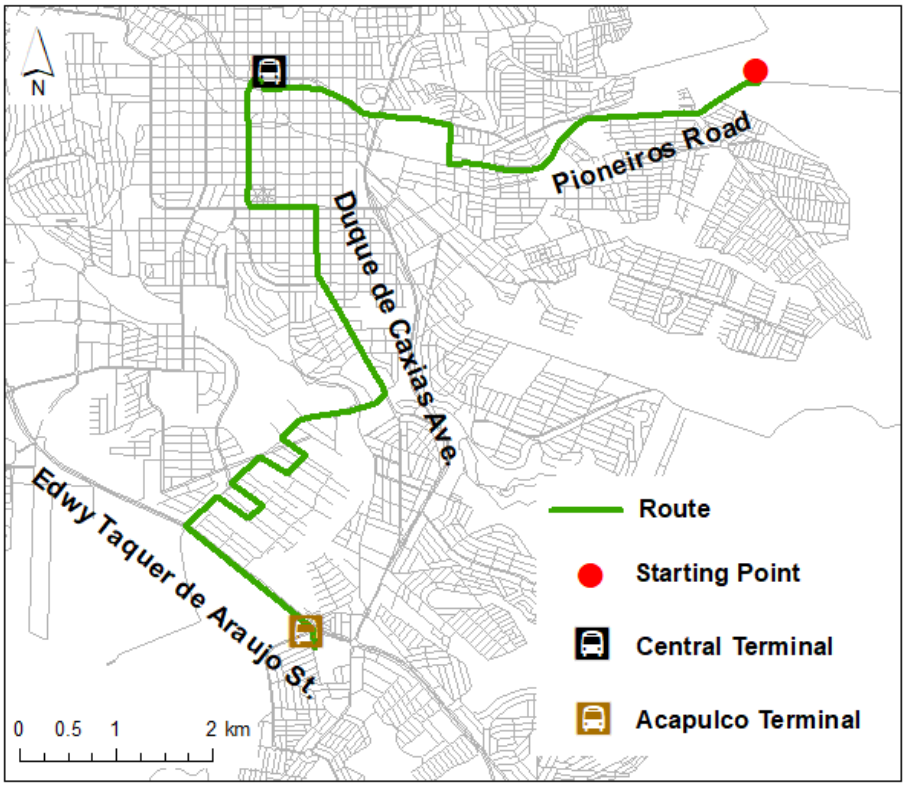

Figure 3-2: Londrina sampling route.

3.1.2 São Paulo

São Paulo city is the capital of the homonymous state in southeastern Brazil (23° 32’ S, 46° 39’ W, elevation 760 m). The city was established in the mid-1500s and has grown to have an urban population of an estimated 12,106,920 inhabitants; however, the metropolis population is nearly double (IBGE, 2017). São Paulo is considered a megacity, defined by the UN as a city with a population larger than ten million (Zhao *et al., 2017*). Sampling took place in São Paulo over a four-day period commencing on June 27, 2016 at approximately 13:45 each day. The sampling route can be seen mapped below in Figure 3-3. This route consisted of a single direction loop within the city core of São Paulo. Sampling commenced on the 8707-10 bus, except for June 28th when sampling began on the 778R-10 bus instead. Both buses took a direct route from the intersection of Consolação Street and Paulista Avenue to the Princesa Isabel bus terminal. From there, the 805L-10 bus was taken which looped through the city and ended at the starting intersection.

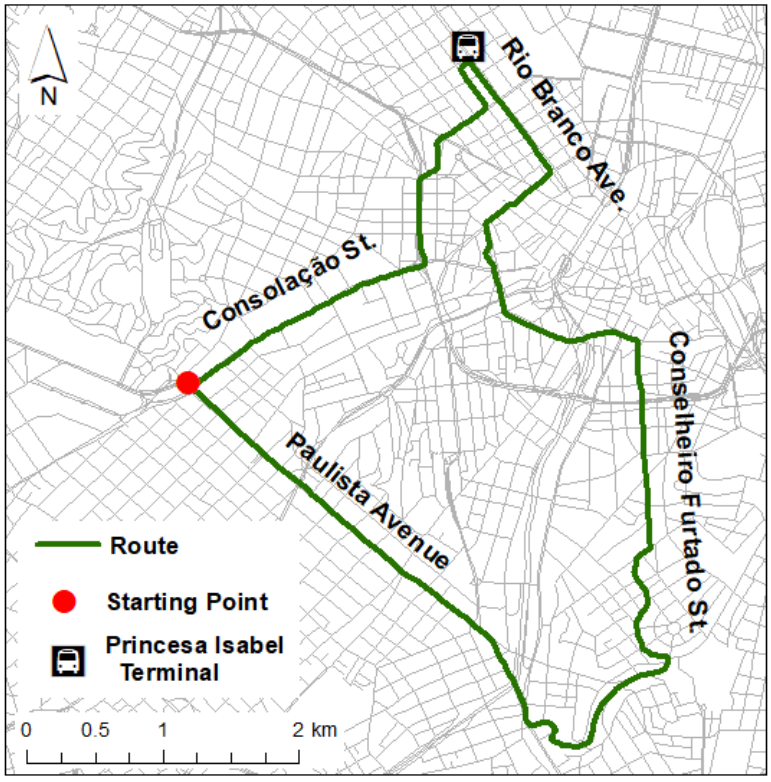

Figure 3-3: São Paulo sampling route.

A study by Castanho and Artaxo (2001) conducted the source apportionment of $PM_{2.5}$ collected over winter 1997 in São Paulo. Vehicle emissions accounted for 28 % of PM during the winter, resuspended soil dust accounted for 25 %, oil combustion accounted for 18 %, sulfates accounted for 23 %, and industrial emissions accounted for 5 %. Another $PM_{2.5}$ source apportionment study was conducted more recently by Andrade *et al.* (2010) over a one-year period from winter 2007 to winter 2008. The average $PM_{2.5}$ mass concentration in São Paulo was 28 $\mu g/m^3$. It was determined that 13 % of the $PM_{2.5}$ mass was associated with resuspended soil and construction and demolition dust, 13 % mass was from oil burning, industrial emissions, and secondary aerosol formation, 12 % mass was from light duty vehicle emissions, and 28 % mass from heavy duty vehicle emissions. The remaining 33 % of the mass that was uncharacterized and assumed to be organic carbon and water.

3.1.3 Curitiba

Curitiba is the capital city of the state of Paraná (25° 25’ S, 49° 16’ W, elevation 935 m). It is located southeast of Londrina and towards the Atlantic coast. Curitiba, also much older than Londrina, was founded in 1693. Curitiba became known for its urban planning in the 1990s. This attracted many new businesses and industries to the city, as well as a significant population growth (Macedo, 2004). The current population in Curitiba is estimated to be 1,908,359 inhabitants making it the largest city in southern Brazil (IBGE, 2017). Sampling in Curitiba took place over a five-day period commencing July 25, 2016. Each sampling period started at approximately 13:40 each day. The sampling route can be seen mapped below in Figure 3-4. Sampling commenced on bus #002 on Desembargador Motta Street and completed the entire counter-clockwise loop until reaching Sete de Setembro Avenue. Bus #001 was then sampled for one entire clockwise loop, starting on Visconde de Guarapuava Avenue, one block north from the departure point of the previous bus.

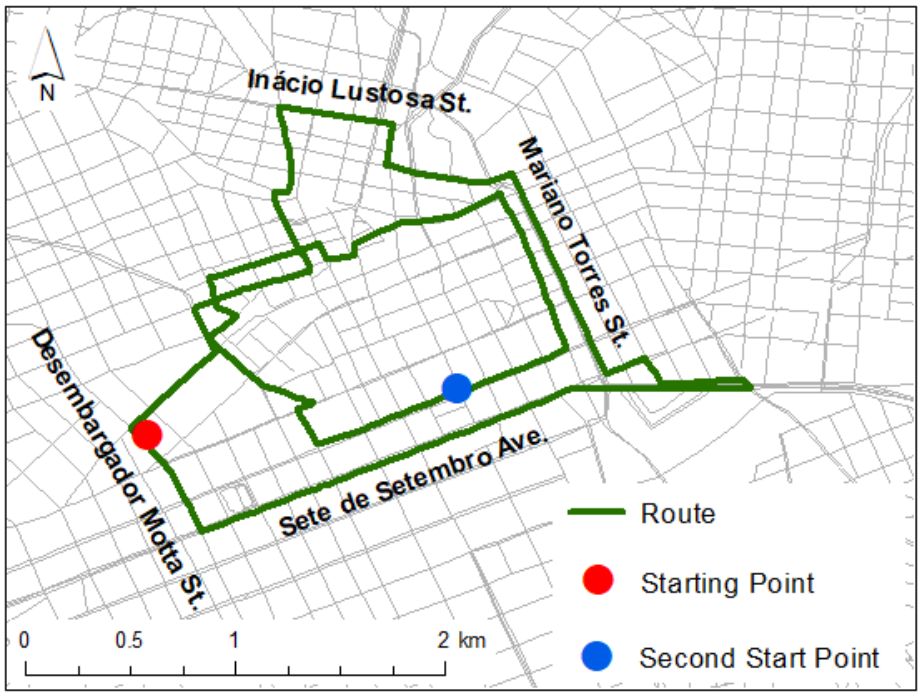

Figure 3-4: Curitiba sampling route.

Andrade *et al.* (2010) included Curitiba in their source apportionment study comparing several cities in Brazil from winter 2007 to winter 2008. The average $PM_{2.5}$ mass concentration was determined to be 16 $\mu g/m^3$. The composition was found to be 40 % crustal emissions and vehicle emissions, 3 % from residual emissions, 15 % from mobile emissions, 13 % from industrial and secondary emissions, and 29 % remained uncharacterized.

3.2 Field Instruments

Three different instruments were used to measure $PM_{2.5}$, BC, and UFP. A Global Positioning System (GPS) receiver was also used to record location information. These instruments were carried together on the bus routes in a duffel bag and are discussed below in detail.

3.2.1 TSI DustTrak 8520

The DustTrak 8520 is a real time particulate matter measuring instrument (Figure 3-5). It operates with a flow rate of 1.7 liters per minute (Lpm) with greased impactors of different aerodynamic cut sizes that can be fitted to the sampling inlet to subsequently remove particles greater than the desired median size cut from the sample air stream. For this study, an impactor plate with a median aerodynamic diameter < 2.5 μm was used to quantify the mass concentration of $PM_{2.5}$ particles. The DustTrak obtains a mass-concentration of the $PM_{2.5}$ through light scattering and photodetection (Wallace *et al.*, 2011). The air sample is lit with a laser source which causes the light to be scattered in all directions from the particles in the air stream. A photodetector collects the light at 90° incident to the laser diode and converts it to a voltage. This voltage is then converted into a mass concentration using the density of the Arizona Test Dust ($\rho = 2.6$ g/m^3). The test dust that the instrument is factory calibrated with typically has a different size distribution than the aerosol being measured since the Arizona test dust only has a distribution range of 0.1 μm to 10 μm. Urban areas are influenced by high concentrations of UFP (Simon *et al.*, 2017). Each sampling location will have different aerosol parameters that affect DustTrak measurements including refractive index, particle shape, particle density, and particle size (Cheng *et al*., 2008). Because urban aerosols have lower density than the Arizona Test Dust aerosols (for example, ρ=1.36- 1.55 g/cm^3 in Shanghai, Yin *et al*., 2015), this results in an overestimation of the air pollution in the sampling area. Kingham *et al.* (2005), Cheng *et al*. (2008), and Li *et al.* (2018) observed overestimations in the range of 1.4 to 3.26 times the actual concentration of $PM_{2.5}$. Due to this overestimation, a correction factor needs to be applied to DustTrak data for accurate analysis.

In a previous study in Londrina, Brazil a correction factor of 0.5 was applied based on a literature review (Targino *et al.*, 2016). When possible, gravimetric measurements are used to determine an environment-specific correction factor since filter-based measurements are a very accurate method of measuring particulate mass. Dr. Targino's research group at UTFPR in Londrina determined correction factors for both Londrina

and Curitiba cities in Brazil; 0.5079 and 0.5199, respectively (M. de Lima Souza, personal communication, April 10, 2017). These correction factors have been applied to the data analyzed in this work. Additionally, since no correction factor was determined for São Paulo, the correction factor from Curitiba was applied. Curitiba is approximately 400 km south-west of São Paulo and has a significantly larger vehicle fleet than Londrina therefore it was assumed that the aerosol parameters in Curitiba would be more similar to those in São Paulo than those in Londrina.

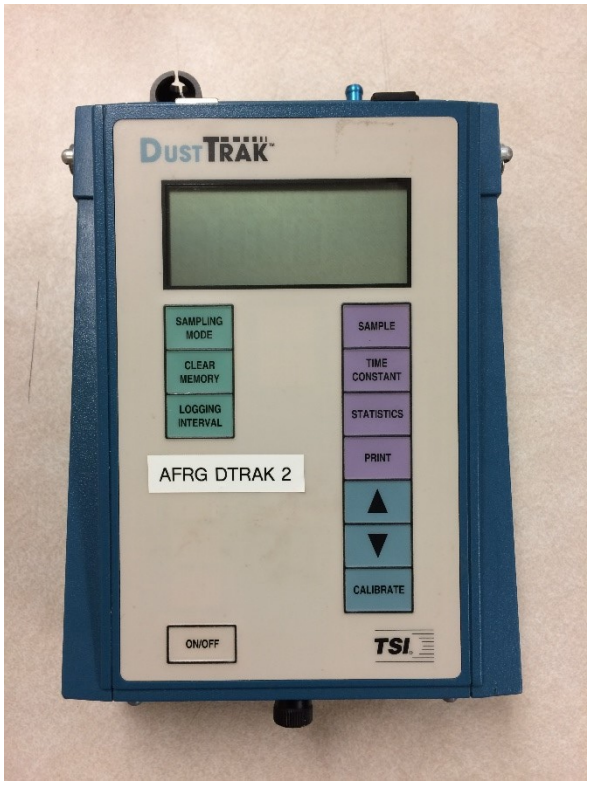

Figure 3-5: Photo of the DustTrak 8520 (Photo by Ellen Patrick).

The flowrate was checked and adjusted if necessary each day prior to data collection. A zero check was performed and the clocks between instruments and the computer were synchronized prior to data collection. Data was downloaded immediately after collection and the instrument was cleaned when required (typically every few days with the exception of São Paulo, where high levels of pollution required the instruments be

cleaned daily). The DustTrak was set to sample at an interval of 1-second and has a particle size limitation of 0.1 μm limiting it from measuring particles classified as ultrafine.

3.2.2 AethLabs AE51

Black carbon concentrations were measured using a microaethalometer AE51. It operates at a user selected flow rate corresponding to the desired type of measurements. The flow rate was set to 150 mL per minute and a time resolution of ten seconds. These rates ensured that the device sampled sufficient aerosol mass in clean environments and a sufficient number of data points in areas of fast transit. The AE51 functions by drawing in air and passing it through a T60 Teflon coated borosilicate glass fiber filter. The calculations behind the attenuation and resulting BC concentration have been outlined extensively in literature. Targino *et al.* (2017) summarizes the theory and equations and the findings are summarized below.

The attenuation (ATN) is measured by monitoring the intensity of an 880 nm radiation beam transmitted through a blank filter spot, and the intensity of radiation transmitted through the filter spot on which the particles accumulate:

$$ATN = 100\ln\frac{I_0}{I} \quad (1)$$

where I_o is the radiation intensity through the blank portion of the filter strip and I is the intensity measured through the particle-laden portion of the filter strip. The BC concentration is calculated using the wavelength-dependent cross-sectional absorption coefficient (σ_λ = 12.5 m^2/g for λ = 880 nm). These calculations can be seen below amalgamated into one equation:

$$BC = \frac{A}{Q}\frac{\Delta ATN}{\Delta t}\frac{1}{\sigma_\lambda} \quad (2)$$

where BC is given in [µg/m^3], A is area of the particle-laden filter spot, Q is the flow rate, ΔATN is the change in attenuation over Δt change in time. Because the attenuation calculation does not differentiate between BC and other light absorbing particulate matter, it is assumed that all the light absorbing material on the filter is BC. However, interferences may occur in environments dominated by mineral dust since these particles absorb radiation at wavelengths similar to carbonaceous aerosols (Moosmüller *et al.,* 2009).

The AE51 used in this study was tested with a TSI zero filter attached to the inlet to determine the instrumental limit of detection (LOD). The LOD is defined as three times the standard deviation of the instrument noise (MacDougall and Crummett, 1980). A zero filter removes all airborne particulate matter from the inlet air stream permitting the operator in this case to quantify instrumental noise. The zero filters used in this set up have a polyethersulfone membrane filter media with a removal efficiency of 99.96 % at 0.45µm (M. Mangin, personal communication, September 22, 2017). These instruments were left to run overnight for a full 12-hour period. For this microaethalometer at a 10-second logging interval, the LOD was determined to be 0.2 µg/m^3.

Figure 3-6: Photo of the AE51 (Photo by Julián Felipe Segura).

3.2.3 TSI P-Trak

The P-Trak Ultrafine Particle Counter 8525 is a real-time instrument that measures UFP concentrations at a user specified logging interval (Figure 3-7). The flow rate is calibrated by the manufacturer to 0.7 Lpm. It is a type of instrument referred to as a condensation particle counter. An isopropyl saturated wick is manually placed into the P-Trak prior to sampling and results in isopropyl alcohol evaporating into the chamber. As particles in the air stream pass through the supersaturated atmosphere, isopropyl alcohol condenses to the particles (Wallace *et al.*, 2011). When the alcohol condenses on the particles, they grow in size allowing them to be detected by the laser diode and photo detector that counts the particles as they pass through (Nikolova *et al.*, 2011). The data is output as the number of particles per cm^3 as opposed to the mass concentration given by the DustTrak or AE51 instruments. The P-Trak detects particles in the size range from 20 nm to 1 µm and has a maximum measurable concentration of 500,000 particles per cm^3 (Wallace *et al*., 2011). The logging interval of the P-Trak was set to 1-second.

Figure 3-7: Photo of the P-Trak 8525 (Photo by Ellen Patrick).

3.2.4 GlobalSat GPS

A GlobalSat GPS (Model DG-100) was carried in the instrument package to record GPS data. GPS coordinates, speed, and elevation were recorded on a 1-second logging interval.

3.3 Pre-Data Collection Preparation

Prior to data collection, practice runs and instrument collocations were carried out in Londrina to ensure that the sampling frequency and flow rates yielded particle concentrations with acceptable signal-to-noise ratios. Sampling runs were also completed to pinpoint any eventual problems that could arise during the data collection in the field. An instrument pack with a DustTrak, AE51, P-Trak, and GPS was used to collect trial data on a bus route.

3.4 Field Methods

Sampling routes were designed ahead of time using the program Google Maps to choose bus routes that maximized the area of the city that was sampled. The routes were designed to cover a large portion of the city, crossing different microenvironments. Conductive tubing was used to connect the inlets of the instruments within the bags to outside of the bag, and instruments were padded with foam to reduce vibrations. The bag was carried on the researcher's lap when riding the bus and taking measurements. The seats on the buses were chosen based on availability, and no specific bus model was prioritised. The bus windows were opened/closed according to the passengers' discretion, but due to the warm weather they were usually kept open. The ventilation settings on the buses were not controlled and whether any ventilation settings were used is unknown.

Exact times were noted for each time the bus route started and ended, each time the bus stopped at a bus stop and a stop light, and each time there was a unique traffic occurrence. After collecting data, the researcher returned to the starting point and

immediately downloaded the data off the instruments. Data was downloaded to a computer as well as an additional copy on Google Drive.

3.5 Analysis Software

3.5.1 MATLAB

MATLAB version R2016b was used for data cleaning and analysis. MATLAB is a programming language that is used to manipulate arrays and matrices of data. Each instrument yielded individual data files which needed to be consolidated with the geolocation data for subsequent mapping. This was done by using a MATLAB script that scanned the GPS, AE51, P-Trak, and DustTrak data files to find coincident time stamps. The GPS and particulate data were subsequently pooled together into their respective times, yielding georeferenced data matrices. Periods with intermittent GPS data due to poor signal reception were discarded. MATLAB was used to produce time series of the data.

3.5.2 ArcGIS

ArcMap is one of the software packages that is part of the ArcGIS Desktop. ArcMap 10.3.1 was used to create maps of the air pollution concentrations throughout the cities. ArcMap is a Geographic Information System (GIS) software that allows the user to display GIS data and manipulate it with different tools. The buffer tool found within ArcGIS was used to extract air pollution data from certain locations, namely bus stops and traffic lights, and the spatial join tool was used to match data points to buffer zones and polygons.

3.5.3 SigmaPlot

SigmaPlot 12 is a statistical software package that was used to conduct statistical analyses of the data. It was used to determine descriptive statistics, construct boxplots, and perform statistical significance testing.

3.6 Analysis Methods

3.6.1 Outlier Detection

Data were cleaned in MATLAB by qualitatively removing outliers. Often very high values were related to peaks observed in high pollution events and therefore a blanket outlier removal was not representative of the dataset. Instead, only outliers that were determined to be erroneous points were removed from the data. Data points were qualitatively determined to be outliers when their value was illogical and could not be attributed to any source other than instrumental error. Since the BC data were sampled at a 10-second logging interval, the $PM_{2.5}$ data were averaged in ten second intervals as well using MATLAB for comparison purposes. The UFP data were left at their 1-second logging interval.

3.6.2 Statistical Tests

Two different statistical tests were employed as part of the statistical tests between datasets. These tests were chosen by the program SigmaPlot as best-fitting for the dataset. For comparing two sets of data, the Mann-Whitney statistical test was used, described in Wijnand (2000). The Mann-Whitney statistical test is used for comparing two sets of nonparametric data and determining if either dataset originated from the same distribution. If the output determines that the null hypothesis is rejected, then the medians of the datasets are statistically significant. For comparing three or more datasets, the Kruskal-Wallis test was used. The Kruskal-Wallis test, described in Ramachandran and Tsokos (2015), was conducted on nonparametric datasets to determine whether the medians of the datasets were statistically significant. Further, Dunn's subtest was run for pairwise comparisons after the Kruskal-Wallis test. Dunn's subtest determines which events are contributing to the statistically significant difference determined from the Kruskal-Wallis test. Descriptive statistics were carried out in SigmaPlot and included: mean, median, standard deviation, and interquartile range (IQR).

3.6.3 Comparisons Between Cities

General descriptive statistics were run in SigmaPlot for each of the three pollutants each day of measurement, as well as for each pollutant within each city. Boxplots and statistical significance tests were composed in SigmaPlot to compare concentrations between cities. Time series were made for each day of measurements and separated by pollutant type in MATLAB. Bus stops and traffic lights, obtained from their times in the field notes, were marked on the time series to visualize the locations of these events. Maps were made in ArcMap for each day of measurements and separated by pollutant type. The routes were separated into polygons of 50 m lengths and the datasets were spatially joined to these polygons. The median value was displayed on the map for each 50 m interval. Locations of vehicle count data were also marked on these maps.

3.6.4 Hotspot and Spike Definition and Detection

A spike is defined as a sudden increase in concentration, approximately double the baseline value (Lim *et al.*, 2015). The identification of a pollution spike indicates a location where air pollution suddenly experienced a notable increase in concentration. Spikes can be identified by observation on time series plots. Finding the true definition of a "hotspot" is difficult as the term is often used colloquially in the field of air quality research without any clear definition provided. A hotspot is defined in this work as a location of highly elevated air pollution concentrations in comparison to the baseline concentrations and neighbouring air pollutant concentrations (Gately *et al.*, 2017). Hotspots are identified and isolated through observation of the air pollutant concentration maps.

3.6.5 Waiting vs. Riding

Using the recorded times from the field notes, the datasets were separated from when the measurements were taking place on the bus versus waiting for the bus in bus terminals and at bus stops. The Mann-Whitney statistical test was conducted to determine if there

was a statistical difference in the particle concentrations between riding the bus and waiting for the bus.

3.6.6 Bus Stop and Traffic Light Particle Concentrations

Google Maps was used to collect the GPS coordinates of each bus stop and traffic light along the bus routes. These coordinates were output as an Excel file and input into ArcMap. The buffer tool was used to draw a 50 m buffer zone around each GPS point, following the methods described in Lim *et al.* (2015). The air pollution datasets were then joined with the buffer zones. Data points that fell within the zone of the traffic lights and bus stops and were also during travel < 2 km/hr were output as separate files. Lim *et al.* (2015) assumed that travel under 2 km/hr would indicate the bus had stopped at the bus stop or traffic light. This assumption was followed for this work. Descriptive statistics were run in SigmaPlot on the datasets.

3.6.7 Particle Concentrations vs. Bus Speed

The $PM_{2.5}$, BC, and UFP concentrations were plotted against speed of the bus to verify if there was a correlation between particle concentrations and bus speed. The bus speeds were binned in segments of 5 km/hr up to 45 km/hr and the mean of each pollutant within these bins was calculated. The 0-5 km/hr bin was disregarded to account for measurements that were taken while waiting for the bus at bus stops and in terminals.

3.7 Ancillary Data

3.7.1 Traffic Volume Data

Traffic counts were available throughout each of the cities. The volumes of traffic flow within each city are important for analysis of pollution hot spots and sources on each measured bus route. The traffic counts for Londrina were collected by various members of Dr. Targino's research group at UTFPR between 2014 and 2016. Measurements were either taken during the 8:00 – 9:00 peak morning traffic flow, or the 16:00 – 17:00 peak

evening traffic flow. Manual counts were performed by recording traffic in two alternating 15-minute periods during the one-hour measurement period. Data was then multiplied by two to obtain a one-hour total vehicle count. The vehicles were counted by their vehicle type: car, motorcycle, bus, and truck (Targino *et al.*, 2016). Traffic points are representative of the total traffic volume on the street (including both directions of traffic) and can be seen below in Figure 3-8.

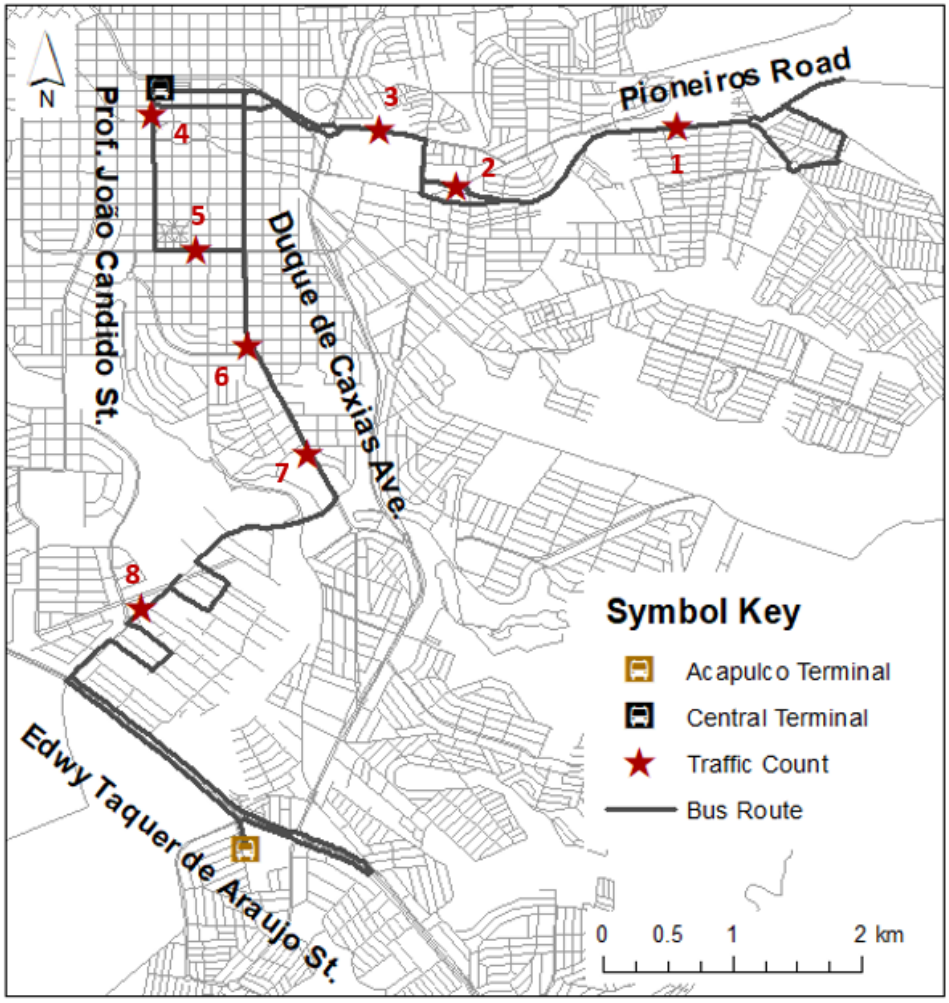

Figure 3-8: Londrina route map with locations of traffic count data.

The counts for cars, motorcycles and mopeds, buses, and trucks can be seen in Table 3-1. The largest count was located at Point 5 which is on Juscelino Kubitscheck Avenue, a main thoroughfare through the city of Londrina.

Table 3-1: Londrina traffic count data over a one-hour period during rush hour.

Traffic	Cars	Motorcycles	Buses	Trucks	Total (Vehicles/hr)
1	838	312	14	36	**1,200**
2	176	68	2	6	**252**
3	1176	314	12	40	**1,542**
4	550	98	346	16	**698**
5	2434	302	12	88	**2,836**
6	698	140	36	14	**888**
7	1362	226	82	30	**1,700**
8	558	72	4	22	**656**

Traffic count data for São Paulo was retrieved from the Traffic Engineering Company (CET) of São Paulo. Vehicle counts were taken over three hours, from 17:00 to 20:00 which encompassed the peak evening traffic flows. The available traffic counts can be seen on the measurement route in Figure 3-9. Five traffic counts are available spread out on the measured route.

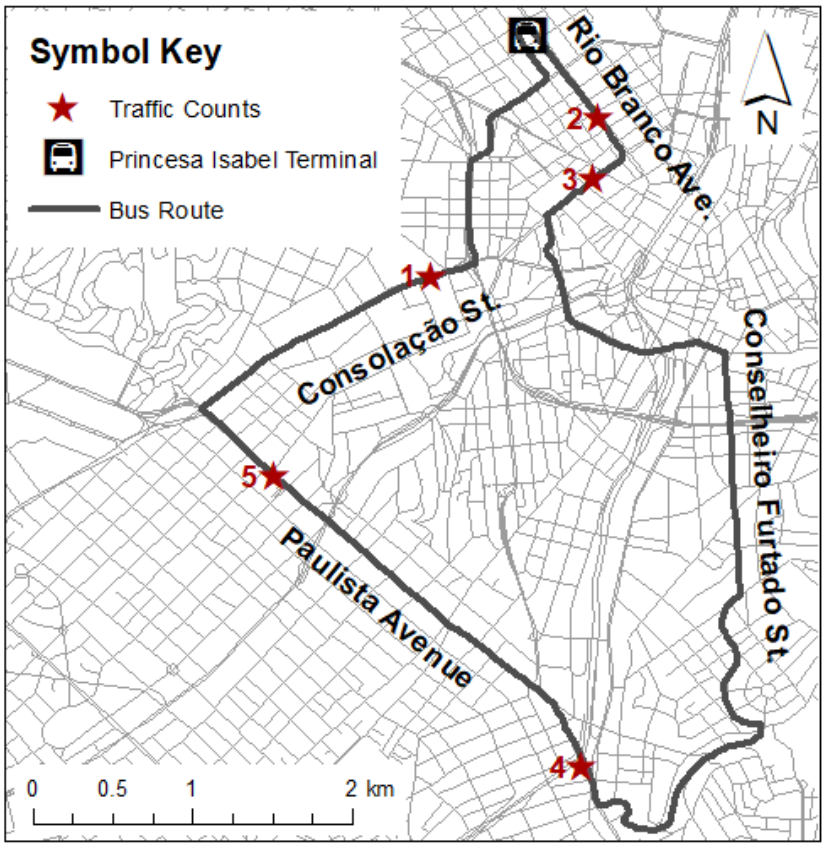

Figure 3-9: São Paulo route map with locations of traffic count data.

The traffic counts include data from cars, motorcycles and mopeds, buses, and trucks and include vehicles traveling in both directions in each road segment. These can be seen in Table 3-2 below. The roads Paulista Avenue and Consolação Street have the highest traffic counts within this dataset due to these being large thoroughfares through São Paulo. Paulista Avenue and Consolação Street consist of eight lanes of traffic, although along Consolação Street two lanes are for buses only. It should be noted as well that the traffic counts along Consolação Street have significantly more diesel fueled vehicles (buses and trucks) than on Paulista Avenue.

Table 3-2: São Paulo traffic count data over a three-hour period during evening rush hour.

Traffic	Cars	Motorcycles	Buses	Trucks	Total	Vehicles/hr
1	14,330	3,692	634	31	**18,687**	**6,229**
2	5,281	1,239	486	42	**7,048**	**2,349**
3	4,502	990	569	30	**6,091**	**2,030**
4	15,429	3,060	449	12	**18,950**	**6,317**
5	11,773	2,405	519	25	**14,722**	**4,907**

Traffic counts for Curitiba are conducted by the Institute of Research and Urban Planning of Curitiba (IPPUC). The measurement route in Curitiba was carried out in the downtown core of the city therefore many traffic counts were available. Traffic counts were taken in 2012 and collected for two hours during the evening peak traffic flows 17:00 to 19:00 (IPPUC, 2012). These traffic count points can be seen below in Figure 3-10.

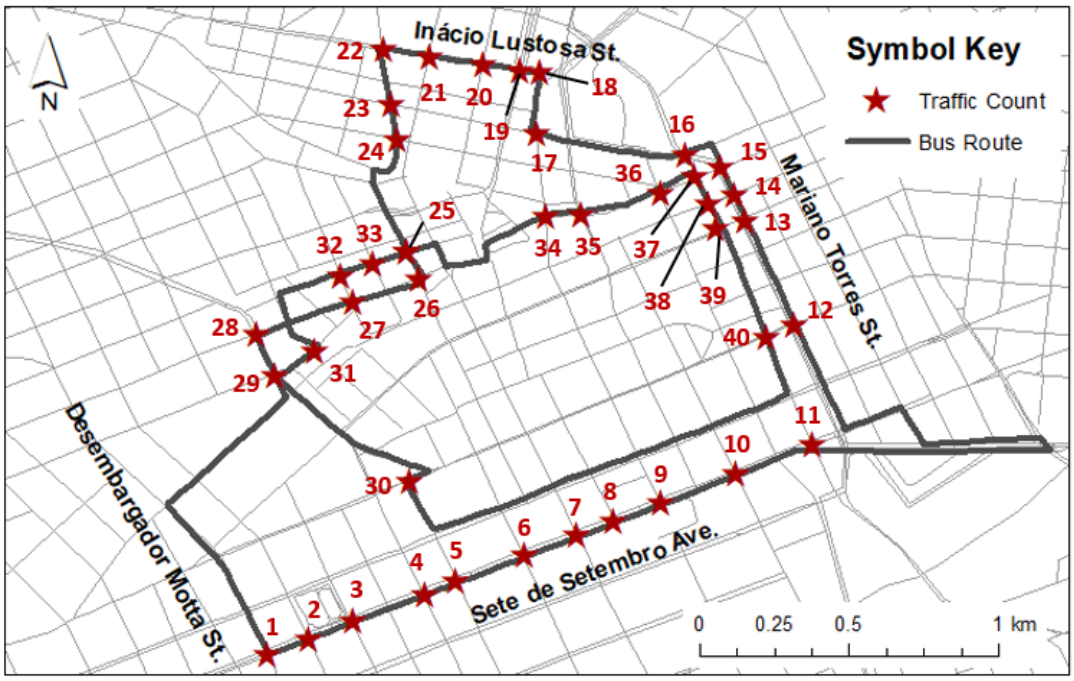

Figure 3-10: Curitiba route map with locations of traffic count data.

The traffic count data includes cars, motorcycles and mopeds, buses, trucks and bicyclists and can be seen in Table 3-3. The Curitiba counts are taken at intersections and include all the vehicles passing through each intersection during the counting period. The total counts include the bicycle values which, although do not contribute to the overall emissions, do give an idea of commuter traffic through each intersection. Point 16 stands out as having a significantly larger traffic flow than the other traffic points. This traffic point is located at an intersection with many different roads coming together.

Table 3-3: Curitiba traffic count data over a two-hour period in evening rush hour.

Traffic	Cars	Motorcycles	Buses	Trucks	Bicycles	Total	Vehicles/hr
1	2244	195	139	21	141	**2,740**	**1,370**
2	1505	150	141	5	122	**1,923**	**962**
3	3023	196	171	12	87	**3,489**	**1,745**
4	2879	163	169	16	61	**3,288**	**1,644**
5	2837	220	152	16	17	**3,242**	**1,621**
6	2820	388	156	29	20	**3,413**	**1,707**
7	2146	180	178	14	29	**2,547**	**1,274**
8	2490	218	266	16	131	**3,121**	**1,561**
9	2446	223	288	15	134	**3,106**	**1,553**
10	2605	257	173	12	87	**3,134**	**1,567**
11	2879	258	211	14	109	**3,471**	**1,736**
12	3969	517	151	44	81	**4,762**	**2,381**
13	2718	380	138	53	44	**3,333**	**1,667**
14	4626	582	261	47	79	**5,595**	**2,798**
15	2201	257	182	20	18	**2,678**	**1,339**
16	7995	-	311	29	-	**8,335**	**4,168**
17	3838	344	77	44	24	**4,327**	**2,164**
18	1378	145	109	17	6	**1,655**	**828**
19	2385	-	33	16	-	**2,434**	**1,217**
20	4090	266	40	28	12	**4,436**	**2,218**
21	2730	155	74	16	10	**2,985**	**1,493**
22	4827	317	83	26	7	**5,260**	**2,630**
23	2018	151	7	19	41	**2,236**	**1,118**
24	2547	273	29	30	3	**2,882**	**1,441**
25	2800	397	107	34	9	**3,347**	**1,674**
26	2921	380	84	49	16	**3,450**	**1,725**
27	2038	209	69	9	14	**2,339**	**1,170**
28	2820	477	58	0	6	**3,361**	**1,681**
29	3857	430	42	4	49	**4,382**	**2,191**
30	3106	458	53	13	5	**3,635**	**1,818**
31	1640	169	41	8	7	**1,865**	**933**
32	562	70	2	0	1	**635**	**318**
33	768	47	3	4	0	**822**	**411**
34	1343	180	32	23	17	**1,595**	**798**
35	1326	153	213	7	91	**1,790**	**895**
36	3351	-	161	17	-	**3,529**	**1,765**
37	2876	-	146	22	-	**2,044**	**1,022**
38	3311	-	199	22	-	**3,532**	**1,766**
39	2277	256	34	7	1	**2,575**	**1,288**
40	2853	350	141	19	6	**3,369**	**1,685**

3.7.2 Meteorological Data

Meteorology data was available for Curitiba and São Paulo. Precipitation was not observed on the days investigated in this study, therefore pollution washout was never of concern. São Paulo meteorological conditions can be seen below in Table 3-4. Data was available from the Environmental Company of the State of São Paulo (CETESB) and includes 24-hour averages (CETESB, 2018). The station Pinheiros (-23.56159, -46.70117) was chosen from the weather stations available due to its proximity to the measurement route. Atmospheric pressure data was unavailable for this station, however other stations in the municipality reported a value of approximately 930 millibars, the atmospheric pressure did not fluctuate during the measurement period. Temperature data was unavailable on June 29th from the Pinheiros station; An average value from another available station was included for this value instead.

Table 3-4: Meteorological data from São Paulo during data collection.

	June 27	**June 28**	**June 29**	**June 30**
Temperature	16.3 °C	17.2 °C	16.4 °C	19.1 °C
Relative Humidity	75 %	72 %	72 %	69 %
Wind Speed	1.2 m/s	1.0 m/s	0.87 m/s	0.74 m/s
Wind Direction	ESE	E	SE	SE

The primary wind direction for this weather station, as shown from the wind rose in Figure 3-11, is the northeast direction. The data for this wind rose were from the four-day measurement period. It should also be noted that although the 24-hour average wind directions show southeast and east directions, the wind during the sampling was a northeast wind for each day of collection.

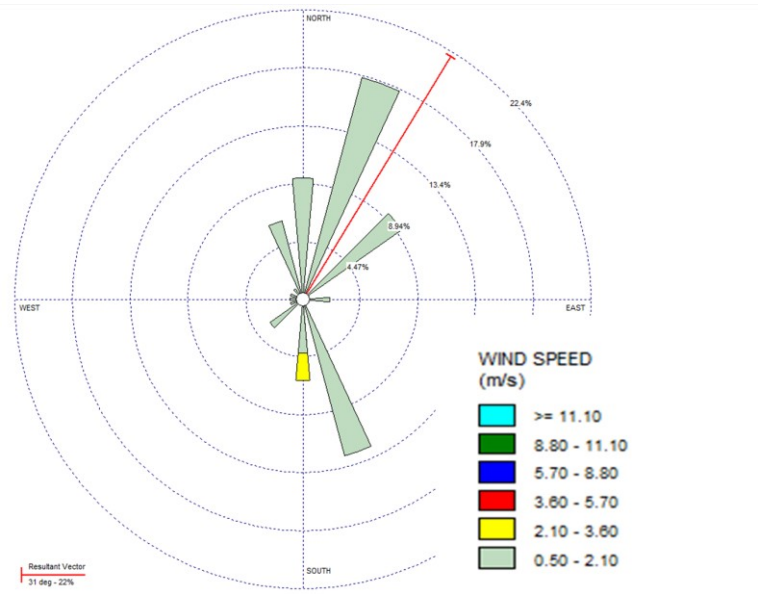

Figure 3-11: Wind rose of São Paulo data during measurement period.

Meteorological data for the Curitiba weather station (-25.44817, -49.23033) can be seen below in Table 3-5. 24-hour averages of the data are included over the measurement campaign. Data were retrieved from the Meteorological System of Parana (SIMEPAR) an online database with weather data for various stations across Parana State (SIMEPAR, 2018). The 24-hour average wind directions are accurate for the wind direction during the sampling, with the exception of July 26th where during the sampling the wind direction was approximately 330 ° (NNW).

Table 3-5: Meteorological data from Curitiba during data collection.

	July 25	July 26	July 27	July 28	July 29
Temperature	15.1 °C	17.5 °C	15.5 °C	9.9 °C	10.3 °C
Relative Humidity	74 %	65 %	53 %	81 %	86 %
Wind Speed	1.6 m/s	2.8 m/s	3.4 m/s	2.2 m/s	2.3 m/s
Wind Direction	63.3 ° (ENE)	179.2 ° (S)	242.4 ° (WSW)	79.5 ° (E)	72.4 ° (ENE)
Atmospheric Pressure	916	912	913	917	918

A wind rose from Curitiba during the measurements can be seen in Figure 3-12. The primary wind direction can be observed from the resultant vector as northeast.

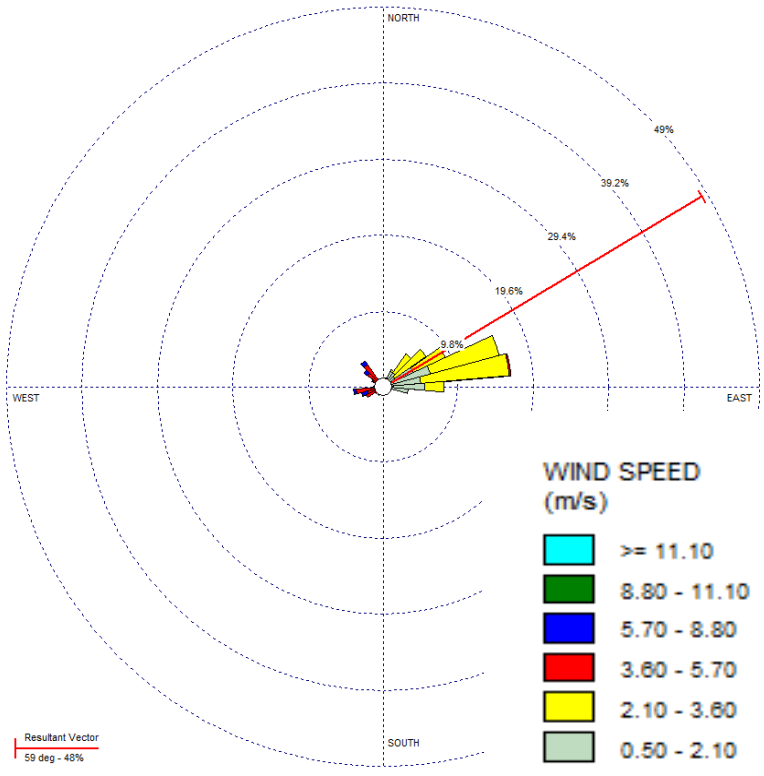

Figure 3-12: Wind rose of Curitiba during measurement period.

Chapter 4 Results and Discussion

4.1 Comparisons Between Cities

Descriptive statistics for each day of measurement are included in the section below for $PM_{2.5}$, BC, and UFP. These statistics include the number of data values (n), mean, standard deviation, median, 95th percentile, 5th percentile, and interquartile range (IQR). The IQR is the range between the 1st and 3rd quartiles of the dataset and is a similar metric to standard deviation for nonparametric statistics. Both mean and median are included for comparison to other studies. Often the mean value is reported despite the data having a nonparametric distribution. The Kruskal-Wallis test, with Dunn's sub-test, was used to determine if there was a significant difference ($\alpha = 0.05$) for each pollutant between the measurement days. The difference in medians was determined to be statistically significant ($p < 0.001$) for all data unless otherwise specified below.

4.1.1 Londrina

Descriptive statistics of $PM_{2.5}$ concentrations for each day of measurement in Londrina can be seen below in Table 4-1. From Dunn's sub-test $p < 0.05$ for all data pairs except between June 23rd and June 24th. The concentrations observed on June 20th are significantly higher (median 25.2 $\mu g/m^3$) compared to the remaining days of measurement. Without meteorological data available for Londrina, it is difficult to say if wind direction was a factor for this higher value.

Table 4-1: Descriptive statistics comparing $PM_{2.5}$ concentrations over five days in Londrina.

	June 20	June 21	June 22	June 23	June 24
n	857	866	867	876	876
Mean (µg/m^3)	27.5	5.59	12.4	14.6	15.8
Standard deviation (µg/m^3)	12.1	2.43	15.6	5.8	8.5
Median (µg/m^3)	25.2	5.4	9.7	13.9	13.7
95th Percentile (µg/m^3)	45.7	8.0	19.7	22.6	27.1
5th Percentile (µg/m^3)	16.5	1.5	3.9	7.1	10.2
IQR (µg/m^3)	9.9	2.7	4.9	6.4	5.4

Descriptive statistics of BC concentrations for each day of measurement in Londrina are presented in Table 4-2. From Dunn's sub-test $p < 0.05$ for all data pairs except between June 23rd and June 24th. Much like with the $PM_{2.5}$ concentrations, the June 20th BC concentrations are much higher than the remaining days of measurement.

Table 4-2: Descriptive statistics comparing BC concentrations over five days in Londrina.

	June 20	June 21	June 22	June 23	June 24
n	856	866	867	876	876
Mean (µg/m^3)	10.02	3.27	7.27	5.35	4.81
Standard deviation (µg/m^3)	12.96	5.31	21.54	6.75	4.77
Median (µg/m^3)	5.73	2.35	3.58	3.46	3.47
95th Percentile (µg/m^3)	35.08	9.70	15.74	16.23	14.19
5th Percentile (µg/m^3)	1.75	0.16	0.48	0.85	0.55
IQR (µg/m^3)	7.80	3.22	4.71	4.03	4.26

Descriptive statistics of UFP concentrations for each day of measurement in Londrina are below in Table 4-3. From Dunn's sub-test $p < 0.05$ for all data pairs except between June 22nd and June 23rd. The median concentration on June 20th can also be observed as much higher than the other medians throughout the measurement days. Despite June 20th having the highest median, it does not have the highest 95th percentile value indicating that baseline values were larger on June 20th, possibly from influences not related to traffic emissions.

Table 4-3: Descriptive statistics comparing UFP concentrations over five days in Londrina.

	June 20	**June 21**	**June 22**	**June 23**	**June 24**
n	8203	8884	8741	8788	8807
Mean (#/cm^3)	24,475	16,718	24,616	22,326	16,499
Standard deviation (#/cm^3)	18,766	11,958	26,704	23,084	15,896
Median (#/cm^3)	19,200	14,700	15,700	15,600	10,900
95th Percentile (#/cm^3)	57,740	38,500	80,650	61,915	44,120
5th Percentile (#/cm^3)	5,750	1,370	3,145	3,300	2,408
IQR (#/cm^3)	24,300	10,600	21,325	15,618	16,510

June 20th concentrations stand out across all pollutants in Londrina compared to the other days. On June 20th, the 5th percentile concentrations were also significantly higher than the other days indicating that background pollution concentrations in Londrina were elevated. The time series below shows that the baseline is elevated on this day and no particular event is contributing to the higher median values. It is possible that air pollution was being influenced by other factors on June 20th apart from vehicle emissions. Targino and Krecl (2016) analysed sources of BC concentrations in Londrina. They concluded that BC concentrations are highly variable due to local waste burning,

which may be contributing to the elevated concentrations observed here on June 20th. The smell of smoke was noted in the field notes on this day.

4.1.2 São Paulo

Descriptive statistics for the $PM_{2.5}$ concentrations in São Paulo can be seen below in Table 4-4. Concentrations on June 28th and June 29th were notably higher than the other days of measurement with median values of 35.5 µg/m^3 and 32.6 µg/m^3, respectively.

Table 4-4: Descriptive statistics comparing $PM_{2.5}$ concentrations over four days in São Paulo.

	June 27	**June 28**	**June 29**	**June 30**
n	349	765	741	694
Mean (µg/m^3)	27.0	37.5	35.5	21.2
Standard deviation (µg/m^3)	7.5	12.1	11.4	7.9
Median (µg/m^3)	25.0	35.5	32.6	19.3
95th Percentile (µg/m^3)	41.2	55.2	57.3	33.0
5th Percentile (µg/m^3)	19.7	22.3	19.2	12.6
IQR (µg/m^3)	8.7	12.1	14.0	7.2

Descriptive statistics for BC concentrations in São Paulo are shown in Table 4-5. From Dunn's sub-test $p < 0.05$ for all data pairs except between June 29th and June 30th. Median values were fairly similar across all days of measurement, ranging from 7 – 10 µg/m^3. Concentrations on June 28th and June 29th were slightly elevated compared to the other days, but not to the same proportion as the $PM_{2.5}$ concentrations on those days.

Table 4-5: Descriptive statistics comparing BC concentrations over four days in São Paulo.

	June 27	**June 28**	**June 29**	**June 30**
n	349	765	741	694
Mean (µg/m^3)	9.47	10.63	12.49	9.47
Standard deviation (µg/m^3)	6.83	12.18	9.92	6.79
Median (µg/m^3)	7.08	8.10	9.78	7.36
95th Percentile (µg/m^3)	24.95	23.95	31.11	22.33
5th Percentile (µg/m^3)	2.57	3.36	3.50	3.43
IQR (µg/m^3)	7.33	6.82	10.44	5.54

Descriptive statistics of UFP concentrations in São Paulo can be seen in Table 4-6. From Dunn's sub-test $p < 0.05$ for all data pairs except between June 27th and June 30th. Median values were elevated on June 28th and June 29th as well, 42,000 particles/cm^3 and 39,900 particles/cm^3.

Table 4-6: Descriptive statistics comparing UFP concentrations over four days in São Paulo.

	June 27	**June 28**	**June 29**	**June 30**
n	4942	7127	7382	6879
Mean (#/cm^3)	38,947	47,940	47,969	39,717
Standard deviation (#/cm^3)	23,654	28,162	31,901	22,046
Median (#/cm^3)	31,600	42,200	39,900	32,700
95th Percentile (#/cm^3)	76,745	96,800	101,000	84,560
5th Percentile (#/cm^3)	9,980	13,500	14,200	20,800
IQR (#/cm^3)	26,400	28,100	28,625	17,500

The larger increases on June 28th and June 29th are associated with all pollutants, however larger differences were observed in the $PM_{2.5}$ and UFP values. Where the meteorological conditions showed no large differences across the days, it is possible that these increased concentrations are from increased emissions and traffic encountered during sampling.

4.1.3 Curitiba

Descriptive statistics for $PM_{2.5}$ concentrations in Curitiba can be seen in Table 4-7. From Dunn's sub-test $p < 0.05$ for all data pairs except between July 26th and July 27th. The median values of July 25th and July 28th stand out as much higher when compared to the other measurement days, 17.3 µg/m^3 and 15.6 µg/m^3, respectively. The wind speeds on these two days were the lowest of the measured days. It is possible that low wind was reducing the ventilation of $PM_{2.5}$ from the streets and contributing to the higher concentrations on these days.

Table 4-7: Descriptive statistics comparing $PM_{2.5}$ concentrations over five days in Curitiba.

	July 25	**July 26**	**July 27**	**July 28**	**July 29**
n	517	555	683	574	833
Mean (µg/m^3)	20.4	10.9	11.3	15.6	12.3
Standard deviation (µg/m^3)	12.6	5.7	5.9	5.4	5.1
Median (µg/m^3)	17.3	10.3	10.5	15.6	10.9
95th Percentile (µg/m^3)	48.0	15.5	19.1	23.9	18.7
5th Percentile (µg/m^3)	12.0	7.4	4.4	7.8	8.9
IQR (µg/m^3)	7.2	3.4	4.4	6.9	2.8

Descriptive statistics of BC concentrations in Curitiba are shown in Table 4-8. The median concentrations on July 26th were particularly low when compared to the other measurement days. The wind direction during this sampling was blowing from the NNW which was different from the other days of measurement. Additionally, the wind velocity was in the range of 4-6 m/s during the measurements which would have promoted ventilation of pollutants from the street. This may account for the lower concentrations of pollution observed that day due to increased ventilation.

Table 4-8: Descriptive statistics comparing BC concentrations over five days in Curitiba.

	July 25	**July 26**	**July 27**	**July 28**	**July 29**
n	517	555	683	574	833
Mean (µg/m^3)	10.49	3.09	3.85	8.98	5.19
Standard deviation (µg/m^3)	18.31	6.80	3.39	7.54	6.46
Median (µg/m^3)	4.71	1.97	3.15	6.24	3.26
95th Percentile (µg/m^3)	41.82	6.98	9.47	23.05	12.52
5th Percentile (µg/m^3)	1.46	0.78	0.79	1.05	1.27
IQR (µg/m^3)	6.99	2.59	2.21	7.24	3.20

Descriptive statistics for the UFP concentrations in Curitiba are in Table 4-9. From Dunn's sub-test $p < 0.05$ for all data pairs except between July 28th and July 29th. The UFP concentrations on July 26th are also much lower when compared to the other days of measurement which could be as a result of the increased wind speed promoting ventilation of UFP as well.

Table 4-9: Descriptive statistics comparing UFP concentrations over five days in Curitiba.

	July 25	**July 26**	**July 27**	**July 28**	**July 29**
n	5567	5485	6793	5749	8335
Mean (#/cm^3)	25,676	19,744	27,899	28,643	28,663
Standard deviation (#/cm^3)	29,823	23,293	15,395	20,125	15,886
Median (#/cm^3)	17,800	12,700	24,000	26,300	25,100
95th Percentile (#/cm^3)	80,360	54,520	59,180	52,110	50,700
5th Percentile (#/cm^3)	7,180	6,070	11,500	7,869	10,220
IQR (#/cm^3)	12,500	12,500	13,100	14,500	13,300

Wind speeds on July 26th and July 27th were stronger than the other days of measurement, as well as from different directions which may have been facilitating better ventilation of air pollution. Lower concentrations were observed on these days for $PM_{2.5}$, however UFP and BC concentrations were only considerably lower on July 26th. Yang *et al.* (2015) observed that BC and UFP had very similar profiles when measured on diesel buses, however, $PM_{2.5}$ concentrations varied because of the mixed local and long-range sources of this metric. Since BC and UFP are both tracers for diesel emissions, Yang *et al.* (2015) suggest that self-pollution from the bus itself may be the cause of this phenomenon which explains why the UFP and BC follow similar pollution profiles.

4.1.4 Overall Cities Comparison

Mean, standard deviation, median, and IQR are included in the tables of descriptive statistics below for each city. The Kruskal-Wallis test, with Dunn's sub-test, was used to determine if there was a significant difference ($\alpha = 0.05$) for the data between the three cities. The difference in medians was determined to be statistically significant ($p < 0.001$) for all pollutants. From Dunn's sub-test, $p < 0.05$ for all data pairs. A box-plot showing the pollutant concentrations is shown in Figure 4-1. The box shows the interquartile range

of the distribution, with the centreline representing the median. The whiskers extend from the 5th to the 95th percentiles with black dots showing the extreme values. This box-plot shows that Londrina consistently had lower pollutant concentrations. São Paulo however, had much higher concentrations across all pollutants which was expected from the much higher-trafficked roads in comparison to Curitiba and Londrina.

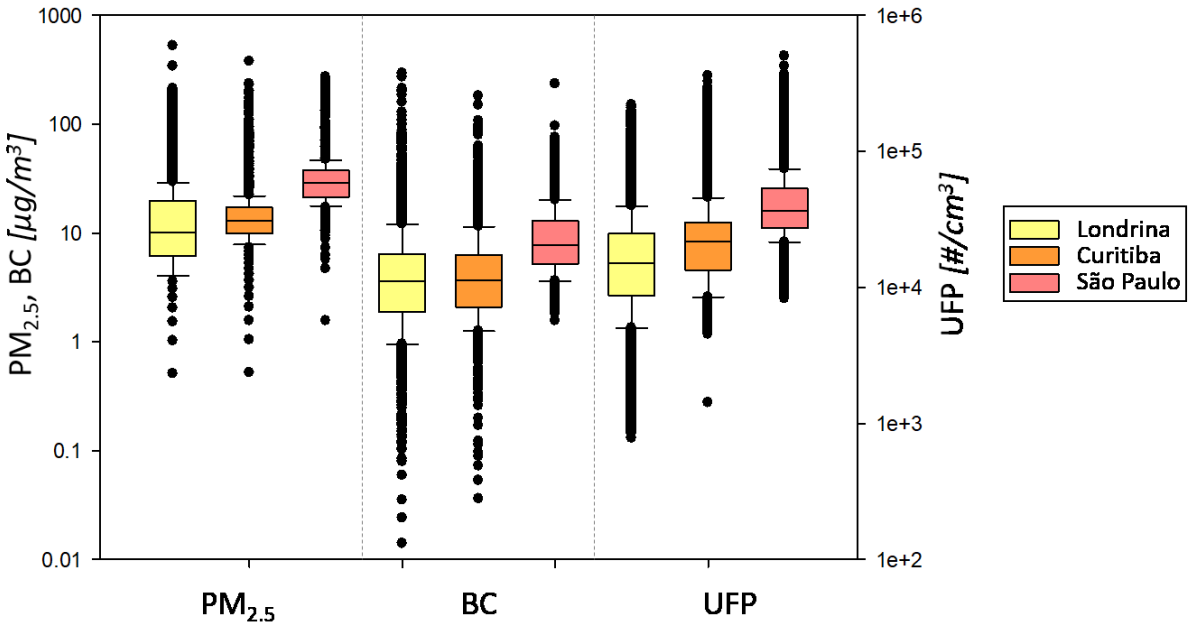

Figure 4-1: Box-plot of pollutant comparison between cities.

The overall $PM_{2.5}$ concentrations between the three cities can be seen compared below in Table 4-10. From the median values, it can be observed that São Paulo had the highest concentrations of the three cities with a median of 29.1 µg/m^3. The median $PM_{2.5}$ concentration of Curitiba (13.0 µg/m^3) was only slightly higher than the $PM_{2.5}$ median value of Londrina (10.2 µg/m^3). The high standard deviations and IQRs can also be attributed to a large range in values across the concentration distribution within each city.

Table 4-10: Descriptive statistics comparing $PM_{2.5}$ concentrations in São Paulo, Curitiba, and Londrina.

	Mean	Standard Deviation	Median	IQR
Londrina	14.7 μg/m^3	14.7 μg/m^3	10.2 μg/m^3	13.7 μg/m^3
São Paulo	31.0 μg/m^3	13.2 μg/m^3	29.1 μg/m^3	16.1 μg/m^3
Curitiba	14.6 μg/m^3	8.9 μg/m^3	13.0 μg/m^3	7.3 μg/m^3

In Table 4-11, the descriptive statistics for BC measurements between the three cities can be seen. Much like with $PM_{2.5}$, the median BC concentrations between Curitiba and Londrina are very similar and only differ by 0.5 μg/m^3.

Table 4-11: Descriptive statistics comparing BC concentrations in São Paulo, Curitiba, and Londrina.

	Mean	Standard Deviation	Median	IQR
Londrina	6.46 μg/m^3	13.70 μg/m^3	3.58 μg/m^3	4.57 μg/m^3
São Paulo	10.53 μg/m^3	9.54 μg/m^3	7.73 μg/m^3	7.78 μg/m^3
Curitiba	6.01 μg/m^3	9.52 μg/m^3	3.63 μg/m^3	4.19 μg/m^3

The UFP descriptive statistics for the three cities can be seen below in Table 4-12. For the UFP concentrations, the medians between all three cities are very different with Londrina having the lowest concentration and São Paulo having the highest.

Table 4-12: Descriptive statistics comparing UFP concentrations in São Paulo, Curitiba, and Londrina.

	Mean	Standard Deviation	Median	IQR
Londrina	19,918 #/cm^3	18,195 #/cm^3	15,000 #/cm^3	19,640 #/cm^3
São Paulo	44,112 #/cm^3	27,388 #/cm^3	36,600 #/cm^3	26,400 #/cm^3
Curitiba	26,051 #/cm^3	22,453 #/cm^3	21,700 #/cm^3	16,700 #/cm^3

4.1.5 Comparison to Other Cities

Results from previous studies investigating exposure to $PM_{2.5}$, BC, and UFP on buses are outlined in Table 4-13,Table 4-14, and Table 4-15 below. These studies are used to compare the results in our study to other examples globally. Many studies report their findings as mean values despite having non-normal distributions, therefore the mean from our experiment is used here for comparison purposes as well.

Targino *et al.* (2018) quantified the mean concentration of BC in Londrina, Brazil as 9.6 μg/m^3. This value is higher than the mean concentration observed in our measurements of Londrina. However, Targino *et al.* (2018) note that the concentrations in the low-traffic regions of their measurements were lower with a mean of 4.7 μg/m^3. Different bus routes were measured in their study as well which could result in the variation between studies. Additionally, measurements were completed in a different season and seasonal effects were not investigated in either study. Other studies are not available for comparison in São Paulo or Curitiba.

Table 4-13: $PM_{2.5}$ concentrations from other bus passenger exposure studies.

Author	Location	Mean Exposure (µg/m^3)
Adams *et al.* (2001)	London, UK	39
Chan *et al.* (2002a)	Hong Kong	Non-Air Conditioned: 93 Air Conditioned: 51
Chan *et al.* (2002b)	Guangzhou, China	Non-Air Conditioned: 145 Air Conditioned: 106
Gomez-Perales *et al.* (2004)	Mexico City, Mexico	71
Kaur *et al.* (2005)	London, UK	35
Knibbs and de Dear (2010)	Sydney, Australia	33.4
Huang *et al.* (2012)	Beijing, China	42.4
Kongtip *et al.* (2012)	Bangkok, Thailand	Non-Air Conditioned: 323.8 Air-Conditioned: 206.5
de Nazelle *et al.* (2012)	Barcelona, Spain	25.9
Both *et al.* (2013)	Jakarta, Indonesia	117
Nyhan *et al.* (2014)	Dublin, Ireland	21.4
Suárez *et al.* (2014)	Santiago, Chile	60.4
Yan *et al.* (2015)	Beijing, China	26.7
Betancourt *et al.* (2017)	Bogotá, Colombia	186
Ham *et al.* (2017)	Sacramento, California	7.5
Okokon *et al.* (2017)	Helsinki, Finland	29
	Rotterdam, Netherlands	21
	Thessaloniki, Greece	85
Qiu *et al.* (2017)	Xi'an, China	Air Conditioned: 54.4 Open Windows: 58.6
This Study	Londrina, Brazil	14.7
	Curitiba, Brazil	14.6
	São Paulo, Brazil	31.0

Table 4-14: BC concentrations from other bus passenger exposure studies.

Author	Location	Mean Exposure (µg/m^3)
Zhang and Zhu (2010)	Beeville, Texas	2.9
Zuurbier *et al.* (2010)	Arnhem, Netherlands	9.0
de Nazelle *et al.* (2012)	Barcelona, Spain	7.6
Vouitsis *et al.* (2014)	Thessaloniki, Greece	7.4
Li *et al.* (2015)	Shanghai, China	7.3
Moreno *et al.* (2015)	Barcelona, Spain	5.5
Yang *et al.* (2015)	Hong Kong	11.6
Williams and Knibbs (2016)	Brisbane, Australia	2.4
Betancourt *et al.* (2017)	Bogotá, Colombia	120
Ham *et al.* (2017)	Sacramento, California	0.95
Okokon *et al.* (2017)	Helsinki, Finland	4.6
	Rotterdam, Netherlands	4.3
	Thessaloniki, Greece	8.5
Rivas *et al.* (2017)	London, UK	5.4
Targino *et al.* (2018)	Londrina, Brazil	9.6
This Study	Londrina, Brazil	6.46
	Curitiba, Brazil	7.63
	São Paulo, Brazil	10.53

Different factors can largely affect the concentrations that are observed in each city including population, bus fleet characteristics, and street configuration. Two other cities in South America have been investigated for their bus passenger exposure to air pollution. Suárez *et al.* (2014) measured $PM_{2.5}$ and UFP on buses in Santiago Chile. Santiago has a population of over 6 million people, a bus fleet of 6,180 diesel buses, and a private vehicle fleet of approximately 1.6 million vehicles. It is located between mountain ranges which inhibits ventilation of the city and contributes to air pollution events. The route was selected due to its high volume of traffic and variation of commuter modes available, and measurements were carried out during morning rush hour. The temperature during measurements ranged from 0 to 10 °C. The exposure concentrations on buses were above those measured at a background site. It was determined that traffic impacts contributed 15 µg/m^3 to the $PM_{2.5}$ in personal exposure

measurements and 30,100 particles/cm^3 for UFP measurements on buses (Suárez *et al.*, 2014). The concentrations observed in Santiago were significantly higher than those observed in this study. Measurements in Santiago were completed during rush hour which would contribute to elevated concentrations due to higher traffic presence on the streets. Additionally, morning measurements can have higher emissions concentrations due to vehicle engines producing more emissions in colder temperatures, typical of early mornings (Gómez-Perales *et al.*, 2007).

Table 4-15: UFP concentrations from other bus passenger exposure studies.

Author	**Location**	**Mean Exposure (particles/cm^3)**
Weichenthal *et al.* (2008)	Montreal, Canada	25,300
Cattaneo *et al.* (2009)	Milan, Italy	117,600
Knibbs and de Dear (2010)	Sydney, Australia	105,000
Zuurbier *et al.* (2010)	Arnhem, Netherlands	36,000
de Nazelle *et al.* (2012)	Barcelona, Spain	55,200
Both *et al.* (2013)	Jakarta, Indonesia	401,000
Ragletti *et al.* (2013)	Basel, Switzerland	14,055
Suárez *et al.* (2014)	Santiago, Chile	70,900
Yan *et al.* (2015)	Beijing, China	Non-Air Conditioned: 8,615 Air Conditioned: 21,806
Betancourt *et al.* (2017)	Bogotá, Colombia	197,000
Grana *et al.* (2017)	Rome, Italy	29,299
Ham *et al.* (2017)	Sacramento, California	13,000
Okokon *et al.* (2017)	Helsinki, Finland	15,000
	Rotterdam, Netherlands	18,000
	Thessaloniki, Greece	50,000
This Study	Londrina, Brazil	19,918
	Curitiba, Brazil	26,057
	São Paulo, Brazil	44,112

Betancourt *et al.* (2017) measured $PM_{2.5}$, BC, and UFP on board buses in Bogotá, Colombia. Bogotá is located on a plateau in the Andes Mountains and has a population of approximately 8 million people. The passenger vehicle fleet consists of approximately 1.4 million cars (Fajardo & Rojas, 2012). Bogotá has both bus rapid transit (BRT) infrastructure as well as traditional bus infrastructure. BRT consists of bus only lanes throughout the city. The values reported above were the highest observed in the study from the three bus routes investigated and came from the BRT route. This route also had significantly higher traffic flow along the road (7,152 vehicles/hour) than the other two bus routes (1,760 and 970 vehicles/hour) which likely contributed to the high concentrations that were observed. Measurements were also taken during morning rush hour. The concentrations pertaining to these three bus routes are summarized in Table 4-16 below. Despite Routes 2 and 3 having significantly lower vehicle counts than Route 1, the pollution concentrations are still quite high in comparison. This could be attributed to the street type where Route 1 is classified as 'Open' and increased ventilation would aid in the removal of pollutants from the roadway. The results from this study are also well above the concentrations observed in our results in Brazil.

Table 4-16: Results from different bus routes in Betancourt et al. (2017).

	Bus Route 1	**Bus Route 2**	**Bus Route 3**
Median $PM_{2.5}$ ($\mu g/m^3$)	118.3	92.9	88.8
Median BC ($\mu g/m^3$)	77.5	55.8	74.7
Median UFP (#/cm^3)	195,000	115,000	164,000
Street Type	Open	Intermediate	Street Canyon
Traffic Count (veh./hr)	7152	970	1760

In the context of the other studies listed above, the results obtained in this study fit well into other bus passenger exposure studies around the world. The $PM_{2.5}$ concentrations from our study are on the lower end of other studies. However, the BC concentrations

from our measurements are within and largely above results from other cities. This could be partially due to different regulations on diesel engine emissions in different countries resulting in higher BC output in Brazil where older diesel engines only meet EURO II and III emissions standards. The UFP results from our study can also be observed within the concentrations measured in other studies. It can be concluded that concentrations on buses are highly variable across different cities. The results from our study are well below those results from other cities in South America. Many factors influence concentrations on-board buses including traffic density, time of measurement, season of measurement, and background concentrations.

4.2 Daily Time Series

Time series for each city are analysed below. Bus stops are marked by the symbol 'X' where traffic lights are marked as the symbol 'O' along the $PM_{2.5}$ profile in each time series. Spikes in the time series can be seen to occur often after a bus stop. This is because as the bus stops, back and/or front doors on the bus open and can allow air pollutants to enter the passenger area within the bus.

4.2.1 Londrina

Figure 4-2 shows the time series on June 20th, 2016. It can be observed during the first bus terminal waiting period at approximately 10:10 that a sharp spike appears across the pollutants. This spike shows up distinctly in both the $PM_{2.5}$ and BC time series graphs. This is presumably because a bus was passing by at that time within the terminal since bus exhaust contains BC. It should also be noted that these spikes do not exhibit the same decay features as observed within bus cabins. Bus terminals are covered, but not protected from the outdoors and therefore air flow is present preventing the accumulation of pollutants as observed within the buses. There are two particularly notable spikes that occur around the same time as bus stops and traffic lights: one from 11:03 – 11:10 and another at 11:45-11:51. These are likely a result of doors opening on the bus and letting air pollution enter on board. Due to the spikes across all three air pollutants, self-pollution

from the bus exhaust fumes may be a contributing factor as well, particularly at the later spike since the bus would have been traveling along a low-trafficked road.

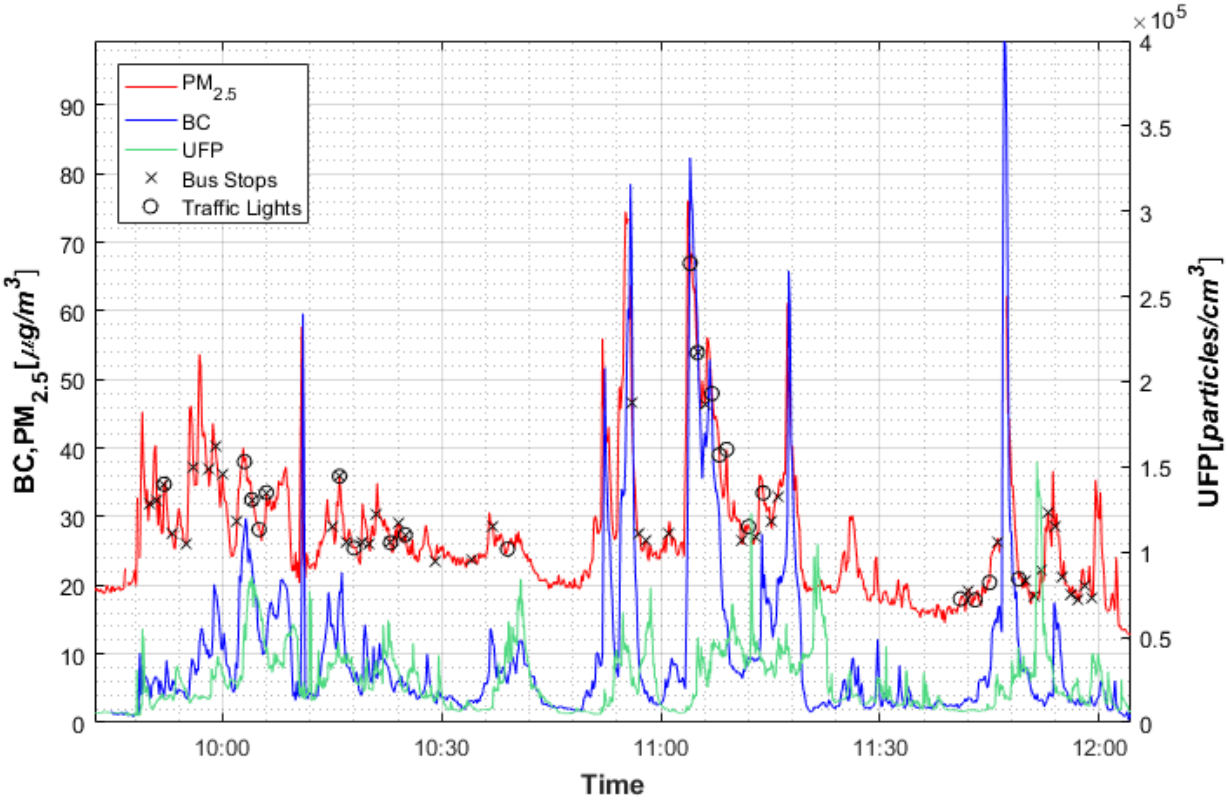

Figure 4-2: Time series in Londrina on June 20th, 2016.

The time series from June 21st, 2016 can be seen below in Figure 4-3. Baseline levels can be observed as significantly lower than the previous day for $PM_{2.5}$ and BC concentrations. There are many small peaks throughout the route that are prevalent across all three pollutants and occur simultaneously with bus stops and traffic lights. A large peak occurs in the dataset from 11:41 – 11:46 in the $PM_{2.5}$ and BC profiles that takes five minutes before the concentrations return to the baseline level. The UFP concentrations are elevated during this period as well, but not to the same extent (the BC concentrations more than quadrupled). There are several bus stops and traffic lights that occur at this

time which could be contributing to the slow decay this peak experienced, likely introducing more pollution to the bus cabin with each stop.

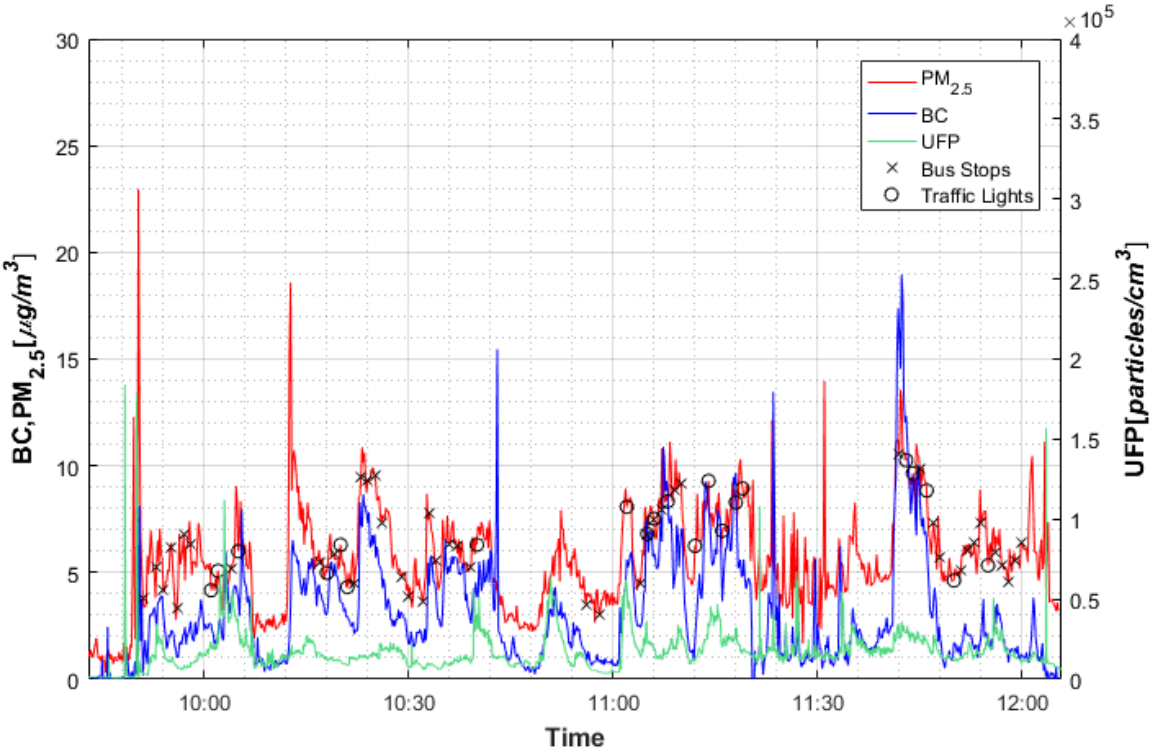

Figure 4-3: Time series in Londrina on June 21st, 2016.

Figure 4-4 below shows the time series from June 22nd, 2016. A very prominent spike in the data is present from 10:54 to 10:58. Due to the proximity of the bus stops to this spike, it is likely that the air pollution within the bus was a result of the doors opening at the bus stop and allowing PM air pollutants to enter within the bus. The very high BC concentration indicates that diesel emissions were possibly present as a result of self-pollution. The extremely high UFP spike at 11:20 occurred shortly after getting off the bus and may have been from the bus's own exhaust when walking nearby.

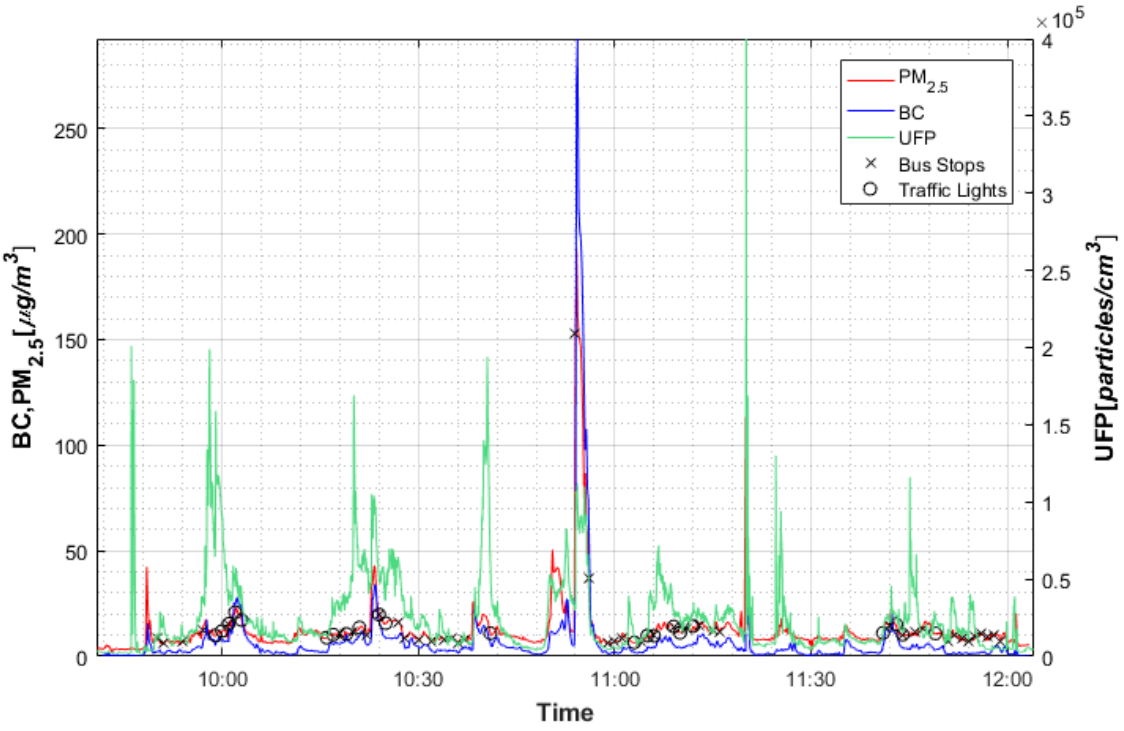

Figure 4-4: Time series in Londrina on June 22nd, 2016.

Figure 4-5 below shows the time series from June 23rd, 2016. High peaks in the data can be observed at approximately 10:10 when at the bus terminal. Much like above, there is no decay period after the spike due to the air circulation at the bus terminal. These UFP spikes are probably not caused by bus emissions since there is no peak present in either of the other pollutants. There is a high spike present across all three pollutants inside the bus from 11:00 to 11:10. Bus stops and traffic lights were present and therefore the high PM pollution levels may be entering the bus at these locations.

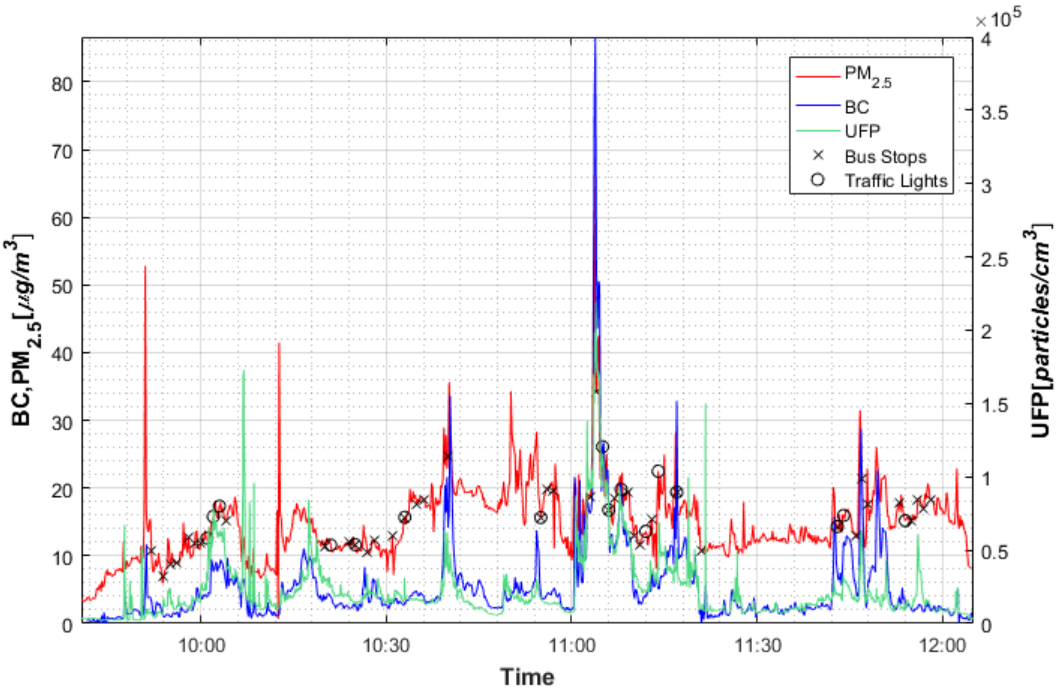

Figure 4-5: Time series in Londrina on June 23rd, 2016.

The final time series from Londrina is in Figure 4-6 below from June 24th, 2016. Higher sustained concentrations are observed for all pollutants from 10:00 to 10:08. The presence of traffic lights and bus stops may be letting pollutants into the bus that are accumulating in the cabin and contributing to the high concentrations. Another peak across all pollutants is observed from 10:54 to 10:57 and is in the presence of two bus stops which could be facilitating the entry of pollution into the bus cabin. There is a final large spike at 11:50 that is very high in the $PM_{2.5}$ profile but also noted in the BC which could be as a result of self-pollution at a bus stop. There are some large peaks at 12:00, however these are shortly after getting off the bus and would be a result of exposure to the bus's own exhaust after disembarking.

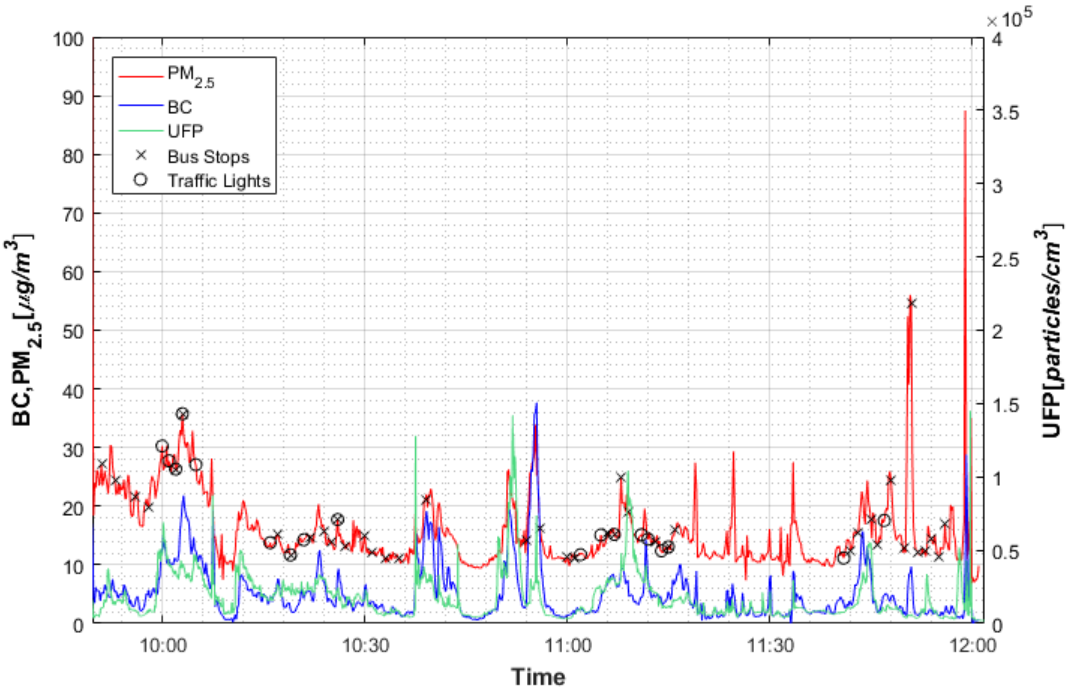

Figure 4-6: Time series in Londrina on June 24th, 2016.

4.2.2 São Paulo

The measurements in São Paulo were taken in the afternoon. Figure 4-7 below shows the temporal distribution of $PM_{2.5}$, BC, and UFP concentrations on June 27th, 2016. The DustTrak was having battery connectivity issues on this day and therefore the $PM_{2.5}$ distribution is incomplete. The measured route commenced at 14:06. There was a waiting period in the Princesa Isabel terminal from 14:26 – 14:42. Characteristic of Brazilian bus terminals, it was sheltered overtop but not completely enclosed in a building thus allowing ambient air to flow freely through the shelter. Some spikes can be noted in the BC and $PM_{2.5}$ distributions during this waiting period, likely from buses driving through the terminal where a BC spike is also present. The next bus was taken from 14:42 – 15:44. It was noted that there was a busy intersection at 15:00 and then a street canyon at 15:06, which may explain the spikes in the data at these times. Additionally, Paulista Avenue was entered at 15:28 until the end of the route which could account for the high spikes observed towards the end of the time series. Paulista Avenue has high traffic (4,907 – 6,317 vehicles/hour depending on the location along Paulista Avenue).

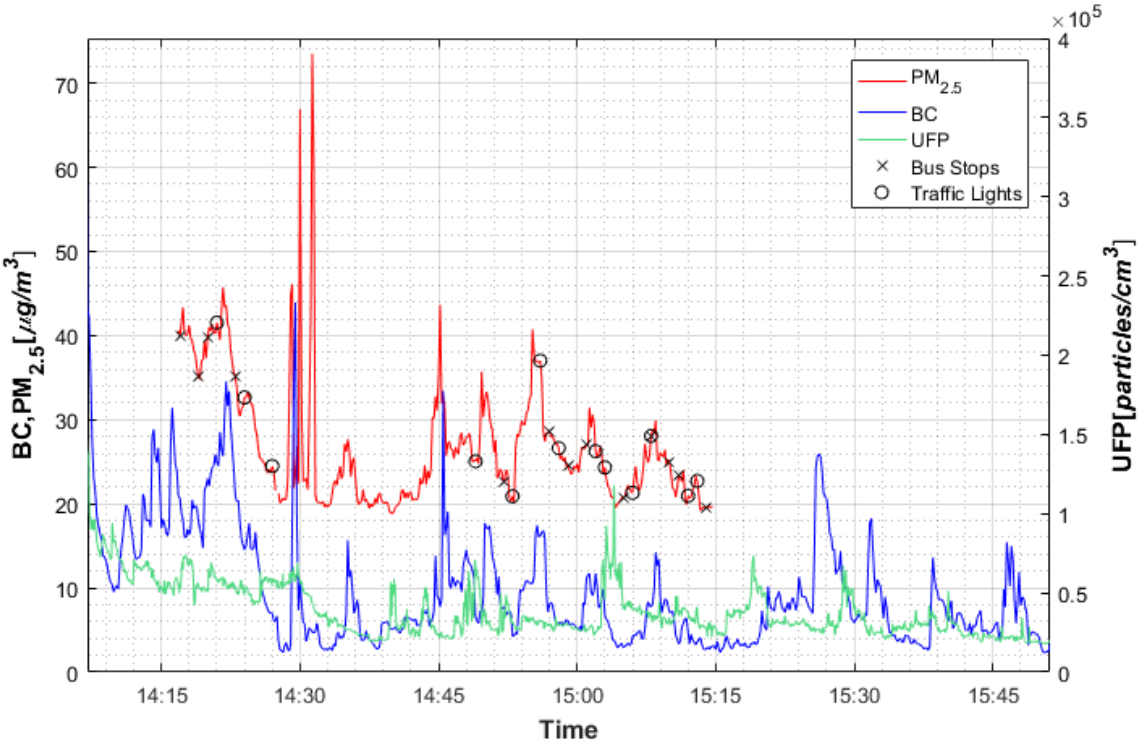

Figure 4-7: Time series in São Paulo on June 27th, 2016.

The time series for June 28th, 2016 is below in Figure 4-8. The baseline levels of all pollutants can be observed as much higher at the start of the measurements, then decreasing to a low during travel through a residential neighbourhood, and finally increasing again when returning to Paulista Avenue towards the end of measurements. There is a prominent spike from 14:20 to 14:28 across all pollutants, but most notably in the BC where concentrations increase by over 20 µg/m^3. The presence of bus stops and traffic lights through this period likely contributed to the drawn-out spike observed here. There is also a spike at the end of the time series, however, this was from disembarking the bus and being exposed to the bus's own exhaust emissions.

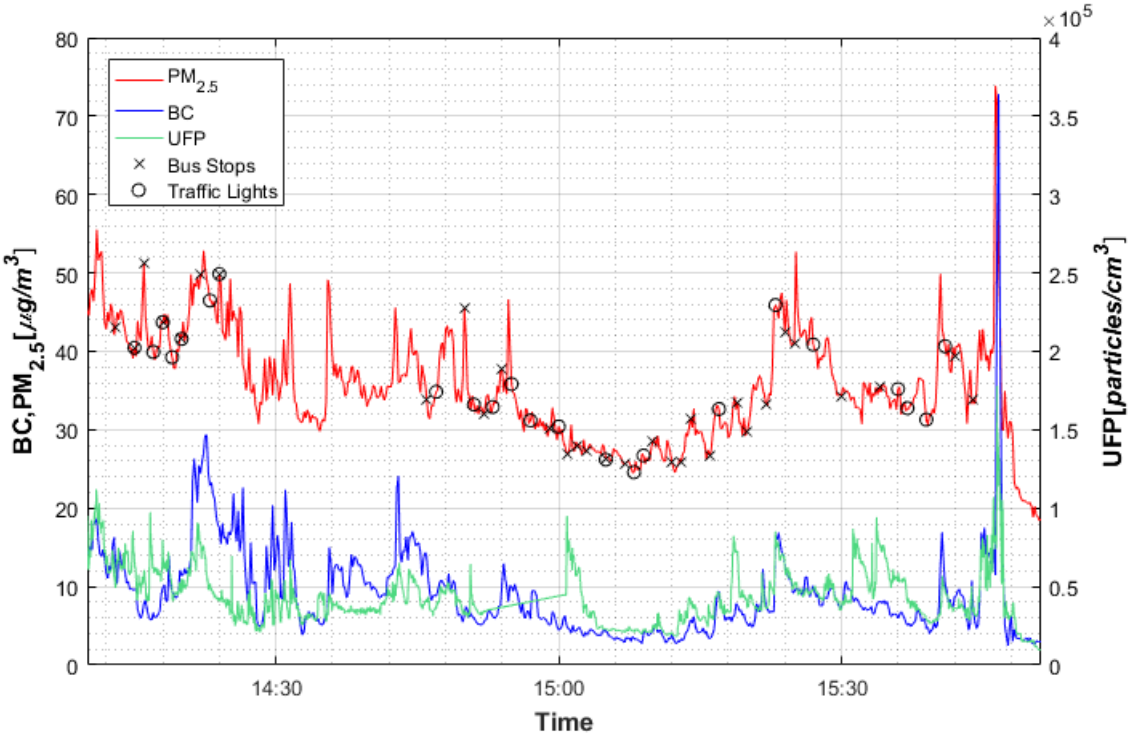

Figure 4-8: Time series in São Paulo on June 28th, 2016.

The time series from June 29th, 2016 can be seen in Figure 4-9. Very high $PM_{2.5}$, BC, and UFP concentrations can be seen from approximately 14:15 until returning to baseline levels at 14:30. It was noted in the field notes that high traffic conditions were occurring along this part of the route, and several bus stops and traffic lights occurred along the segment. More traffic was encountered from 15:15 until the end of the route, however these concentrations do not reach the same peaks observed in the earlier traffic. The traffic along the beginning of the route was along narrower roads than the traffic towards the end, perhaps leading to the higher concentrations observed due to reduced ventilation of the emissions in the street. Most of the peaks observed in this time series are clearly observed across all pollutants. The presence of BC in the peaks indicates that the increased concentrations were from the penetration of exhaust emissions into the bus, likely from open windows and open doors.

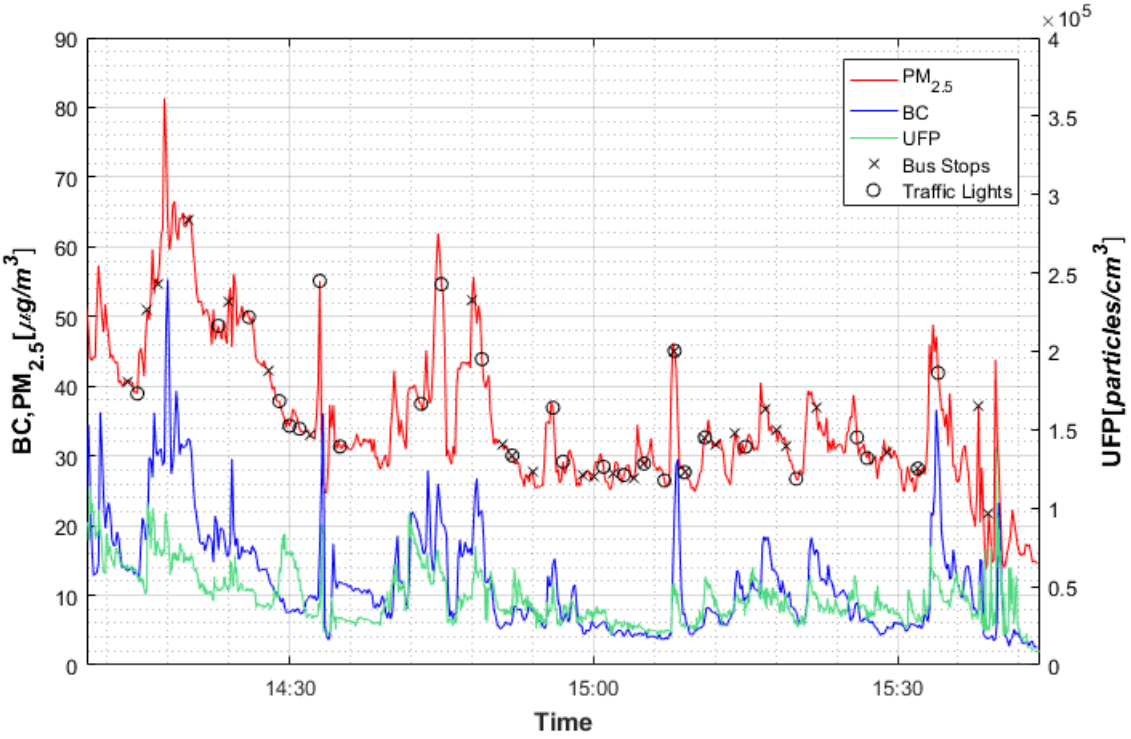

Figure 4-9: Time series in São Paulo on June 29th, 2016.

The final time series in São Paulo is from June 30th, 2016 and can be seen in Figure 4-10. A spike can be seen across all pollutants from 13:42 – 13:46. This occurs near the start of the route and can be seen to occur at the same time as many bus stops and traffic lights. There is another large spike in the data at 14:02, most prominently in the $PM_{2.5}$ series. This spike occurred when disembarking from the bus and is attributed to the bus's own exhaust. Finally, there is a spike from 14:07 – 14:10 that has high concentrations in both $PM_{2.5}$ and BC. The bus had just turned on and was exiting the terminal, which could explain the high BC concentrations observed here. Following this spike there is another spike from 14:10 – 14:15 where bus stops and traffic lights occurred.

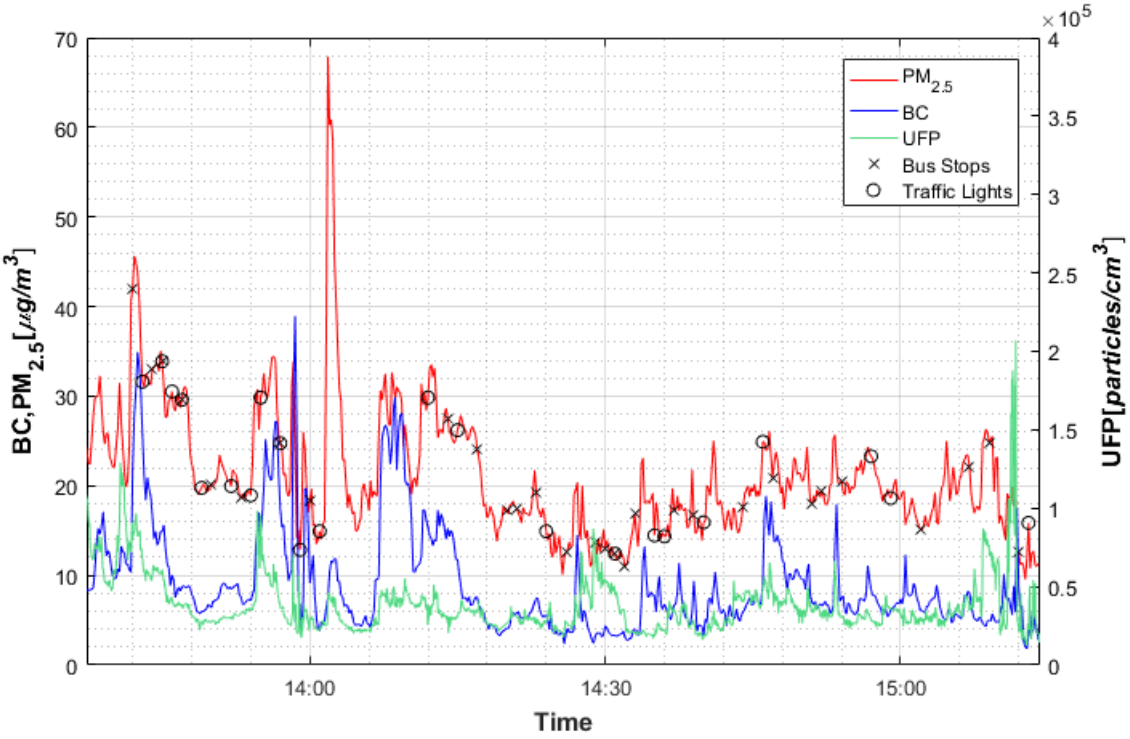

Figure 4-10: Time series in São Paulo on June 30th, 2016.

4.2.3 Curitiba

Measurements in Curitiba took place in the afternoon. The buses for the routes measured in Curitiba were smaller than traditional public buses. The seating also varied, unlike traditional bus seats in rows, some of these buses had seating around the perimeter of the bus. Figure 4-11 shows the $PM_{2.5}$, BC, and UFP concentrations on July 25th, 2016. The bus route started at a bus stop on the side of the road. The field notes specified that commencing at 14:16, high traffic was encountered, and the bus was traveling behind a large truck. In the time series, concentrations across all pollutants increase rapidly representing a large drawn out spike in the data from 14:17 – 14:23. This is likely because the air pollutants were continuously entering the bus through the open windows and accumulating within the bus passenger cabin. The high presence of BC in this peak further confirms this since there was a diesel truck in front of the bus during this period. Another spike is observed from 14:39 – 14:42. Again, BC and UFP concentrations are elevated indicating the infiltration of diesel exhaust emissions into the bus, perhaps at the

traffic light. From 14:48 – 14:53 a bus change was made, this included walking one block to the next bus stop. A few high UFP and BC spikes can be noted during this time, likely as an influence from passing cars.

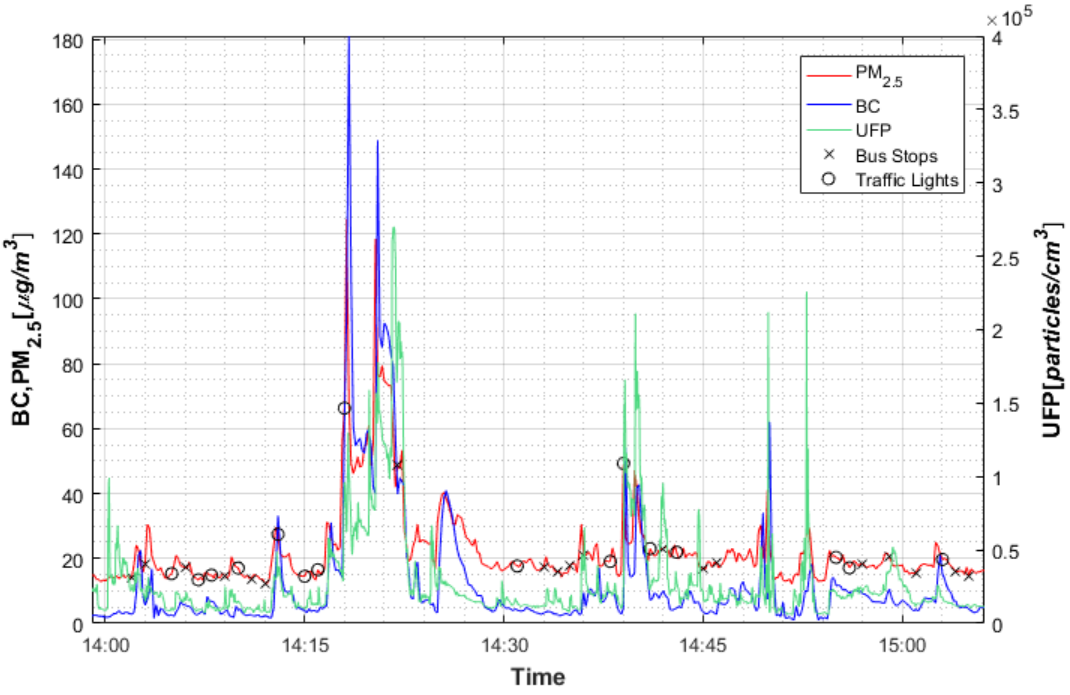

Figure 4-11: Time series in Curitiba on July 25th, 2016.

The $PM_{2.5}$, BC, and UFP concentrations on July 26th, 2016 are in Figure 4-12. Many spikes can be seen in the time series, more notably in the BC and UFP than the $PM_{2.5}$ series. Many of these spikes can be seen to be occurring at the location of traffic lights and bus stops, with the exception of the spike at 14:38 which occurred during disembarking the bus and can be attributed to the bus's own exhaust outdoors. High traffic conditions were noted in the field notes on the second bus trip from 14:46 – 15:08. It is possible that high traffic was leading to high exhaust emissions in the road that were infiltrating into the bus at traffic lights and bus stops leading to the many spikes in the data.

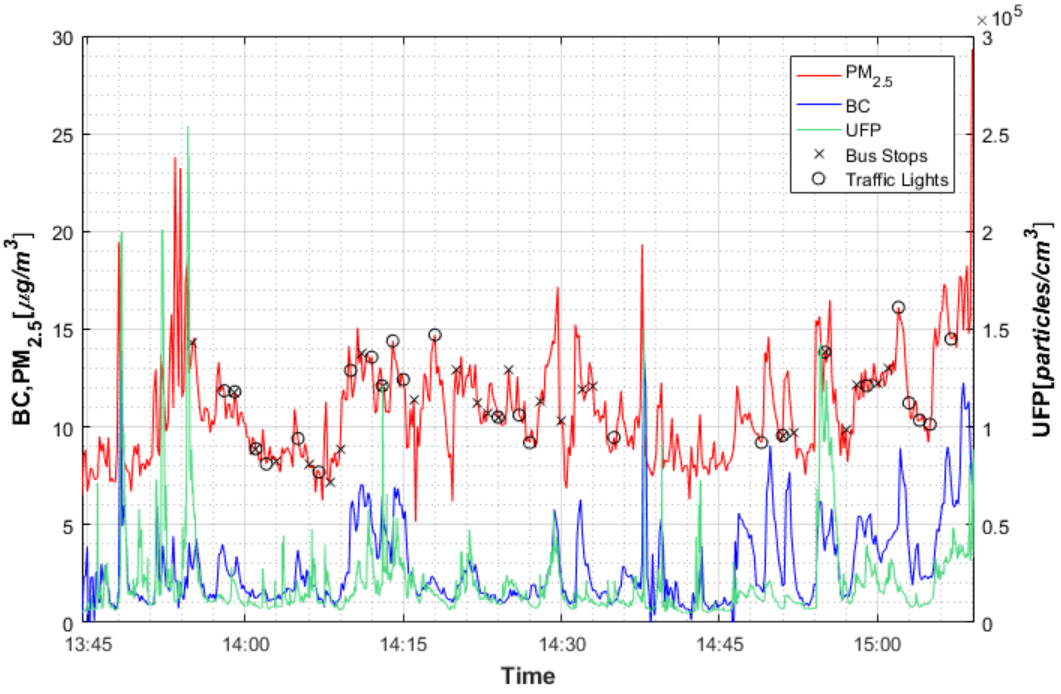

Figure 4-12: Time series in Curitiba on July 26th, 2016.

$PM_{2.5}$, BC, and UFP concentrations are in the time series below from July 27th, 2016 in Figure 4-13. Heavy traffic was noted at several times throughout the bus trip at 14:15, 14:39, and 14:47 which may be contributing factors to the spikes observed in the time series at these periods. The spike from 14:20 – 14:26 is particularly large. The high traffic conditions may have attributed to the high concentrations of pollution observed in the bus here, likely as a result from infiltration into the bus at the bus stop and two traffic lights during this peak. An interesting observation can be seen from 2:50pm – 3:05pm when walking to the second bus. In the $PM_{2.5}$ and BC time series, very low values can be seen. It is known that exhaust emission concentrations decrease rapidly away from the street and may be the case here for the low concentrations.

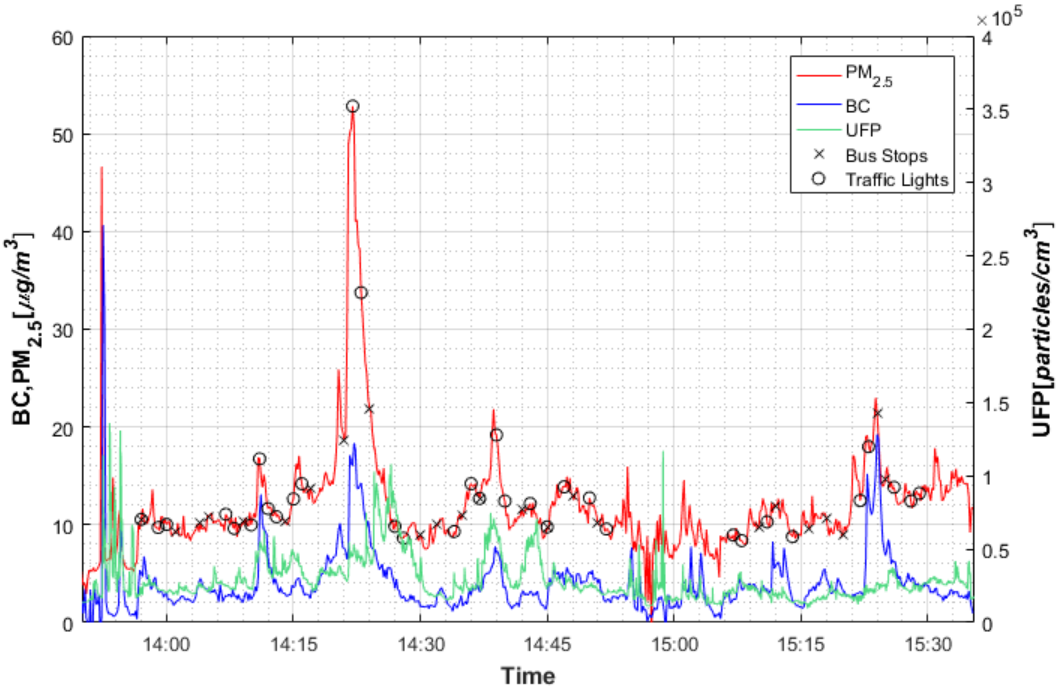

Figure 4-13: Time series in Curitiba on July 27th, 2016.

The time series of $PM_{2.5}$, BC, and UFP concentrations from July 28th, 2016 are shown in Figure 4-14 below. A large peak can be observed in the data at 14:53 which is the same time that the second bus arrived at the bus stop. It is possible that this large spike is from the bus's own exhaust emission as it approached the stop. Heavy traffic was encountered from 15:09 – 15:20, which corresponds with spikes in both the BC and $PM_{2.5}$ time series. A final spike is also observed from 15:16 – 15:24 where several traffic lights were encountered.

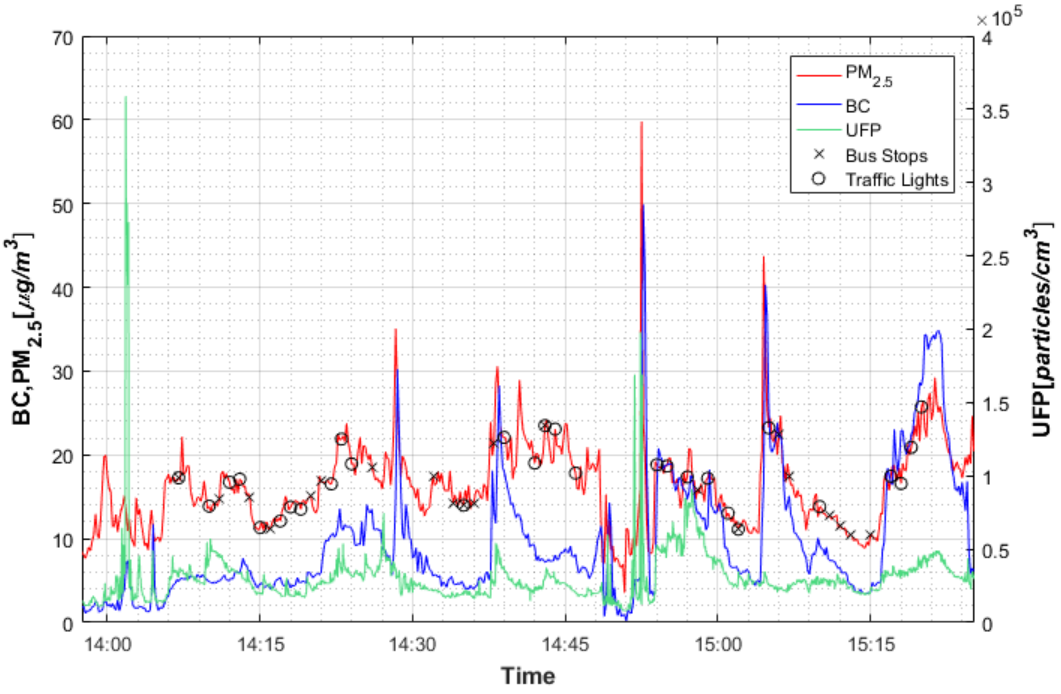

Figure 4-14: Time series in Curitiba on July 28th, 2016.

The final time series in Curitiba is from July 29th, 2016 and can be seen in Figure 4-15. High traffic was noted at 14:42. At the first instance of traffic, no notable spikes are in the $PM_{2.5}$ or BC series, however the UFP series does show an increase at this time perhaps indicating that infiltration of non-diesel exhaust emissions was occurring. Spikes across all pollutants can be observed from 15:15 – 15:19, however this was when travel between buses was occurring and would be from passing cars. High traffic was indicated in the notes again at 15:40. In this case, a large peak can be seen in $PM_{2.5}$ and BC with both pollutants increasing over 40 µg/m^3, as well as an increase in UFP. There were two traffic lights along this period and exhaust emissions were likely infiltrating into the bus resulting in this final large peak prior to the end of the bus route.

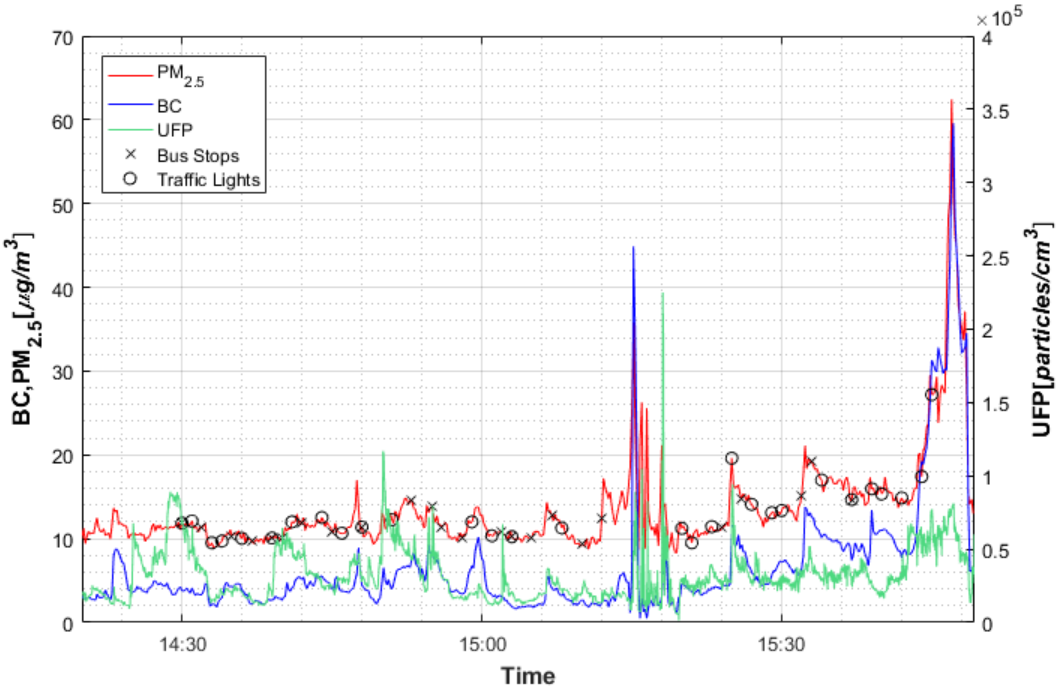

Figure 4-15: Time series in Curitiba on July 29th, 2016.

4.3 Route Pollution Maps

Maps of each pollutant for each day of measurements were made. Maps containing aggregated data for all days of measurement are included in text; the individual daily maps can be found in Appendix B. Locations of bus terminals and traffic count points are symbolized on the maps.

4.3.1 Londrina

In Londrina, high concentrations of $PM_{2.5}$, BC, and UFP were frequently noted in the downtown core of the city (near the Central Terminal). Rural and residential areas, most notably between the university and the downtown as well as between the downtown and Acapulco Terminal, experienced lower PM concentrations. Edwy Taquer de Araujo Street, near Acapulco Terminal, also visibly experienced higher concentrations. Despite this road being a low traffic road, it runs along the sides of a major highway. Between

each direction of Edwy Taquer de Araujo Street is a four-lane highway which could be contributing to the elevated concentrations observed.

Figure 4-16 is a map of the $PM_{2.5}$ concentrations in Londrina. Elevated concentrations can be observed in the downtown core, particularly along Sergipe Street (> 20 µg/m^3). The streets in the downtown of Londrina are very narrow and Sergipe Street has been studied for its street canyon configuration and resulting high air pollution concentrations (Krecl *et al.*, 2016). Edwy Taquer de Araujo Street also has elevated $PM_{2.5}$ concentrations for most of the measured section (> 20 µg/m^3). As was expected, the roads near the university have low vehicle traffic (1,200 vehicles/hour at the point closest to the university) and therefore low $PM_{2.5}$ concentrations are observed (less than 10 µg/m^3). The route between Duque de Caxias Avenue and Edwy Taquer de Araujo Street is also through a residential neighbourhood with low traffic (656 vehicles/hour) and low $PM_{2.5}$ concentrations (primarily 10 - 15 µg/m^3) can be observed here as well. However, as the road nears the highway, $PM_{2.5}$ concentrations can be seen to increase up to 20 µg/m^3.

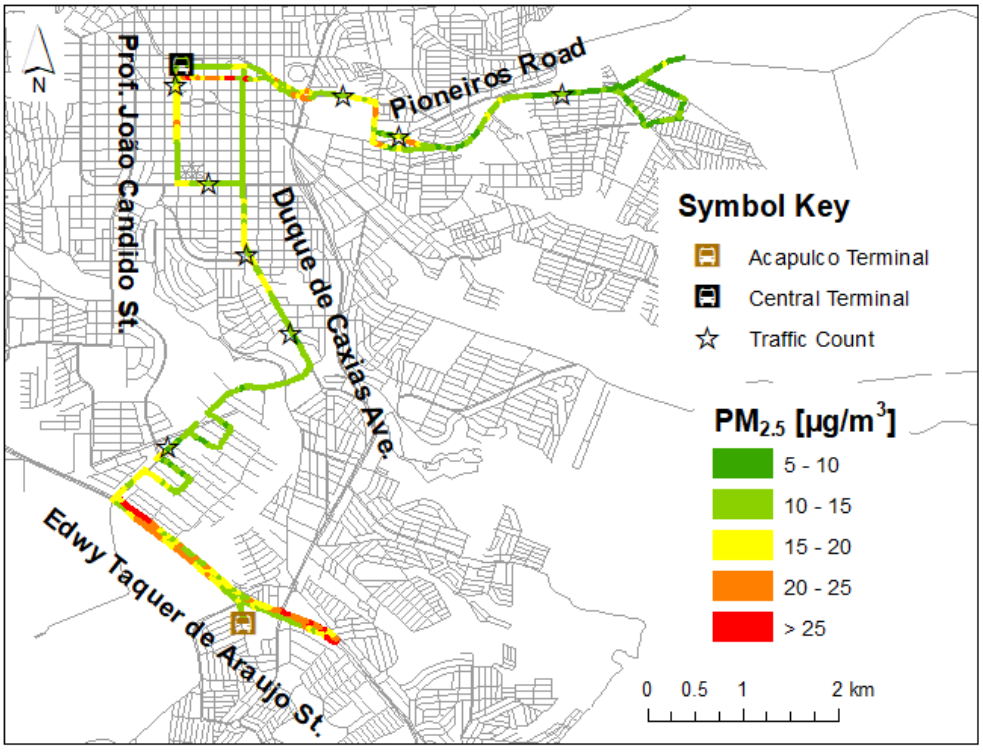

Figure 4-16: Map of $PM_{2.5}$ concentrations in Londrina.

Figure 4-17 below is a map of BC concentrations throughout Londrina. Similar to the $PM_{2.5}$ concentrations seen on the above map, elevated concentrations can be seen at particular intersections in the same general area as the elevated $PM_{2.5}$ concentrations (in the downtown and along Edwy Taquer de Araujo Street). Pioneiros Road and the residential area between Duque de Caxias Avenue and Edwy Taquer de Araujo Street both have very low BC concentrations (< 6 µg/m^3). Both of these roads experience low bus and truck traffic (approximately 4 % the total traffic) and therefore low BC is expected since the diesel emissions along these roads is reduced. In the downtown of Londrina, particularly near the Central Terminal, a significant number of buses travel along the roads. The traffic count point closest to the Central Terminal is composed of 50 % bus traffic, therefore increased BC concentrations are to be expected. Edwy Taquer de Araujo Street also has elevated BC concentrations which could be as a result of the highway traffic.

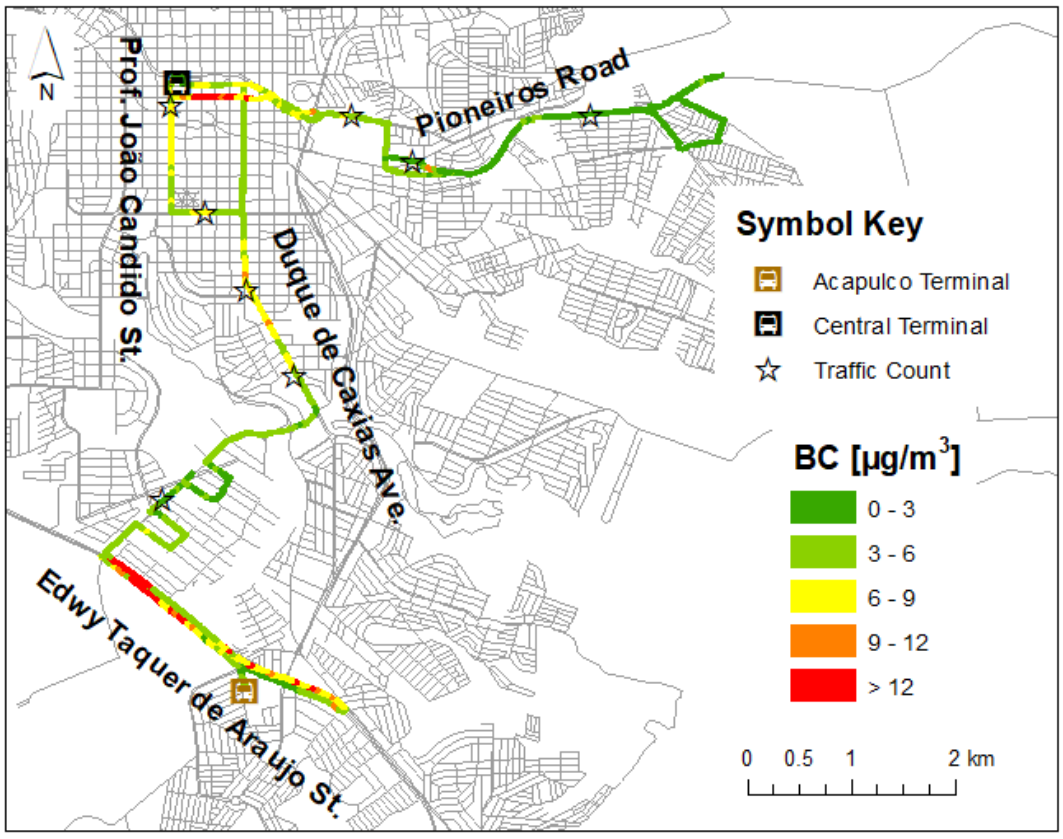

Figure 4-17: Map of BC concentrations in Londrina on June 23, 2016.

Figure 4-18 below shows the UFP concentrations throughout Londrina. Elevated and reduced concentrations can be observed in the same areas as the above two maps. The highest UFP concentrations are observed in the downtown core of Londrina and along Edwy Taquer de Araujo Street. High UFP concentrations (> 40,000 particles/cm^3) can also be seen along Duque de Caxias Avenue. Duque de Caxias Avenue is a busy main thoroughfare through Londrina with six-lanes (the outer lane in either direction however, is primarily a parking-only lane). The vehicle counts ranged from 888 to 1,700 vehicles/hour with 6 - 7% diesel buses and trucks.

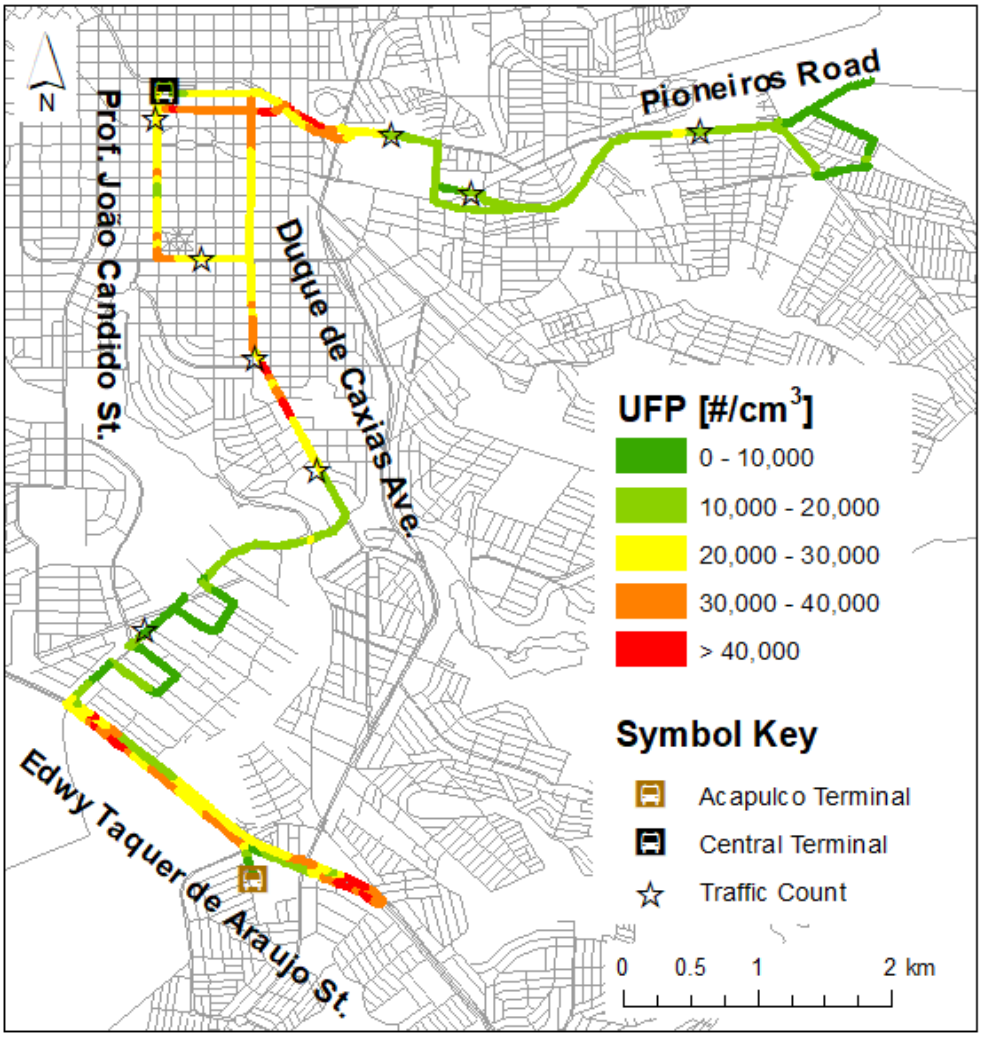

Figure 4-18: Map of UFP concentrations in Londrina on June 24, 2016.

4.3.2 São Paulo

Figure 4-19 shows the $PM_{2.5}$ concentrations throughout São Paulo. Elevated concentrations can be seen most prominently along Consolação Street and towards the Princesa Isabel Terminal (majority 40 - 50 µg/m^3). Consolação Street consists of eight-lanes of traffic (the inner lanes are designated bus lanes) with buildings flanking either side. The traffic flow on this street is 6,229 vehicles/hour. The routes approaching the bus terminal are narrow and characterized in the field notes consistently as having high traffic, especially through intersections. The $PM_{2.5}$ concentrations along Conselheiro Furtado Street and approaching Paulista Avenue are much lower (consistently < 30 µg/m^3) than the other streets. Although vehicle count data is not available for this segment of the route, it travels through a primarily residential neighbourhood and lower vehicle traffic can be expected. The concentrations along Paulista Avenue are remarkably lower than Consolação Street, despite having high traffic (4,907 - 6,317 vehicles/hour). The traffic along Paulista Avenue was slow moving and primarily stop and go through intersections. Paulista Avenue was also more open than Consolação Street or the narrow streets near the bus terminal which may have facilitated pollutant ventilation.

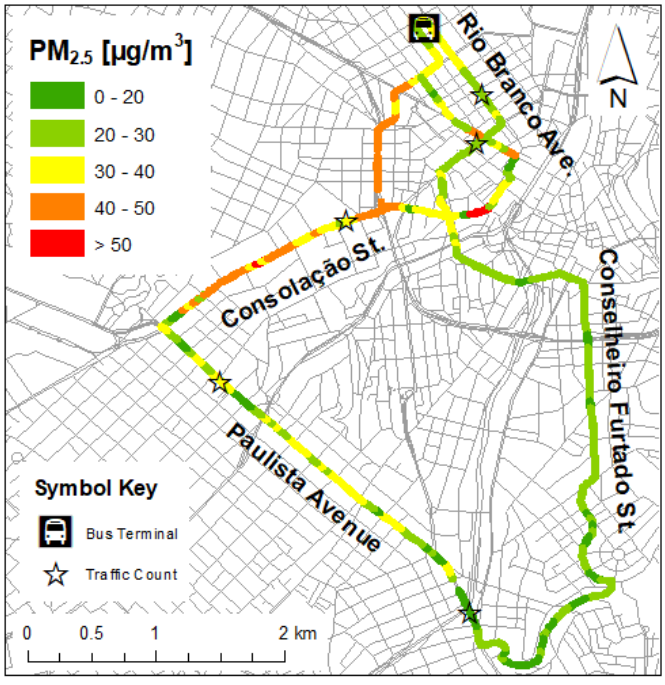

Figure 4-19: Map of $PM_{2.5}$ concentrations in São Paulo.

Figure 4-20 below shows the BC emissions throughout São Paulo. The BC concentrations along Consolação Street are more elevated than other areas along the route with many isolated areas reaching over 20 µg/m^3. When traveling in the bus-specific lane along Consolação Street, it is possible that the other bus traffic in front of the bus was contributing to the higher concentrations of BC on board (Hill *et al*., 2005). Over 200 buses/hour travel along Consolação Street. The area around the bus terminal also had some pockets of higher emissions. These roads likely had many buses traveling to and from the bus station. Paulista Avenue, which as observed above has a high vehicle count, does not have any significant BC events compared to Consolação Street. This could be partially because the street is more open and facilitates ventilation. Paulista Avenue also however, has less bus traffic than Consolação Street. From the two vehicle count points along Paulista Avenue, 150 - 175 buses/hour travel along the street which may also contribute to the lower BC concentrations.

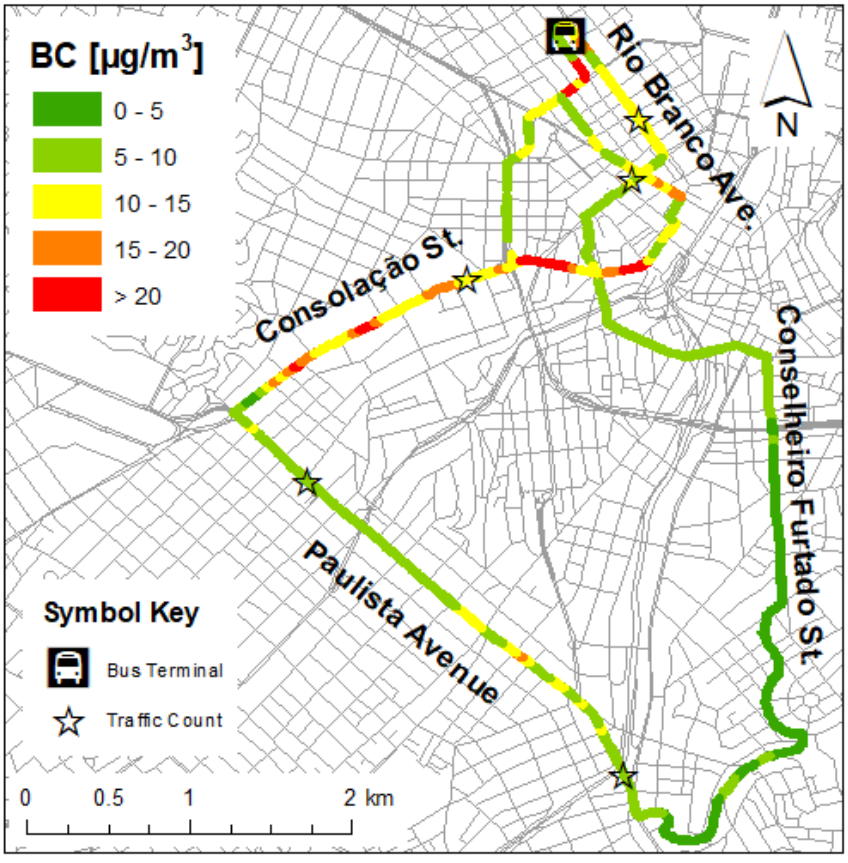

Figure 4-20: Map of BC concentrations in São Paulo.

Figure 4-21 below is a map of the UFP concentrations throughout São Paulo. A similar trend can be observed in this map as was seen in the maps above. Consolação Street can be observed to have elevated UFP concentrations the entire length of the street with some sections reaching over 75,000 particles/cm^3. These high concentrations could be as a result of both diesel emissions from the bus-only lane, as well as elevated levels of car traffic which are also known to emit high amounts of UFP (Morawska *et al.*, 2008). The majority of Conselheiro Furtado Street, a residential area, has very low UFP concentrations (< 30,000 particles/cm^3). Paulista Avenue does not have as high of UFP concentrations as other high traffic sections of the route (primarily < 45,000 particles/cm^3) which may be from the open street configuration, less diesel vehicles, and a lower vehicle speed due to high traffic. Park *et al.* (2011) show that UFP emissions from low accelerations and low cruising speeds are significantly lower than high accelerations and high cruising speeds in gasoline-powered vehicles.

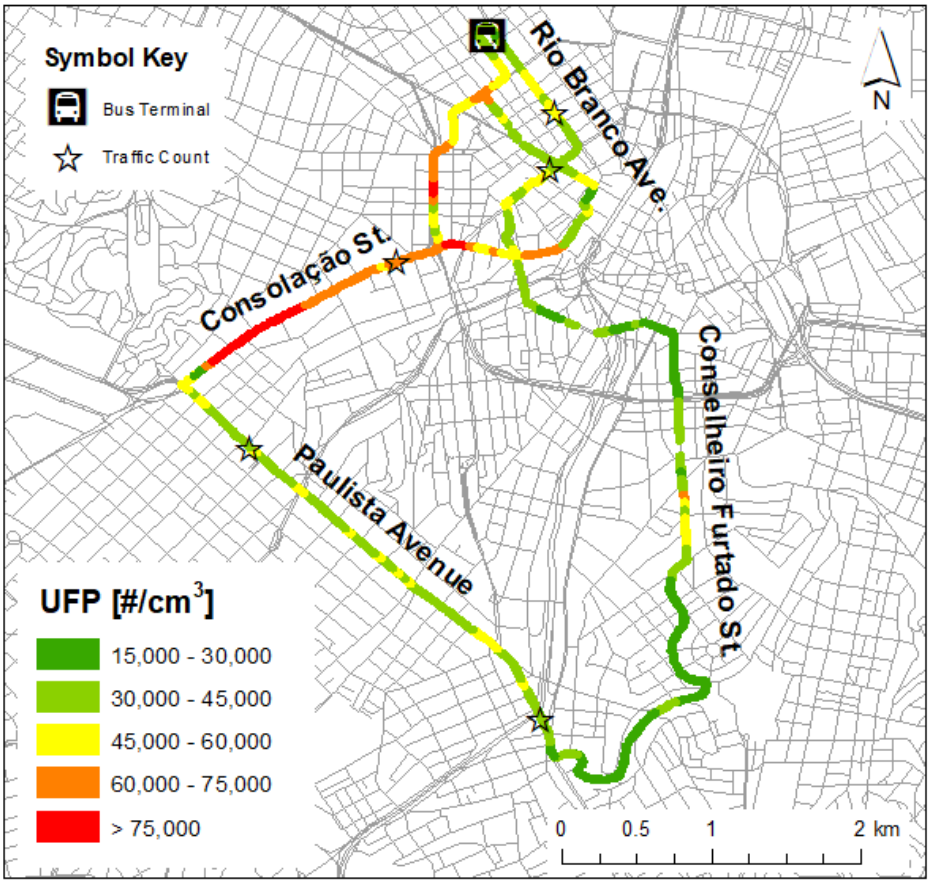

Figure 4-21: Map of UFP concentrations in São Paulo.

4.3.3 Curitiba

Figure 4-22 shows the $PM_{2.5}$ concentrations in Curitiba. The majority of the sampled route has $PM_{2.5}$ concentrations 10 – 15 $\mu g/m^3$. Elevated concentrations can be seen most notably along Mariano Torres Street and the surrounding region. The traffic counts on Mariano Torres Street are high (1,339 – 2,798 vehicles/hour along the measured section). The only location on the map with $PM_{2.5}$ concentrations exceeding 20 $\mu g/m^3$ is just past the north corner of Mariano Torres Street heading towards Inácio Lustosa Street. This was a very busy intersection during the measurement routes, and vehicle counts at the closest point are the highest on the measured route (4,168 vehicles/hour). The high vehicle density coupled with the slow intersection at this location may have resulted in the higher $PM_{2.5}$ concentrations. Sete de Setembro Avenue, which is a major road in the city of Curitiba, does not have any notable $PM_{2.5}$ events. This could be because there is a BRT lane down the centre of the street separating the large mass transit buses from the car lanes. The car lanes are single lanes on the sides of the bus lanes with a maximum speed limit of 30 km/hr (Trisotto, 2014).

Curitiba also has a traffic calmed area where the speed limit is 40 km/hr for much of the downtown core, which encompasses most of the measured route from this study (Prefeitura de Curitiba, 2015). Park *et al.* (2011) showed that driving at slower cruise speeds and slower accelerations does not largely affect $PM_{2.5}$ emissions from gas vehicles, however it does result in increased emissions from diesel vehicles. Jayaratne *et al.* (2009) showed that coming to an abrupt stop and then accelerating away (for example, at a pedestrian crossing or a traffic light) will contribute to higher vehicle emissions. In Curitiba where vehicles in the traffic calmed area are not driving faster than 40 km/hr, there would not be significant abrupt stopping or accelerating away which could be why the $PM_{2.5}$ emissions throughout the city are somewhat even with small instances of increases or decreases.

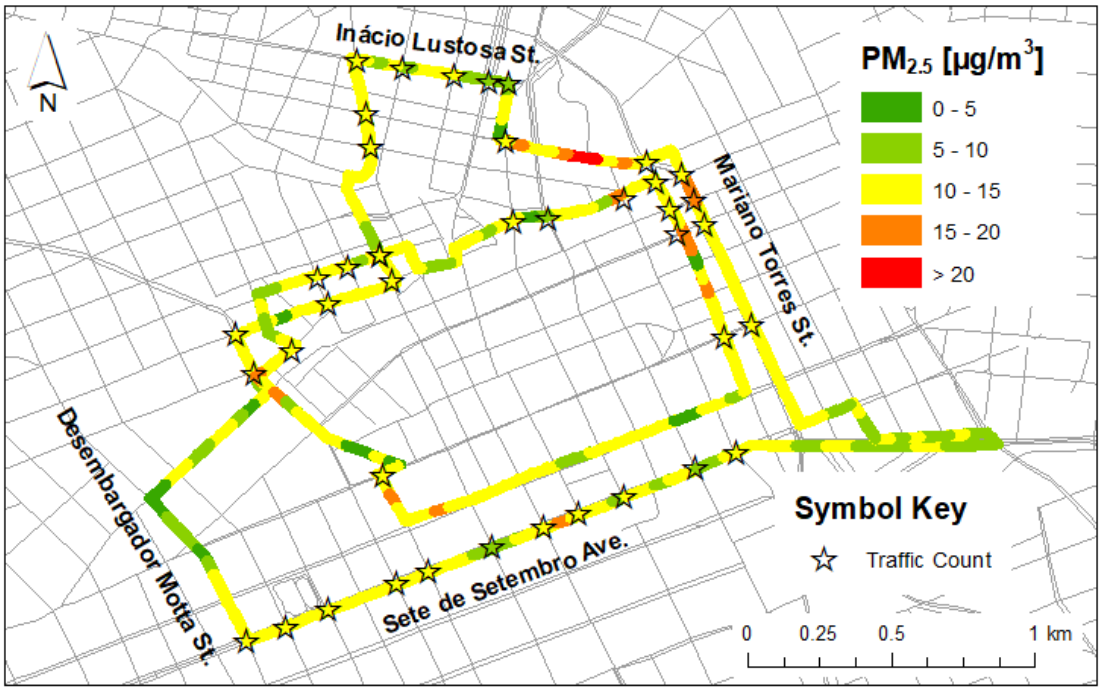

Figure 4-22: Map of $PM_{2.5}$ concentrations in Curitiba.

Figure 4-23 shows the BC concentrations in Curitiba. Elevated BC concentrations can be seen along the north corner of Mariano Torres Street, as well as the length of the street parallel to it called Tibagi Street. Both streets are one-way streets running in opposite directions. Mariano Torres Street flows northbound with six lanes, and Tibagi Street flows southbound with only three lanes. Both streets are flanked by many buildings on either side which could inhibit pollutant dispersion and ventilation. The bus counts also made up 5-7 % the vehicle counts through the intersections approaching the corner for both Mariano Torres Street and Tibagi Street. These factors may contribute to the elevated BC concentrations observed here. The other area of elevated concentrations is on the road approaching Desembargador Motta Street where concentrations exceeded 12 µg/m^3. Traffic was often encountered in this region during measurements, however the data in this section is not overly reliable due to a consistently poor GPS signal when traveling along this part of the route. The vehicle counts at the closest intersection however, do show elevated traffic counts (2,191 vehicles/hour) with a 10 % bus composition.

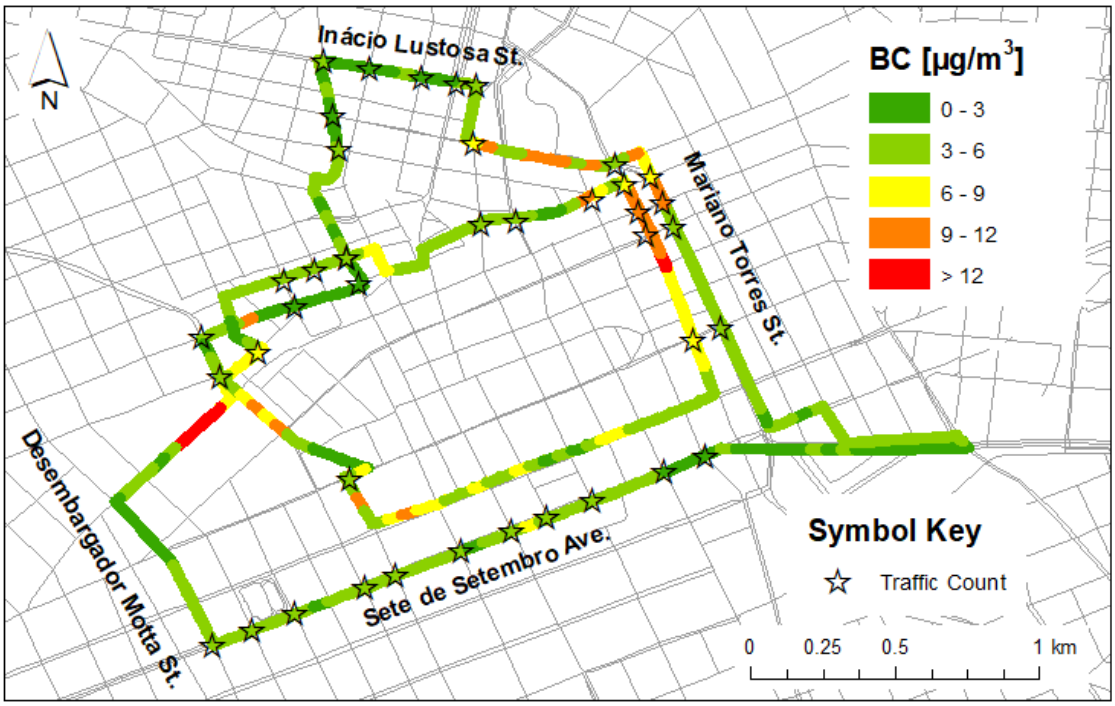

Figure 4-23: Map of BC concentrations in Curitiba.

Figure 4-24 is a map of the UFP concentrations throughout Curitiba. The locations identified with higher concentrations on the UFP map are also areas that had higher concentrations on both the BC and $PM_{2.5}$ maps. Much like with the $PM_{2.5}$ map, the UFP concentrations do not show as much variation with concentrations primarily in the 20,000 – 30,000 particles/cm^3 range. The UFP concentrations however were very high along Inácio Lustosa Street despite the $PM_{2.5}$ and BC data not showing this trend. The speed data along this section was generally slow (< 20km/hr) however this was not a unique characteristic for the streets in Curitiba. The street configuration does show buildings flanking either side of the narrow four lane road (one lane is used as a parking lane). It is possible that the high UFP concentrations are as a result of poor street ventilation. Additionally, there is no BRT line along this road, so diesel traffic would be limited to trucks and fewer buses which could account for the lower BC concentrations that were observed.

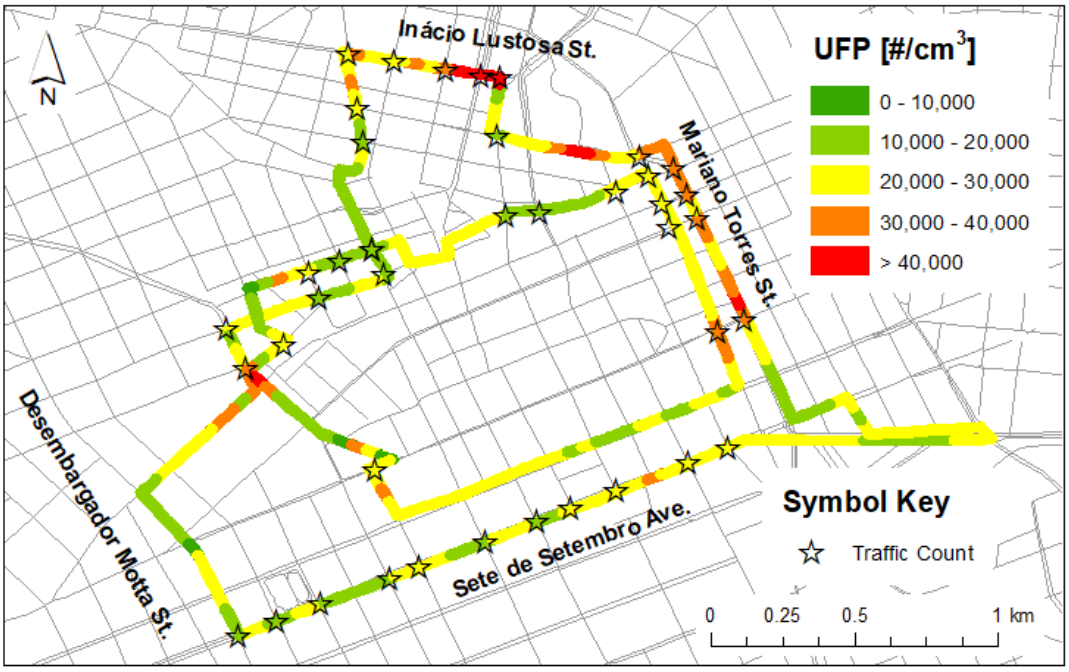

Figure 4-24: Map of UFP concentrations in Curitiba.

4.4 Riding Buses Compared to Waiting for Buses

Previous statistics so far have included the air pollution concentrations for the entire bus trips. The concentrations discussed here were separated into two categories: riding buses and periods of waiting for buses (in terminals and at bus stops). Only $PM_{2.5}$ and BC results are discussed in this section. The descriptive statistics include mean, standard deviation, median, and IQR. A box-plot showing this data is in Figure 4-25. In general, concentrations while waiting for the bus are lower than while riding the bus. The only exception can be observed in São Paulo where the concentrations are very similar.

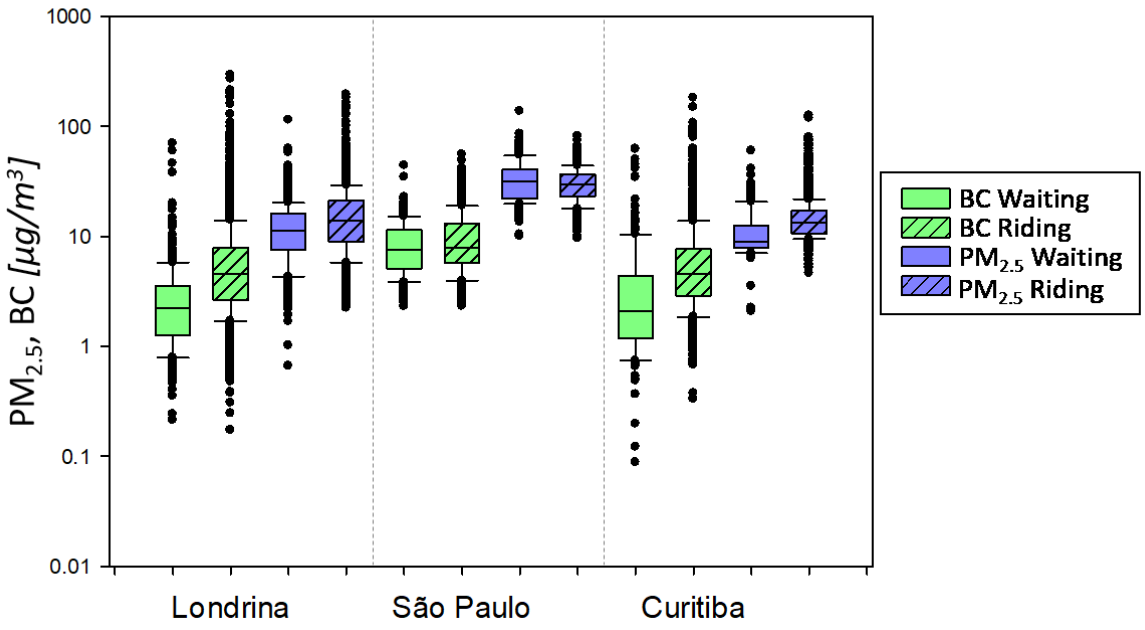

Figure 4-25: Box-plot of riding and waiting for buses.

4.4.1 Londrina

The waiting periods in Londrina took place at the university bus stop and in two bus terminals: Central Terminal and Acapulco Terminal. These terminals during off-peak hours did not experience much traffic. The general air pollutant concentrations were lower in these terminals, as was observed in the time series, aside from the occasional spike from a passing bus. A table of the descriptive statistics for both $PM_{2.5}$ and BC is in Table 4-17. Mann-Whitney rank sum tests were performed for both datasets. The difference in the medians was determined to be statistically significant ($p < 0.001$). For both the $PM_{2.5}$ and BC concentrations, the riding concentrations were much higher than the waiting concentrations. In particular, the BC median riding concentration was 41% larger than that waiting. This indicates that the concentrations while riding the buses were elevated than when standing at the side of the road or in a terminal.

Table 4-17: Riding vs. waiting $PM_{2.5}$ and BC concentrations comparison in Londrina.

	Mean ($\mu g/m^3$)	Standard Deviation ($\mu g/m^3$)	Median ($\mu g/m^3$)	IQR ($\mu g/m^3$)
$PM_{2.5}$ riding	16.8	13.4	14.0	12.3
$PM_{2.5}$waiting	12.3	7.7	11.3	8.4
BC riding	7.54	13.82	4.52	5.22
BC waiting	3.05	4.59	2.22	2.31

4.4.2 São Paulo

The waiting periods in São Paulo took place at a bus stop and in the Princesa Isabel Terminal. The bus stop for this route was located in the median of Consolação Street, an eight-lane main road with over 6,000 vehicles/hour. Due to this bus stop being in the median of the road, waiting passengers will be exposed to elevated levels of emissions from the passing cars since the stop is essentially in the street. Additionally, this stop was served by many buses. The terminal however, was less busy. Isolated spikes in the time series above were noticed from passing buses, however the general concentrations of PM were quite low. The general statistics from both $PM_{2.5}$ and BC can be seen in Table 4-18. From the Mann-Whitney rank sum test, the $PM_{2.5}$ medians in the datasets were statistically significant ($p < 0.001$) and the BC medians were statistically significant ($p = 0.014$). Unlike the Londrina data however, the median waiting concentration for $PM_{2.5}$ was slightly above the median riding concentration, while the median BC waiting concentration however, is slightly below the median riding concentration. This indicates that the in-bus concentrations were not largely different from the outdoor waiting concentrations.

Table 4-18: Riding vs. waiting $PM_{2.5}$ and BC concentrations comparison in São Paulo.

	Mean ($\mu g/m^3$)	**Standard Deviation ($\mu g/m^3$)**	**Median ($\mu g/m^3$)**	**IQR ($\mu g/m^3$)**
$PM_{2.5}$ Riding	30.6	13.8	29.4	13.1
$PM_{2.5}$ Waiting	33.7	14.4	31.8	18.7
BC Riding	10.13	6.63	7.86	7.40
BC Waiting	8.76	5.09	7.55	6.33

4.4.3 Curitiba

In Curitiba, the waiting periods took place at the side of the roads. The first waiting period was at a bus stop on the side of the road, and the second period involved walking one block to another bus stop on the side of the road. The second bus stop was located on a main road which had slow moving traffic (generally under 20 km/hr) during the waiting period. The descriptive statistics for both $PM_{2.5}$ and BC can be seen in Table 4-19. The Mann-Whitney rank sum test determined that the difference in medians of the $PM_{2.5}$ and BC data was significant ($p < 0.001$). As can be seen in the median values, the $PM_{2.5}$ riding concentrations are 50% higher when compared to the waiting concentrations and the BC riding concentrations are 35 % higher. This indicates that vehicle emissions from the road were infiltrating into the bus passenger cabin.

Table 4-19: Riding vs. waiting $PM_{2.5}$ and BC concentrations comparison in Curitiba.

	Mean ($\mu g/m^3$)	Standard Deviation ($\mu g/m^3$)	Median ($\mu g/m^3$)	IQR ($\mu g/m^3$)
$PM_{2.5}$ Riding	15.2	8.3	13.3	6.4
$PM_{2.5}$ Waiting	11.5	6.8	8.9	4.7
BC Riding	7.24	10.26	4.56	4.75
BC Waiting	4.72	8.13	2.11	3.22

4.5 Influence of Bus Stops and Traffic Lights

It is hypothesized that when the bus stops at a bus stop or traffic light, PM from nearby road traffic enters the bus through the open windows and doors. Data at bus stops and traffic lights were separated and compared to the full dataset to observe the influence of these events. The mean, standard deviation, median, IQR, and percent change were included in the descriptive statistics. The percent change is the percent increase or decrease of the median when compared to the original full dataset.

4.5.1 $PM_{2.5}$

The $PM_{2.5}$ concentrations were investigated at bus stops for Londrina, São Paulo, and Curitiba and the descriptive statistics can be seen in Table 4-20. The largest percent increase was observed for the city of Londrina with almost a 15 % increase of $PM_{2.5}$ at bus stops. São Paulo observed a moderate increase of 7 % and Curitiba observed a small decrease of 3 %.

Table 4-20: Descriptive statistics of $PM_{2.5}$ concentrations at bus stops.

	Mean ($\mu g/m^3$)	Standard Deviation ($\mu g/m^3$)	Median ($\mu g/m^3$)	IQR ($\mu g/m^3$)	% Change
Londrina	14.1	8.3	11.7	6.9	14.7
São Paulo	31.8	12.2	31.2	15.9	7.2
Curitiba	14.0	9.1	12.6	9.8	-3.1

The descriptive statistics for the influence of $PM_{2.5}$ at traffic lights is shown in Table 4-21. An increase was observed for all three cities with Londrina again having the most notable increase of nearly 17 %. São Paulo and Curitiba observed increases of 8.2 % and 6.2 %, respectively. The increases in $PM_{2.5}$ concentrations observed at traffic lights are higher than the increases at bus stops.

Table 4-21: Descriptive statistics of $PM_{2.5}$ concentrations at traffic lights.

	Mean ($\mu g/m^3$)	Standard Deviation ($\mu g/m^3$)	Median ($\mu g/m^3$)	IQR ($\mu g/m^3$)	% Change
Londrina	14.0	8.6	11.9	5.9	16.7 %
São Paulo	32.5	12.3	31.5	15.3	8.2 %
Curitiba	15.0	6.7	13.8	8.5	6.2 %

4.5.2 BC

The descriptive statistics of BC concentrations at bus stops can be seen in Table 4-22. The largest percent increase in concentrations was observed in Londrina with a 32 % increase in total BC concentrations at bus stops. São Paulo observed an increase of 10 %. Curitiba however saw a decrease in BC concentrations at bus stops of almost 7 %.

Table 4-22: Descriptive statistics of BC concentrations at bus stops.

	Mean ($\mu g/m^3$)	Standard Deviation ($\mu g/m^3$)	Median ($\mu g/m^3$)	IQR ($\mu g/m^3$)	% Change
Londrina	9.68	16.61	4.73	7.67	32.1 %
São Paulo	11.21	10.10	8.52	7.82	10.2 %
Curitiba	6.19	11.27	3.39	4.24	-6.6 %

The BC concentrations at traffic lights for all three cities is in Table 4-23 below. An increase between the concentrations at traffic lights and the overall concentrations is notable across both Londrina and São Paulo. In Londrina, an increase of 30 % was observed. São Paulo had an increase of 22%. Curitiba however had a decrease of 4.4 % in BC concentrations at traffic lights.

Table 4-23: Descriptive statistics of BC concentrations at traffic lights.

	Mean ($\mu g/m^3$)	Standard Deviation ($\mu g/m^3$)	Median ($\mu g/m^3$)	IQR ($\mu g/m^3$)	% Change
Londrina	8.16	12.58	4.65	7.29	29.9 %
São Paulo	11.73	10.10	9.43	8.36	22.0 %
Curitiba	6.52	12.06	3.47	4.25	-4.4 %

4.5.3 UFP

The descriptive statistics for the UFP concentrations at bus stops can be seen below in Table 4-24. Londrina exhibited the largest percent increase at bus stops with an increase of 35 % in UFP concentrations. São Paulo observed an increase of 6 % and Curitiba saw a large decrease in UFP concentrations of 30 %.

Table 4-24: Descriptive statistics of UFP concentrations at bus stops.

	Mean (#/cm^3)	Standard Deviation (#/cm^3)	Median (#/cm^3)	IQR (#/cm^3)	% Change
Londrina	23,600	14,409	20,200	15,000	34.7 %
São Paulo	46,030	22,846	38,950	28,500	6.4 %
Curitiba	19,198	16,166	15,100	19,850	-30.4 %

The descriptive statistics for the UFP concentrations at traffic lights are in Table 4-25. A very large increase of over 50 % is observed in the Londrina data comparing the traffic light concentrations to the original dataset. São Paulo exhibits an increase of 9 % and Curitiba an increase of 10 % in the UFP concentration at traffic lights.

Table 4-25: Descriptive statistics of UFP concentrations at traffic lights.

	Mean (#/cm^3)	Standard Deviation (#/cm^3)	Median (#/cm^3)	IQR (#/cm^3)	% Change
Londrina	26,029	14,265	23,500	17,900	56.7 %
São Paulo	46,313	22,744	39,800	28,100	8.7 %
Curitiba	28,567	16,344	23,900	20,500	10.1 %

From the above results bus stops and traffic lights showed increases in the different pollutants in São Paulo and Londrina. Curitiba was the only city that experienced decreases and only small increases in certain scenarios. It is possible that because in Curitiba the traffic travels slower through traffic calmed areas, pollution is readily entering the bus through the open windows therefore when the bus pulls to the side of the road at a bus stop, the concentrations outside of the bus are now lower than in the street due to being further away from vehicle exhaust. Large increases in BC were observed in

Londrina and São Paulo at traffic lights and in Londrina at bus stops. Self-pollution from the bus's own exhaust may be influencing the concentrations at traffic lights and bus stops. A study by Marshall and Behrentz (2005) measured self-pollution of diesel-powered school buses and found that self-pollution was significant for all buses measured. It was noted however, in Harik *et al.* (2017) that self-pollution of a vehicle seems to increase with speed therefore wind direction may also influence emissions entering the bus with winds from the back of the bus blowing tailpipe and engine emissions forward towards the open windows and bus doors (Hill *et al.*, 2005). Yang *et al.* (2015) noted that BC and UFP concentrations were higher in diesel buses than other modes of transport suggesting that self-pollution and penetration of pollution from the street was likely occurring.

4.6 Bus Speed Relation to Particle Concentrations

The mean pollutant concentrations were plotted versus their corresponding bus speeds, in quantiles of 5 km/hr up to 45 km/hr, to identify relationships between these variables. In the below figures, $PM_{2.5}$ and BC are plot on the y-axis in $\mu g/m^3$ versus bus speed in km/hr. In the below UFP plots, UFP concentrations are plot on the y-axis in particles/cm^3 versus bus speed in km/hr. Error plots are included alongside the mean concentration plots. The error bars represent one standard deviation away from each mean value.

4.6.1 Londrina

In Figure 4-26a it can be seen that the $PM_{2.5}$ concentrations increase with increasing speed up until 25 km/hr followed by a sharp decrease. A small increase in concentration occurs from 40-45 km/hr. The same trend can be observed when looking at the plot with error bars in Figure 4-28b.

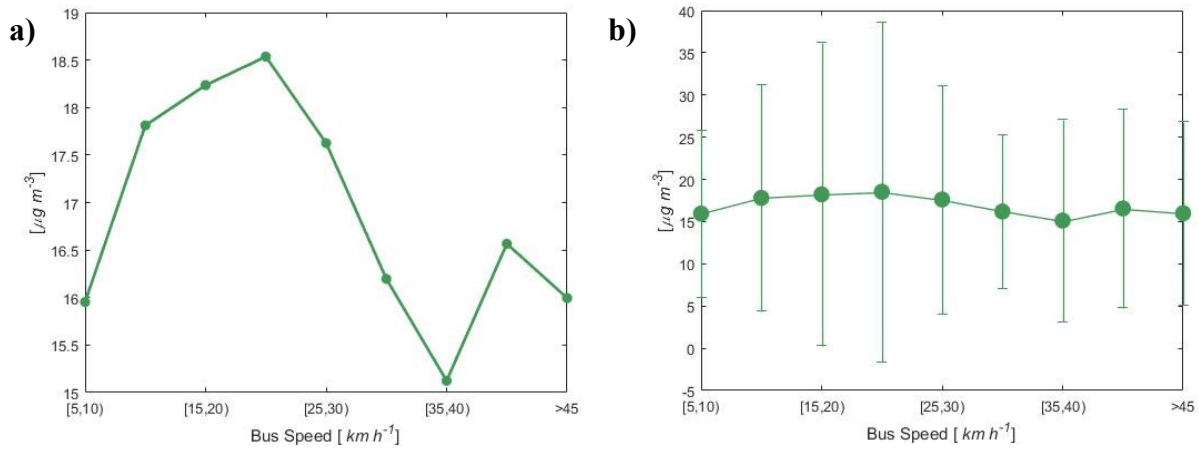

Figure 4-26: a) Londrina $PM_{2.5}$ concentrations vs. bus speed b) Londrina $PM_{2.5}$ concentrations vs. bus speed with error bars.

Similar results can be observed in the BC plot in Figure 4-27a and Figure 4-27b. Concentrations of BC increase up until a speed of 25 km/hr followed by a sharp decrease in speed, with a small increase from 40-45 km/hr.

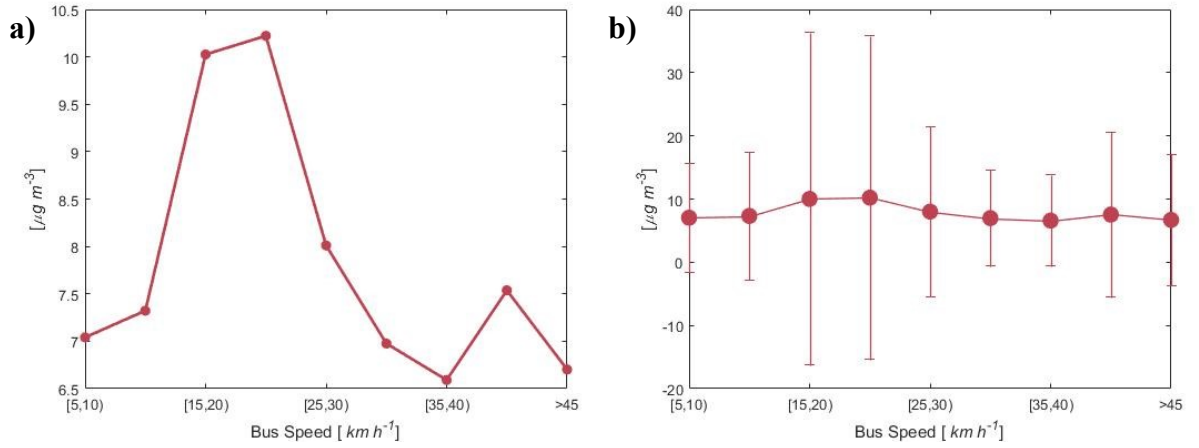

Figure 4-27: a) Londrina BC concentrations vs. bus speed b) Londrina BC concentrations vs. bus speed with error bars.

When observing the relation between UFP and speed, an initial increase followed by a decrease in concentrations is also observed with increasing speeds. From Figure 4-28a the maximum concentration occurs at 20 km/hr followed by a decrease in concentration with a small increase from 35-40 km/hr. The plot with error bars in Figure 4-30b also shows this trend.

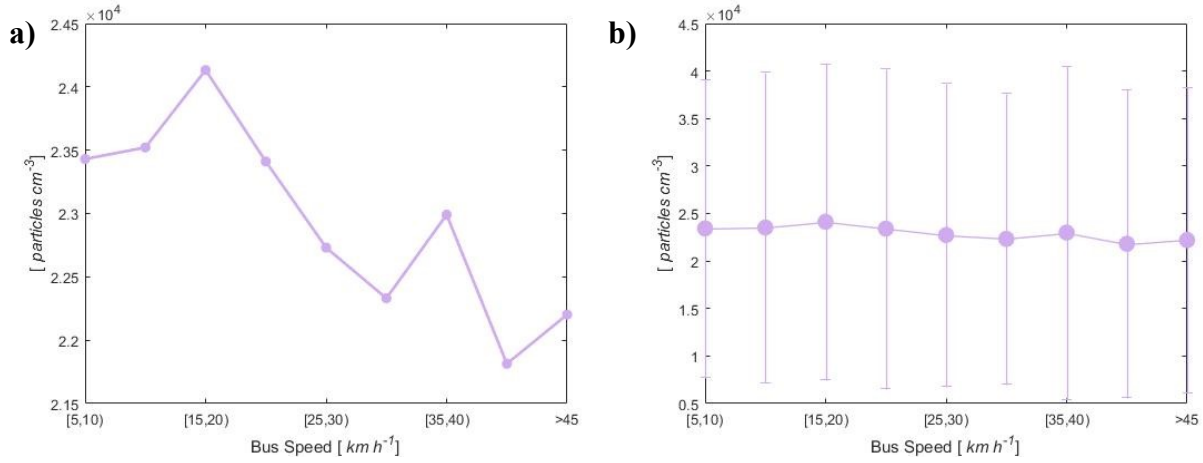

Figure 4-28: a) Londrina UFP concentrations vs. bus speed b) Londrina UFP concentrations vs. bus speed with error bars.

Although the error bars are very large, the trends are not lost. The decreasing trend observed in Londrina suggests that as the bus was moving at faster speeds, higher air flow entered into the bus through the open windows and ventilation system, thus flushing out the accumulated pollutants. The bus may also be moving faster due to being in less congested areas of the city therefore cleaner air is present outdoors. Similar trends were observed in Targino *et al.* (2018) where BC concentrations on bus routes in Londrina were investigated. Additionally, pollution infiltration into a vehicle tends to increase with speed (Xu & Zhu, 2013). This may be the reason that the increase in pollutants is seen initially in the pollutant profiles for Londrina. However, when the bus is above the speed of 25 km/hr, it is traveling on the cleaner roads and therefore less polluted air is infiltrating into the cabin. The maximum concentration in the UFP plots is observed to occur 5 km/hr before the $PM_{2.5}$ and BC maximums. This could be because UFP undergo processes over time where they grow into larger particles. Perhaps this difference in

maximum occurs because the UFP reach a maximum value before the $PM_{2.5}$ due to this time delay in growth.

4.6.2 São Paulo

The trends observed in São Paulo are entirely opposite from those in Londrina. From the plot of $PM_{2.5}$ concentrations versus bus speeds in Figure 4-29a, it can be observed that concentrations increase with increasing speed. In the error plot Figure 4-29b, the increasing trend is not as sharp however, it is still noticeable.

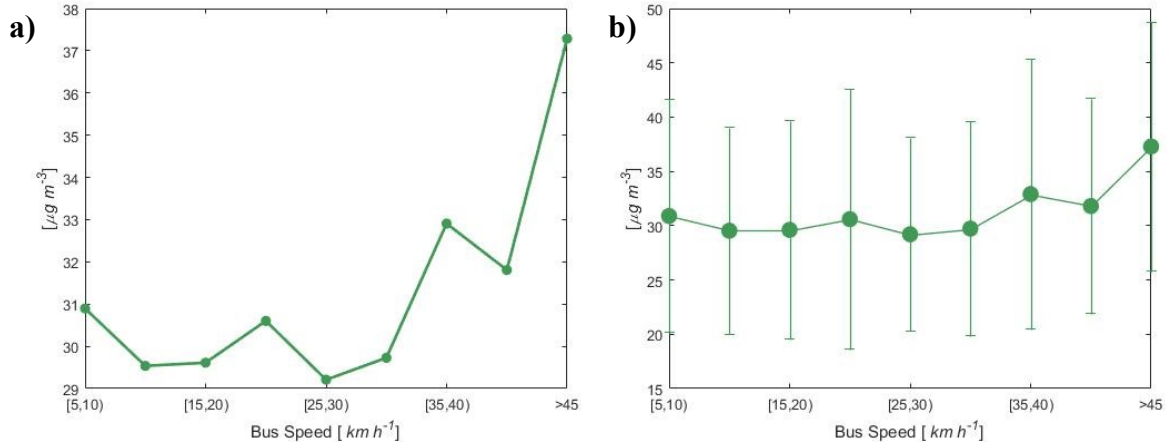

Figure 4-29: a) São Paulo $PM_{2.5}$ concentrations vs. bus speed b) São Paulo $PM_{2.5}$ concentrations vs. bus speed with error bars.

Similar observations can be made in Figure 4-30a and Figure 4-30b which show a trend of increasing BC concentrations with increasing bus speed. Like in the $PM_{2.5}$ plots, the error plot does not show as sharp of an increase.

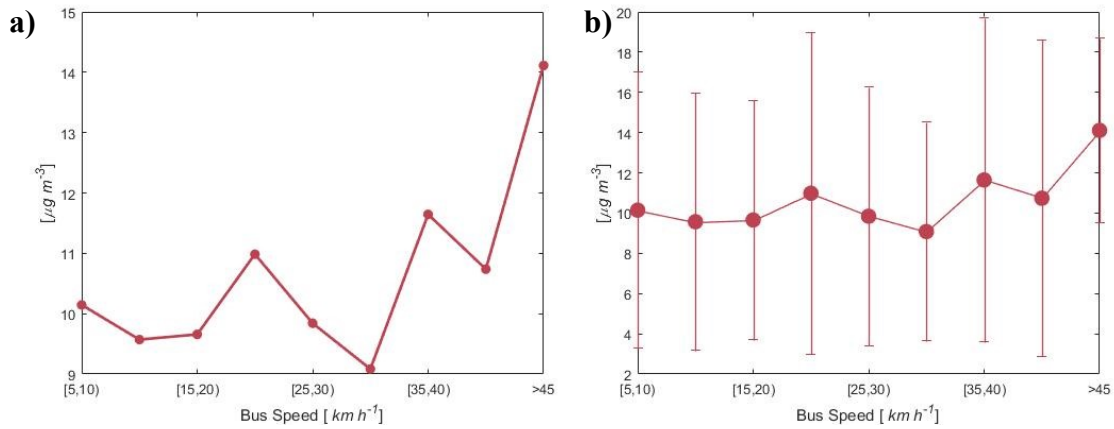

Figure 4-30: a) São Paulo BC concentrations vs. bus speed b) São Paulo BC concentrations vs. bus speed with error bars.

The UFP concentrations versus bus speed show the most defined increase of the pollutant plots in São Paulo, and can be observed in Figure 4-31a. The increase in UFP concentrations becomes sharp above 35 km/hr. In Figure 4-31b the same trend is observed with the error considered.

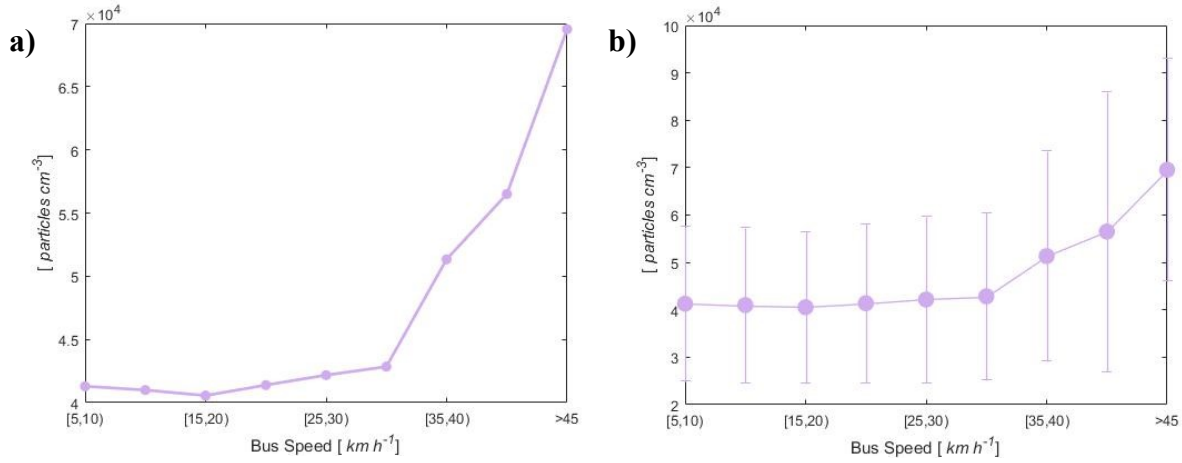

Figure 4-31: a) São Paulo UFP concentrations vs. bus speed b) São Paulo UFP concentrations vs. bus speed with error bars.

The trends observed in São Paulo are opposite the trends observed in Londrina. In São Paulo, there were clear increases across all pollutants with an increase in speed. In São Paulo, unlike Londrina, the areas that the bus is able to travel at higher speeds along this particular route are still very congested and highly trafficked roads resulting in higher concentrations of pollutants in the ambient air outside of the bus. This profile follows those that have been previously studied. As a vehicle speed increases, infiltration into the passenger cabin will be higher through larger leakage, a greater air exchange rate, and greater particle penetrations (Xu & Zhu, 2013).

4.6.3 Curitiba

In Curitiba, the trends are similar to both Londrina and São Paulo. In Figure 4-32a, the $PM_{2.5}$ shows an increasing trend in concentration with increasing bus speed, much like in the São Paulo dataset. The error plot in Figure 4-32b exhibits this same trend.

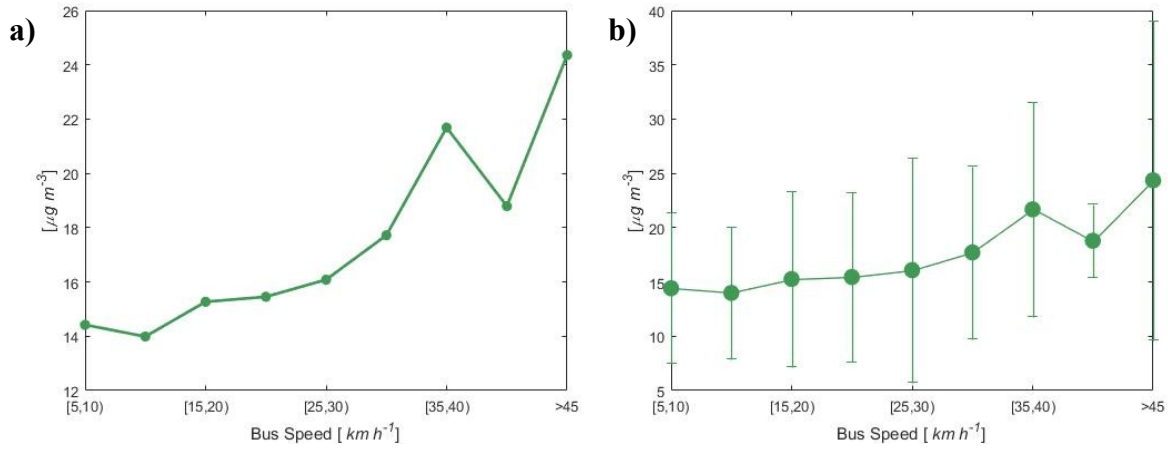

Figure 4-32: a) Curitiba $PM_{2.5}$ concentrations vs. bus speed b) Curitiba $PM_{2.5}$ concentrations vs. bus speed with error bars.

The BC concentrations also show an increasing trend with speed from the mean plot and the error plot, in Figure 4-33a and Figure 4-33b below. The increasing trend in the error plot however is not as clear as the previous plots.

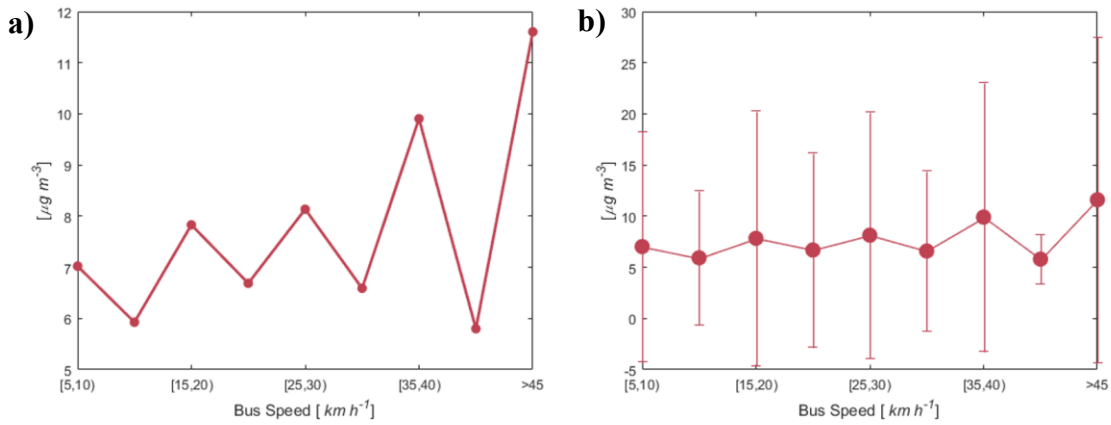

Figure 4-33: a) Curitiba BC concentrations vs. bus speed b) Curitiba BC concentrations vs. bus speed with error bars.

The UFP plots for Curitiba in Figure 4-34a and Figure 4-34b below exhibit an opposite trend to the $PM_{2.5}$ plot, and is similar to that observed in Londrina. The UFP concentrations decrease in concentration with increasing speed.

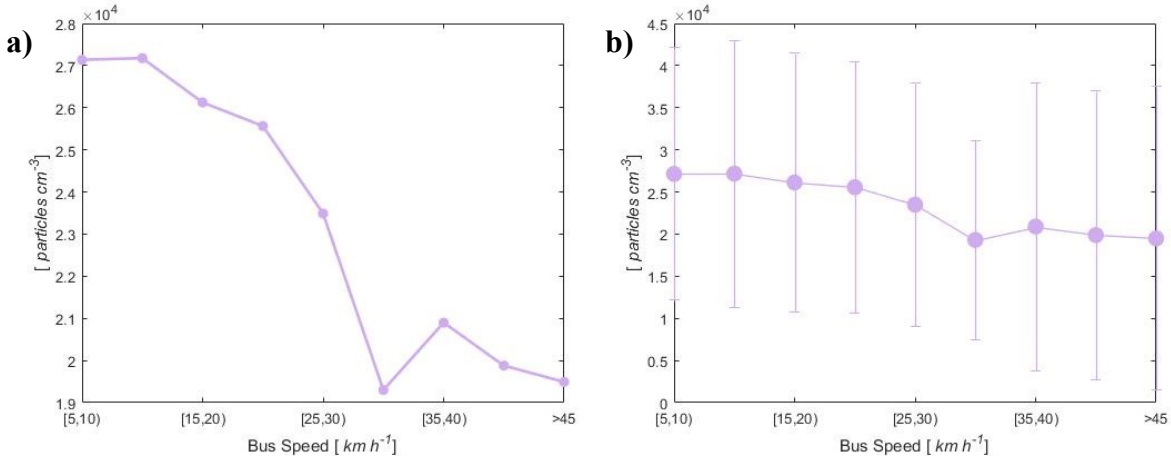

Figure 4-34: a) Curitiba UFP concentrations vs. bus speed b) Curitiba UFP concentrations vs. bus speed with error bars.

The Curitiba pollutant concentration trends with speed are more difficult to interpret than the previous other cities. The decrease in UFP observed is similar to Londrina, however it could be occurring due to the particles growing into larger particles which would result in

the increase of $PM_{2.5}$ concentrations observed. The $PM_{2.5}$ and BC both showed increases in concentration with speed, similar to what was observed in São Paulo.

Particles enter the vehicle cabin through the mechanical air supply and through leakage in the cracks in the vehicle. The amount of particle penetration is highly dependent on the pressure differential between inside the vehicle cabin and the outdoors. Lee (2013) investigated the effects of ventilation settings and driving speeds on the infiltration of UFPs into various different types of passenger vehicles. It was concluded that properly maintained cabin pressurization will prevent the infiltration of UFPs. As driving speed increases, the pressure field within the passenger cabin and around the outer surface of the vehicle changes. Typically, higher vehicle speeds lead to a higher PM penetration factor (Xu & Zhu, 2013). Higher vehicle speed leads to larger leakage, greater air exchange rate, and greater particle penetration (Xu & Zhu, 2013). Also, a higher flowrate through the mechanical ventilation system will increase UFP flow into the cabin due to lower removal efficiencies through the filter (if present) at higher flowrates. When ventilation settings are on however, the air pressure within the vehicle cabin increases thus promoting the removal of UFP. A higher mechanical airflow into the cabin can also reduce the pressure differential between inside the cabin and outdoors and can reduce leakage into the cabin. However, particles are also more likely to deposit within the vehicle cabin when ventilation settings are low (Xu & Zhu, 2013). The amount of particle penetration entering the vehicle cabin is different for every vehicle scenario. In the case of buses in Brazil, the windows were also open which adds a further complexity. Leakage into the bus is no doubt higher than if the windows were kept closed, as well as large cracks in the doors of the bus contribute to further leakage.

4.7 São Paulo Public Results

The CETESB has many air quality monitoring stations set up throughout the Municipality of São Paulo and not all stations measure the same pollutants. Data was retrieved and analysed from stations closest to the sampling route for comparison purposes to the results seen above.

The closest station to the measurement route, Cerqueira César, unfortunately only had data for PM_{10} and nitrogen dioxide (NO_2). A time series for this data on June 27th, 2016 can be seen in Figure 4-35. The measurements in São Paulo took place between the morning and afternoon rush hour pollution peaks. However, at this station, the PM_{10} concentrations are still quite elevated in the mid-afternoon. The minimum concentrations for both PM_{10} and NO_2 occurred early morning prior to the morning rush-hour. Concentrations remain elevated for the entire day.

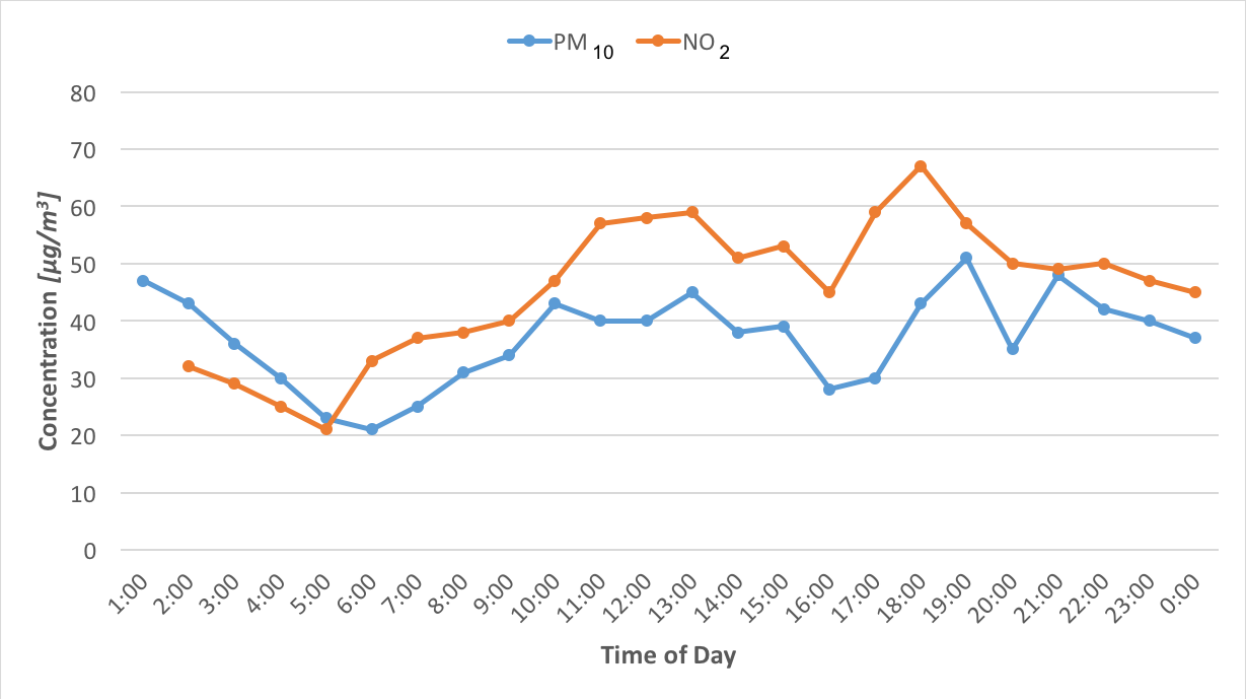

Figure 4-35: Cerqueira César station on June 27th, 2016.

Figure 4-36 below shows the 24-hour time series of hourly data at the Ibirapuera air quality station. Rises in the NO_2 and PM_{10} are clear during morning and evening rush hour, with a larger peak occurring during the evening rush hour. The delayed formation of ozone (O_3) can be observed with the peak occurring in the mid-afternoon. O_3 production requires NO_2, sunlight, and hydrocarbons hence the peak observed when

sunlight is at its strongest (Jacob, 1999). Measurements were taken during the mid-afternoon when pollutant levels, except for O_3, were lower than during rush hour.

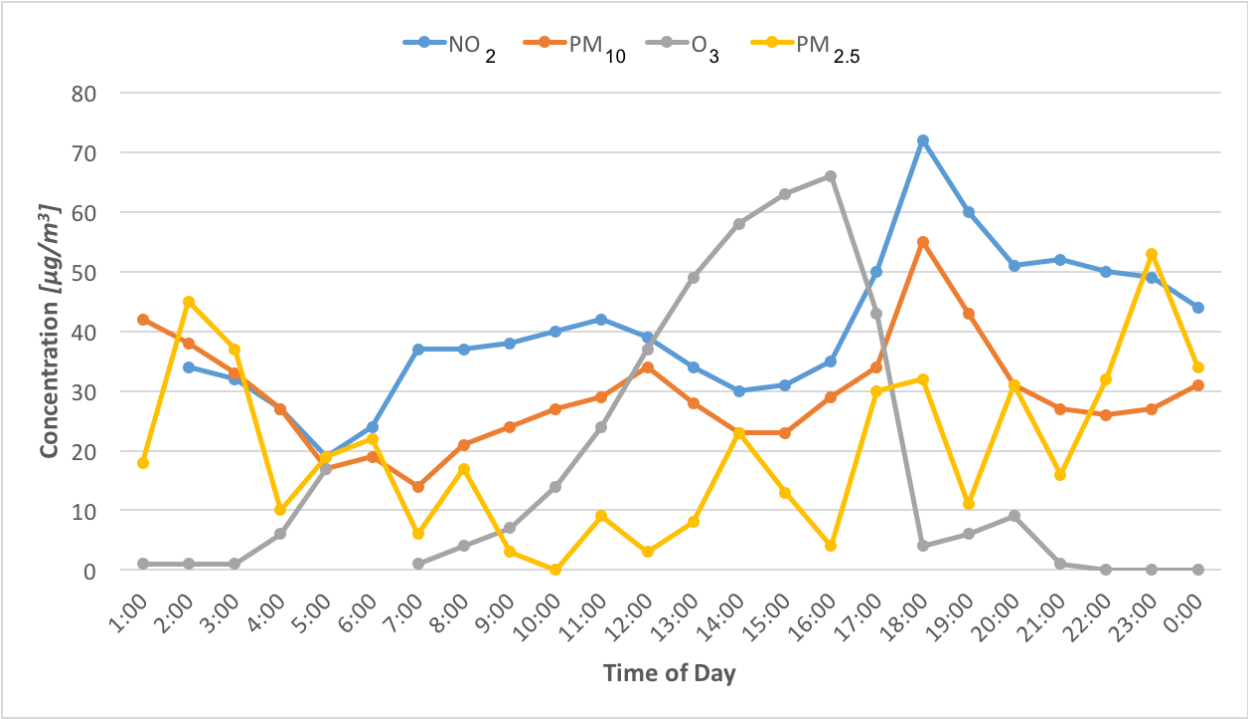

Figure 4-36: Ibirapuera station on June 27th, 2016.

The PM_{10} concentrations were also retrieved from the database and mapped. Very few stations have $PM_{2.5}$ data however, PM_{10} data was available for most monitoring stations. The one-hour averages were taken from data at 2pm for all sampling days since this hour period occurred during the measurement campaign in São Paulo. Figure 4-37 shows a map of these PM_{10} concentrations throughout the city on June 27th, 2016. The wind during this hour was blowing from the northeast direction. PM_{10} concentrations can be seen elevated downwind from the downtown core.

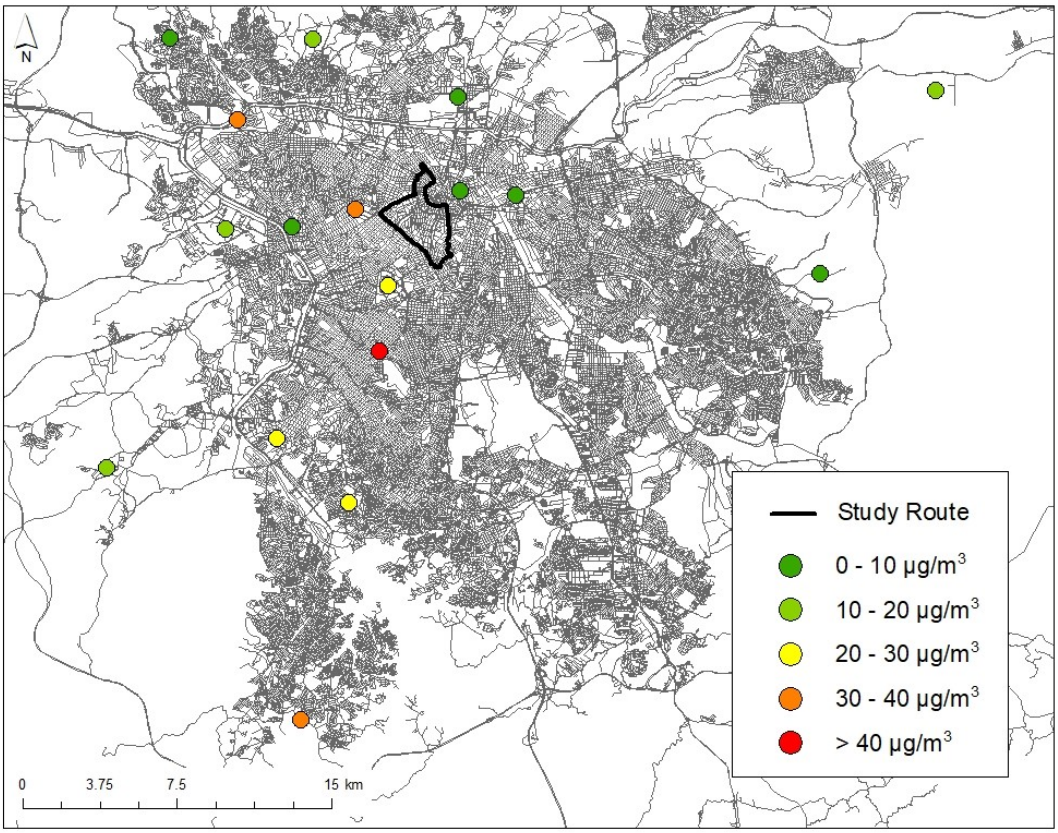

Figure 4-37: June 27, 2016 São Paulo Government PM_{10} monitoring stations.

4.8 Limitations

The main limitation of this study is the limited quantity of measurements. Measurements were only taken on two bus routes in each city which may not be representative of the entire bus fleet, land use throughout the cities, or road and traffic conditions. Measurements also took place at off-peak commuting hours likely resulting in much lower exposures than would be experienced by passengers traveling at peak hours when there are significantly more vehicles on the roads. Lastly, measurements were only conducted for a one-week period in the winter. Seasonality trends may exist, and these were not investigated.

Chapter 5 Conclusions and Recommendations

The bus mode of public transport results in a disproportionately higher passenger exposure to air pollution than other methods of transportation. High concentrations of PM in roads can lead to higher concentrations in buses. Buses stop frequently at bus stops for passengers to get on and off, as well as typically travel down main roads with high traffic characteristics. These events can allow outdoor air pollution to enter the bus passenger cabin. As well, this problem is further compounded for buses during warm weather as bus windows are left open to provide air circulation for the comfort of the passengers. Three pollutants associated with vehicle exhaust are $PM_{2.5}$, BC, and UFP. The many negative health effects due to exposure to these components of PM are well known. This thesis work was focused on quantifying and identifying the factors responsible for increased bus passenger exposure to these air pollutants in Brazil.

Air pollution studies involving different modes of transportation in Brazil are in their infancy. Vehicle emission regulations lag behind those in Europe, and those that exist only apply to new vehicles. The national air quality standards in Brazil have also not been updated since their implementation in 1990. For these reasons, Brazil was chosen as a unique environment for the location of this study. Measurements were conducted inside bus cabins in three different sized cities: Londrina, Curitiba, and São Paulo.

It was concluded that São Paulo, the largest city measured, had the highest concentrations of all three pollutants followed by Curitiba then Londrina. The main factors impacting on-board concentrations were primarily traffic lights and bus stops for São Paulo and Londrina, as was observed in the time series and the analysis of bus stop and traffic light concentrations. Curitiba however, did not observe a high increase in concentrations at locations corresponding to bus stops and traffic lights. Instead, the results of this thesis work suggest that high traffic conditions contributed heavily to elevated concentrations. A possible reason for this discrepancy was that the downtown core of Curitiba is a traffic-

calmed area and has imposed speed limits lower than those observed in Londrina and São Paulo. At a lower vehicle speed, pollutants may readily enter the passenger cabin as the bus is traveling down the road, and the lower speed may reduce the amount of ventilation through the cabin. When investigating the speed of the bus and its relation to on-board air pollution, it was found that each city had a unique profile. In Londrina, PM concentrations decreased with speed. In São Paulo, PM concentrations increased with speed. The relationship between concentrations and speed in Curitiba varied for the different pollutant types. The amount of infiltration of PM at increasing speeds is highly dependent on the pressurization of the vehicle and each vehicle will have a unique profile.

It was also observed that within the bus, pollution concentrations would accumulate and sometimes resulted in spikes that kept increasing. These often occurred when several bus stops and/or traffic lights occurred in succession, clearly through an elevated pollution area so each time the bus stopped more PM entered the bus. Within the bus cabin, PM pollutants exhibited a slower decay rate due to the PM being essentially trapped in the cabin where air flow is minimal. Spikes that occurred in open ventilation settings, for example at bus terminals or along the street, did not exhibit this same decay feature. If windows are open on the bus, as they frequently were in these measurements, ventilation can be increased within the bus thus aiding to remove the pollutants from the bus cabin. However, the open windows also facilitate the direct entry of air pollution from the street into the bus.

From the pollution maps, some trends between all cities were apparent. When the bus was traveling through residential neighbourhoods (in Londrina and São Paulo since Curitiba measurements were only taken in the urban centre), concentrations were lower. As the bus traveled into the downtown centre along busy roads, PM concentrations increased. Concentrations were notably larger along narrow roads, likely due to the road being a street canyon and vehicle emissions accumulating in the street.

Buses often operate with their windows open when weather is warm, however this can lead to increased PM concentrations in the vehicle cabin. It is recommended that further studies be conducted on buses in Brazil comparing the PM concentrations in buses under different ventilation scenarios to investigate the ideal method to reduce pollution concentrations within buses. Since vehicle traffic contributed to concentrations of air pollution with the cabin, further studies are necessary to simultaneously assess the pollution concentrations outside of the bus compared to inside the bus while the bus is completing its route. This is necessary to understand how pollution concentrations from outside of the bus influence concentrations within the bus in more detail and under different traffic scenarios.

References

Adams, H. S., Nieuwenhuijsen, M. J., Colvile, R. N., McMullen, M. A. S., & Khandelwal, P. (2001). Fine particle (PM2.5) personal exposure levels in transport microenvironments, London, UK. *The Science of the Total Environment*, *279*(1–3), 29–44. https://doi.org/10.1016/S0048-9697(01)00723-9

Andrade, M. de F., de Miranda, R. M., Fornaro, A., Kerr, A., Oyama, B., de Andre, P. A., & Saldiva, P. (2012). Vehicle emissions and PM2.5 mass concentrations in six Brazilian cities. *Air Quality, Atmosphere & Health*, *5*(1), 79–88. https://doi.org/10.1007/s11869-010-0104-5

Andrade, M. de F., Kumar, P., de Freitas, E. D., Ynoue, R. Y., Martins, J., Martins, L. D., … Zhang, Y. (2017). Air quality in the megacity of São Paulo: Evolution over the last 30 years and future perspectives. *Atmospheric Environment*, *159*, 66–82. https://doi.org/10.1016/j.atmosenv.2017.03.051

Andreae, M. O., & Gelencsér, A. (2006). Black carbon or brown carbon? The nature of light-absorbing carbonaceous aerosols. *Atmospheric Chemistry and Physics*, *6*(10), 3131–3148.

Betancourt, R. M., Galvis, B., Balachandran, S., Ramos-Bonilla, J. P., Sarmiento, O. L., Gallo-Murcia, S. M., & Contreras, Y. (2017). Exposure to fine particulate, black carbon, and particle number concentration in transportation microenvironments. *Atmospheric Environment*, *157*, 135–145. https://doi.org/10.1016/j.atmosenv.2017.03.006

Bond, T. C., & Bergstrom, R. W. (2006). Light Absorption by Carbonaceous Particles: An Investigative Review. *Aerosol Science and Technology*, *40*(1), 27–67. https://doi.org/10.1080/02786820500421521

Bond, T. C., Doherty, S. J., Fahey, D. W., Forster, P. M., Berntsen, T., DeAngelo, B. J., … Zender, C. S. (2013). Bounding the role of black carbon in the climate system: A scientific assessment: BLACK CARBON IN THE CLIMATE SYSTEM. *Journal of Geophysical Research: Atmospheres*, *118*(11), 5380–5552. https://doi.org/10.1002/jgrd.50171

Borken, J., Steller, H., Merétei, T., & Vanhove, F. (2007). Global and Country Inventory of Road Passenger and Freight Transportation: Fuel Consumption and Emissions of Air Pollutants in Year 2000. *Transportation Research Record: Journal of the Transportation Research Board*, *2011*, 127–136. https://doi.org/10.3141/2011-14

Both, A. F., Westerdahl, D., Fruin, S., Haryanto, B., & Marshall, J. D. (2013). Exposure to carbon monoxide, fine particle mass, and ultrafine particle number in Jakarta, Indonesia: Effect of commute mode. *Science of The Total Environment*, *443*, 965–972. https://doi.org/10.1016/j.scitotenv.2012.10.082

Brace, M. D., Stevens, E., Taylor, S. M., Butt, S., Sun, Z., Hu, L., … Gibson, M. D. (2014). "The air that we breathe": assessment of laser and electrosurgical dissection devices on operating theater air quality. *Journal of Otolaryngology - Head & Neck Surgery*, *43*(1), 39. https://doi.org/10.1186/s40463-014-0039-1

Brook, R. D. (2004). Air Pollution and Cardiovascular Disease: A Statement for Healthcare Professionals From the Expert Panel on Population and Prevention Science of the American Heart Association. *Circulation*, *109*(21), 2655–2671. https://doi.org/10.1161/01.CIR.0000128587.30041.C8

Buccolieri, R., Sandberg, M., & Di Sabatino, S. (2010). City breathability and its link to pollutant concentration distribution within urban-like geometries. *Atmospheric Environment*, *44*(15), 1894–1903.

CAF. (2009). *Observatorio de Movilidad Urbana para América Latina: Información para mejores políticas y mejores ciedades*. Retrieved from www.caf.com/publicaciones

Cao, J., Chow, J. C., Lee, F. S. C., & Watson, J. G. (2013). Evolution of PM2.5 Measurements and Standards in the U.S. and Future Perspectives for China. *Aerosol and Air Quality Research*. https://doi.org/10.4209/aaqr.2012.11.0302

Castanho, A. D. A., & Artaxo, P. (2001). Wintertime and summertime São Paulo aerosol source apportionment study. *Atmospheric Environment*, *35*, 4889–4902.

Castro, L. M., Pio, C. A., Harrison, R. M., & Smith, D. J. T. (1999). Carbonaceous aerosol in urban and rural European atmospheres: estimation of secondary organic carbon concentrations. *Atmospheric Environment*, *33*(17), 2771–2781.

Cattaneo, A., Garramone, G., Taronna, M., Peruzzo, C., & Cavallo, D. M. (2009). Personal exposure to airborne ultrafine particles in the urban area of Milan. *Journal of Physics: Conference Series*, *151*, 012039. https://doi.org/10.1088/1742-6596/151/1/012039

CET. (2013). *Pesquisa de Monitoração da Fluidez* (Desempenho do Sistema Viário Principal: Volume e Velocidade - 2012).

CETESB. (2018). Qualidade do Ar. Retrieved February 12, 2018, from http://sistemasinter.cetesb.sp.gov.br/Ar/php/mapa_qualidade_rmsp.php

Chan, L. Y., Lau, W. L., Lee, S. C., & Chan, C. Y. (2002a). Commuter exposure to particulate matter in public transportation modes in Hong Kong. *Atmospheric Environment*, *36*(21), 3363–3373. https://doi.org/10.1016/S1352-2310(02)00318-7

Chan, L. Y., Lau, W. L., Zou, S. C., Cao, Z. X., & Lai, S. C. (2002b). Exposure level of carbon monoxide and respirable suspended particulate in public transportation modes while commuting in urban area of Guangzhou, China. *Atmospheric Environment*, *36*(38), 5831–5840.

Chen, R., Hu, B., Liu, Y., Xu, J., Yang, G., Xu, D., & Chen, C. (2016). Beyond PM2.5: The role of ultrafine particles on adverse health effects of air pollution. *Biochimica et Biophysica Acta (BBA) - General Subjects*, *1860*(12), 2844–2855. https://doi.org/10.1016/j.bbagen.2016.03.019

Cheng, Y.-H., Lin, Y.-L., & Liu, C.-C. (2008). Levels of PM10 and PM2.5 in Taipei Rapid Transit System. *Atmospheric Environment*, *42*(31), 7242–7249. https://doi.org/10.1016/j.atmosenv.2008.07.011

Costabile, F., Birmili, W., Klose, S., Tuch, T., Wehner, B., Wiedensohler, A., … Sonntag, A. (2009). Spatio-temporal variability and principal components of the particle number size distribution in an urban atmosphere. *Atmospheric Chemistry and Physics*, *9*(9), 3163–3195.

Cyrys, J., Stölzel, M., Heinrich, J., Kreyling, W. G., Menzel, N., Wittmaack, K., … Wichmann, H.-E. (2003). Elemental composition and sources of fine and ultrafine ambient particles in Erfurt, Germany. *Science of the Total Environment*, *305*(1), 143–156.

de Miranda, R. M., Lopes, F., do Rosário, N. É., Yamasoe, M. A., Landulfo, E., & de Fatima Andrade, M. (2017). The relationship between aerosol particles chemical composition and optical properties to identify the biomass burning contribution to fine particles concentration: a case study for São Paulo city, Brazil. *Environmental Monitoring and Assessment*, *189*(1). https://doi.org/10.1007/s10661-016-5659-7

de Nazelle, A., Fruin, S., Westerdahl, D., Martinez, D., Ripoll, A., Kubesch, N., & Nieuwenhuijsen, M. (2012). A travel mode comparison of commuters' exposures to air pollutants in Barcelona. *Atmospheric Environment*, *59*, 151–159.

DENATRAN. (2018). Departamento Nacional de Transito. Retrieved February 20, 2018, from http://www.denatran.gov.br/

Dockery, D. W., Pope, C. A., Xu, X., Spengler, J. D., Ware, J. H., Fay, M. E., … Speizer, F. E. (1993). An association between air pollution and mortality in six U.S. cities. *The New England Journal of Medicine*, *329*(24), 1753–1759. https://doi.org/10.1056/NEJM199312093292401

Dockery, D. W., & Stone, P. H. (2007). *Cardiovascular risks from fine particulate air pollution*. Mass Medical Soc.

Dons, E., Panis, L. I., Van Poppel, M., Theunis, J., & Wets, G. (2012). Personal exposure to black carbon in transport microenvironments. *Atmospheric Environment*, *55*, 392–398.

Ehn, M., Thornton, J. A., Kleist, E., Sipilä, M., Junninen, H., Pullinen, I., … Mentel, T. F. (2014). A large source of low-volatility secondary organic aerosol. *Nature*, *506*(7489), 476–479. https://doi.org/10.1038/nature13032

Fajardo, O. A., & Rojas, N. Y. (2012). Particulate matter exposure of bicycle path users in a high-altitude city. *Atmospheric Environment*, *46*, 675–679.

Fruin, S., Westerdahl, D., Sax, T., Sioutas, C., & Fine, P. M. (2008). Measurements and predictors of on-road ultrafine particle concentrations and associated pollutants in Los Angeles. *Atmospheric Environment*, *42*(2), 207–219. https://doi.org/10.1016/j.atmosenv.2007.09.057

Fuzzi, S., Baltensperger, U., Carslaw, K., Decesari, S., Denier van der Gon, H., Facchini, M. C., … Gilardoni, S. (2015). Particulate matter, air quality and climate: lessons learned and future needs. *Atmospheric Chemistry and Physics*, *15*(14), 8217–8299. https://doi.org/10.5194/acp-15-8217-2015

Geller, M. D., Fine, P. M., & Sioutas, C. (2004). The Relationship between Real-Time and Time-Integrated Coarse (2.5–10 μm), Intermodal (1–2.5 μm), and Fine (<2.5 μm) Particulate Matter in the Los Angeles Basin. *Journal of the Air & Waste Management Association*, *54*(9), 1029–1039. https://doi.org/10.1080/10473289.2004.10470980

Geller, M. D., Ntziachristos, L., Mamakos, A., Samaras, Z., Schmitz, D. A., Froines, J. R., & Sioutas, C. (2006). Physicochemical and redox characteristics of particulate matter (PM) emitted from gasoline and diesel passenger cars. *Atmospheric Environment*, *40*(36), 6988–7004.

Gibson, M. (2004). *Source apportionment of PM10 in Glasgow* (PhD). University of Strathclyde.

Gibson, M. D., Haelssig, J., Pierce, J. R., Parrington, M., Franklin, J. E., Hopper, J. T., … Ward, T. J. (2015). A comparison of four receptor models used to quantify the boreal wildfire smoke contribution to surface $PM_{2.5}$ in Halifax, Nova Scotia during the BORTAS-B experiment. *Atmospheric Chemistry and Physics*, *15*(2), 815–827. https://doi.org/10.5194/acp-15-815-2015

Gibson, M. D., Heal, M. R., Bache, D. H., Hursthouse, A. S., Beverland, I. J., Craig, S. E., … Jones, C. (2009). Using Mass Reconstruction along a Four-Site Transect as a Method to Interpret PM_{10} in West-Central Scotland, United Kingdom. *Journal of the Air & Waste Management Association*, *59*(12), 1429–1436. https://doi.org/10.3155/1047-3289.59.12.1429

Gibson, M. D., Heal, M. R., Li, Z., Kuchta, J., King, G. H., Hayes, A., & Lambert, S. (2013). The spatial and seasonal variation of nitrogen dioxide and sulfur dioxide in Cape Breton Highlands National Park, Canada, and the association with lichen abundance. *Atmospheric Environment*, *64*, 303–311. https://doi.org/10.1016/j.atmosenv.2012.09.068

Gibson, M. D., Pierce, J. R., Waugh, D., Kuchta, J. S., Chisholm, L., Duck, T. J., … Palmer, P. I. (2013). Identifying the sources driving observed $PM_{2.5}$ temporal variability over Halifax, Nova Scotia, during BORTAS-B. *Atmospheric Chemistry and Physics*, *13*(14), 7199–7213. https://doi.org/10.5194/acp-13-7199-2013

Gómez-Perales, J. E., Colvile, R. N., Fernández-Bremauntz, A. A., Gutiérrez-Avedoy, V., Páramo-Figueroa, V. H., Blanco-Jiménez, S., … Hidalgo-Navarro, M. (2007). Bus, minibus, metro inter-comparison of commuters' exposure to air pollution in Mexico City. *Atmospheric Environment*, *41*(4), 890–901.

Gómez-Perales, J. E., Colvile, R. N., Nieuwenhuijsen, M. J., Fernandez-Bremauntz, A., Gutierrez-Avedoy, V. J., Paramo-Figueroa, V. H., … Bernabe-Cabanillas, R. (2004). Commuters' exposure to PM2. 5, CO, and benzene in public transport in the metropolitan area of Mexico City. *Atmospheric Environment*, *38*(8), 1219–1229.

Grana, M., Toschi, N., Vicentini, L., Pietroiusti, A., & Magrini, A. (2017). Exposure to ultrafine particles in different transport modes in the city of Rome. *Environmental Pollution*, *228*, 201–210. https://doi.org/10.1016/j.envpol.2017.05.032

Ham, W., Vijayan, A., Schulte, N., & Herner, J. D. (2017). Commuter exposure to PM 2.5, BC, and UFP in six common transport microenvironments in Sacramento, California. *Atmospheric Environment*, *167*, 335–345. https://doi.org/10.1016/j.atmosenv.2017.08.024

Han, Y.-Y., Donovan, M., & Sung, F.-C. (2010). Increased urinary 8-hydroxy-2′-deoxyguanosine excretion in long-distance bus drivers in Taiwan. *Chemosphere*, *79*(9), 942–948. https://doi.org/10.1016/j.chemosphere.2010.02.057

Harik, G., El-Fadel, M., Shihadeh, A., Alameddine, I., & Hatzopoulou, M. (2017). Is in-cabin exposure to carbon monoxide and fine particulate matter amplified by the vehicle's self-pollution potential? Quantifying the rate of exhaust intrusion. *Transportation Research Part D: Transport and Environment*, *54*, 225–238. https://doi.org/10.1016/j.trd.2017.05.009

Harrison, R. M., Jones, A. M., & Lawrence, R. G. (2003). A pragmatic mass closure model for airborne particulate matter at urban background and roadside sites. *Atmospheric Environment*, *37*(35), 4927–4933.

Harrison, R. M., & Yin, J. (2000). Particulate matter in the atmosphere: which particle properties are important for its effects on health? *The Science of the Total Environment*, *249*(1–3), 85–101. https://doi.org/10.1016/S0048-9697(99)00513-6

Hill, L. B., Zimmerman, N. J., & Gooch, J. (2005). *A multi-city investigation of the effectiveness of retrofit emissions controls in reducing exposures to particulate matter in school buses*. Clean Air Task Force Boston, MA.

Hinds, W. C. (1999). *Aerosol Technology* (Second Edition). New York, NY, USA: John Wiley & Sons, Inc.

Huang, J., Deng, F., Wu, S., & Guo, X. (2012). Comparisons of personal exposure to PM2.5 and CO by different commuting modes in Beijing, China. *Science of The Total Environment*, *425*, 52–59. https://doi.org/10.1016/j.scitotenv.2012.03.007

IBGE. (2017). Instituto Brasileiro de Geografia e Estatística. Retrieved February 17, 2018, from https://ibge.gov.br/

ICCT. (2017). *Effect of P-8 standards on bus system costs in Brazil*. Retrieved from https://www.theicct.org/publications/effect-p-8-standards-bus-system-costs-brazil

IPPUC. (2012). Pesquisa Contagem de Tráfego. Retrieved February 12, 2018, from http://www.ippuc.org.br/mostrarpagina.php?pagina=335&idioma=1&ampliar=n%E3o

Jacob, D. J. (1999). *Atmospheric Chemistry*. Princeton, New Jersey: Princeton University Press.

Jacobson, M. Z. (2001). Strong radiative heating due to the mixing state of black carbon in atmospheric aerosols. *Nature*, *409*, 695.

Janssen, N. A., Hoek, G., Simic-Lawson, M., Fischer, P., Keuken, M., Atkinson, R. W., … Cassee, F. R. (2011). Black carbon as an additional indicator of the adverse health effects of airborne particles compared with PM10 and PM2. 5. *Environmental Health Perspectives*, *119*(12), 1691–1699. https://doi.org/10.1289/ehp.1003369

Kaur, S., Nieuwenhuijsen, M., & Colvile, R. (2005). Personal exposure of street canyon intersection users to PM 2.5, ultrafine particle counts and carbon monoxide in Central London, UK. *Atmospheric Environment*, *39*(20), 3629–3641.

Keuken, M. P., Moerman, M., Voogt, M., Blom, M., Weijers, E. P., Röckmann, T., & Dusek, U. (2013). Source contributions to PM2. 5 and PM10 at an urban background and a street location. *Atmospheric Environment*, *71*, 26–35.

Kingham, S., Durand, M., Aberkane, T., Harrison, J., Gaines Wilson, J., & Epton, M. (2006). Winter comparison of TEOM, MiniVol and DustTrak PM10 monitors in a woodsmoke environment. *Atmospheric Environment*, *40*(2), 338–347. https://doi.org/10.1016/j.atmosenv.2005.09.042

Kingham, S., Pearce, J., & Zawar-Reza, P. (2007). Driven to injustice? Environmental justice and vehicle pollution in Christchurch, New Zealand. *Transportation Research Part D: Transport and Environment*, *12*(4), 254–263. https://doi.org/10.1016/j.trd.2007.02.004

Kittelson, D. B. (1998). Engines and nano-particles: a review. *Journal of Aerosol Science*, *29*(5/6), 575–588.

Knibbs, L. D., & de Dear, R. J. (2010). Exposure to ultrafine particles and PM2.5 in four Sydney transport modes. *Atmospheric Environment*, *44*(26), 3224–3227. https://doi.org/10.1016/j.atmosenv.2010.05.026

Kongtip, P., Anthayanon, T., Yoosook, W., & Onchoi, C. (2012). Exposure to Particulate Matter, CO2, CO, VOCs among Bus Drivers in Bangkok. *J Med Assoc Thai*, *95*(Suppl. 6), S169–S178.

Krecl, P., Targino, A. C., Johansson, C., & Ström, J. (2015). Characterisation and Source Apportionment of Submicron Particle Number Size Distributions in a Busy Street Canyon. *Aerosol and Air Quality Research*. https://doi.org/10.4209/aaqr.2014.06.0108

Krecl, P., Targino, A. C., Wiese, L., Ketzel, M., & de Paula Corrêa, M. (2016). Screening of short-lived climate pollutants in a street canyon in a mid-sized city in Brazil. *Atmospheric Pollution Research*, *7*(6), 1022–1036. https://doi.org/10.1016/j.apr.2016.06.004

Kulmala, M., Vehkamäki, H., Petäjä, T., Dal Maso, M., Lauri, A., Kerminen, V.-M., … McMurry, P. H. (2004). Formation and growth rates of ultrafine atmospheric particles: a review of observations. *Journal of Aerosol Science*, *35*(2), 143–176. https://doi.org/10.1016/j.jaerosci.2003.10.003

Kumar, P., de Fatima Andrade, M., Ynoue, R. Y., Fornaro, A., de Freitas, E. D., Martins, J., … Morawska, L. (2016). New directions: From biofuels to wood stoves: The modern and ancient air quality challenges in the megacity of São Paulo. *Atmospheric Environment*, *140*, 364–369. https://doi.org/10.1016/j.atmosenv.2016.05.059

Kumar, P., Fennell, P., & Britter, R. (2008). Measurements of particles in the 5–1000 nm range close to road level in an urban street canyon. *Science of The Total Environment*, *390*(2–3), 437–447. https://doi.org/10.1016/j.scitotenv.2007.10.013

Kumar, P., Morawska, L., Birmili, W., Paasonen, P., Hu, M., Kulmala, M., … Britter, R. (2014). Ultrafine particles in cities. *Environment International*, *66*, 1–10. https://doi.org/10.1016/j.envint.2014.01.013

Kupiainen, K., & Klimont, Z. (2007). Primary emissions of fine carbonaceous particles in Europe. *Atmospheric Environment*, *41*(10), 2156–2170. https://doi.org/10.1016/j.atmosenv.2006.10.066

Lee, E. S. (2013). *Passenger Exposures to Ultrafine Particles and In-cabin Air Quality Control* (PhD). University of California Los Angeles.

Li, B., Lei, X., Xiu, G., Gao, C., Gao, S., & Qian, N. (2015). Personal exposure to black carbon during commuting in peak and off-peak hours in Shanghai. *Science of The Total Environment*, *524–525*, 237–245. https://doi.org/10.1016/j.scitotenv.2015.03.088

Li, Z., Che, W., Frey, H. C., & Lau, A. K. H. (2018). Factors affecting variability in PM 2.5 exposure concentrations in a metro system. *Environmental Research*, *160*, 20–26. https://doi.org/10.1016/j.envres.2017.09.006

Lim, S., Dirks, K. N., Salmond, J. A., & Xie, S. (2015). Determinants of spikes in ultrafine particle concentration whilst commuting by bus. *Atmospheric Environment*, *112*, 1–8. https://doi.org/10.1016/j.atmosenv.2015.04.025

MacDougall, D., & Crummett, W. B. (1980). Guidelines for data acquisition and data quality evaluation in environmental chemistry. *Analytical Chemistry*, *52*(14), 2242–2249.

Macedo, J. (2004). Curitiba. *Cities*, *21*(6), 537–549. https://doi.org/10.1016/j.cities.2004.08.008

MacNeill, M., Kearney, J., Wallace, L., Gibson, M., Héroux, M. E., Kuchta, J., … Wheeler, A. J. (2014). Quantifying the contribution of ambient and indoor-generated fine particles to indoor air in residential environments. *Indoor Air*, *24*(4), 362–375. https://doi.org/10.1111/ina.12084

Marshall, J. D., & Behrentz, E. (2005). Vehicle Self-Pollution Intake Fraction: Children's Exposure to School Bus Emissions. *Environmental Science & Technology*, *39*(8), 2559–2563. https://doi.org/10.1021/es040377v

Marshall, J. D., Brauer, M., & Frank, L. D. (2009). Healthy Neighborhoods: Walkability and Air Pollution. *Environmental Health Perspectives*, *117*(11), 1752–1759. https://doi.org/10.1289/ehp.0900595

Martins, L. D., da Silva Júnior, C. R., Solci, M. C., Pinto, J. P., Souza, D. Z., Vasconcellos, P., … de Andrade, J. B. (2012). Particle emission from heavy-duty engine fuelled with blended diesel and biodiesel. *Environmental Monitoring and Assessment*, *184*(5), 2663–2676. https://doi.org/10.1007/s10661-011-2142-3

Mohankumar, S., & Senthilkumar, P. (2017). Particulate matter formation and its control methodologies for diesel engine: A comprehensive review. *Renewable and Sustainable Energy Reviews*, *80*, 1227–1238. https://doi.org/10.1016/j.rser.2017.05.133

Moosmüller, H., Chakrabarty, R. K., & Arnott, W. P. (2009). Aerosol light absorption and its measurement: A review. *Journal of Quantitative Spectroscopy and Radiative Transfer*, *110*(11), 844–878. https://doi.org/10.1016/j.jqsrt.2009.02.035

Morawska, L., Ristovski, Z., Jayaratne, E. R., Keogh, D. U., & Ling, X. (2008). Ambient nano and ultrafine particles from motor vehicle emissions: characteristics, ambient processing and implications on human exposure. *Atmospheric Environment*, *42*(35), 8113–8138.

Moreno, T., Reche, C., Rivas, I., Cruz Minguillón, M., Martins, V., Vargas, C., … Gibbons, W. (2015). Urban air quality comparison for bus, tram, subway and pedestrian commutes in Barcelona. *Environmental Research*, *142*, 495–510. https://doi.org/10.1016/j.envres.2015.07.022

Nikolova, I., Janssen, S., Vos, P., Vrancken, K., Mishra, V., & Berghmans, P. (2011). Dispersion modelling of traffic induced ultrafine particles in a street canyon in Antwerp, Belgium and comparison with observations. *Science of The Total Environment*, *412–413*, 336–343. https://doi.org/10.1016/j.scitotenv.2011.09.081

Nogueira, T., Cordeiro, D. de S., Muñoz, R. A. A., Fornaro, A., Miguel, A. H., & Andrade, M. de F. (2015). Bioethanol and Biodiesel as Vehicular Fuels in Brazil — Assessment of Atmospheric Impacts from the Long Period of Biofuels Use. In K. Biernat (Ed.), *Biofuels - Status and Perspective*. InTech. https://doi.org/10.5772/60944

Nyhan, M., McNabola, A., & Misstear, B. (2014). Comparison of particulate matter dose and acute heart rate variability response in cyclists, pedestrians, bus and train passengers. *Science of The Total Environment*, *468–469*, 821–831. https://doi.org/10.1016/j.scitotenv.2013.08.096

Oberdörster, G., Oberdörster, E., & Oberdörster, J. (2005). Nanotoxicology: An Emerging Discipline Evolving from Studies of Ultrafine Particles. *Environmental Health Perspectives*, *113*(7), 823–839. https://doi.org/10.1289/ehp.7339

O'dowd, C. D., Aalto, P., Hmeri, K., Kulmala, M., & Hoffmann, T. (2002). Aerosol formation: Atmospheric particles from organic vapours. *Nature*, *416*(6880), 497–498.

Okokon, E. O., Yli-Tuomi, T., Turunen, A. W., Taimisto, P., Pennanen, A., Vouitsis, I., … Lanki, T. (2017). Particulates and noise exposure during bicycle, bus and car commuting: A study in three European cities. *Environmental Research*, *154*, 181–189. https://doi.org/10.1016/j.envres.2016.12.012

Onat, B., & Stakeeva, B. (2013). Personal exposure of commuters in public transport to PM2.5 and fine particle counts. *Atmospheric Pollution Research*, *4*(3), 329–335. https://doi.org/10.5094/APR.2013.037

O'Neill, M. S., Jerrett, M., Kawachi, I., Levy, J. I., Cohen, A. J., Gouveia, N., … Conditions, S. (2003). Health, Wealth, and Air Pollution: Advancing Theory and Methods. *Environmental Health Perspectives*, *111*(16), 1861–1870. https://doi.org/10.1289/ehp.6334

Park, S. S., Kozawa, K., Fruin, S., Mara, S., Hsu, Y.-K., Jakober, C., … Herner, J. (2011). Emission Factors for High-Emitting Vehicles Based on On-Road Measurements of Individual Vehicle Exhaust with a Mobile Measurement Platform. *Journal of the Air & Waste Management Association*, *61*(10), 1046–1056. https://doi.org/10.1080/10473289.2011.595981

Pérez-Martínez, P. J., Miranda, R. M., Nogueira, T., Guardani, M. L., Fornaro, A., Ynoue, R., & Andrade, M. F. (2014). Emission factors of air pollutants from vehicles measured inside road tunnels in São Paulo: case study comparison. *International Journal of Environmental Science and Technology*, *11*(8), 2155–2168. https://doi.org/10.1007/s13762-014-0562-7

Peters, J., Van den Bossche, J., Reggente, M., Van Poppel, M., De Baets, B., & Theunis, J. (2014). Cyclist exposure to UFP and BC on urban routes in Antwerp, Belgium. *Atmospheric Environment*, *92*, 31–43. https://doi.org/10.1016/j.atmosenv.2014.03.039

Pope, C. A. (2000). Epidemiology of fine particulate air pollution and human health: biologic mechanisms and who's at risk? *Environmental Health Perspectives*, *108*(Suppl 4), 713–723.

Pope, C. A., Burnett, R. T., Thun, M. J., Calle, E. E., Krewski, D., Ito, K., & Thurston, G. D. (2002). Lung Cancer, cardiopulmonary mortality, and long-term exposure to fine particulate air pollution. *The Journal of the American Medical Association*, *287*(9), 1132–1141.

Prefeitura de Curitiba. (2015, September 18). Prefeitura cria Área Calma no Centro, com velocidade reduzida, mais árvores e melhorias na acessibilidade. Retrieved February 16, 2018, from http://www.curitiba.pr.gov.br/noticias/prefeitura-cria-area-calma-no-centro-com-velocidade-reduzida-mais-arvores-e-melhorias-na-acessibilidade/37602

Putaud, J.-P., Van Dingenen, R., Alastuey, A., Bauer, H., Birmili, W., Cyrys, J., … Hansson, H.-C. (2010). A European aerosol phenomenology–3: Physical and chemical characteristics of particulate matter from 60 rural, urban, and kerbside sites across Europe. *Atmospheric Environment*, *44*(10), 1308–1320.

Qiu, Z., Song, J., Xu, X., Luo, Y., Zhao, R., Zhou, W., … Hao, Y. (2017). Commuter exposure to particulate matter for different transportation modes in Xi'an, China. *Atmospheric Pollution Research*, *8*(5), 940–948. https://doi.org/10.1016/j.apr.2017.03.005

Ragettli, M. S., Corradi, E., Braun-Fahrländer, C., Schindler, C., de Nazelle, A., Jerrett, M., … Phuleria, H. C. (2013). Commuter exposure to ultrafine particles in difference urban locations, transportation modes and routes. *Measurement and Modeling of Short-and Long-Term Commuter Exposure to Traffic-Related Air Pollution*, *77*, 11.

Ramachandran, K., & Tsokos, C. (2015). *Mathematical Statistics with Applicatoins in R* (Second Edition). Oxford, UK: Academic Press.

Ramanathan, V., & Carmichael, G. (2008). Global and regional climate changes due to black carbon. *Nature Geoscience*, *1*(4), 221–227. https://doi.org/10.1038/ngeo156

Ré-Poppi, N., Almeida, F. F. P., Cardoso, C. A. L., Raposo, J. L., Viana, L. H., Silva, T. Q., … Ferreira, V. S. (2009). Screening analysis of type C Brazilian gasoline by gas chromatography – Flame ionization detector. *Fuel*, *88*(3), 418–423. https://doi.org/10.1016/j.fuel.2008.10.014

Rivas, I., Kumar, P., & Hagen-Zanker, A. (2017). Exposure to air pollutants during commuting in London: Are there inequalities among different socio-economic groups? *Environment International*, *101*, 143–157. https://doi.org/10.1016/j.envint.2017.01.019

Sánchez-Ccoyllo, O. R., Ynoue, R. Y., Martins, L. D., Astolfo, R., Miranda, R. M., Freitas, E. D., … Andrade, M. F. (2009). Vehicular particulate matter emissions in road tunnels in Sao Paulo, Brazil. *Environmental Monitoring and Assessment*, *149*(1–4), 241–249. https://doi.org/10.1007/s10661-008-0198-5

Silverman, D. T., Samanic, C. M., Lubin, J. H., Blair, A. E., Stewart, P. A., Vermeulen, R., … Attfield, M. D. (2012). The Diesel Exhaust in Miners Study: A Nested Case-Control Study of Lung Cancer and Diesel Exhaust. *JNCI Journal of the National Cancer Institute*, *104*(11), 855–868. https://doi.org/10.1093/jnci/djs034

Simepar. (2018). Tecnologia e Informações Ambientais. Retrieved February 12, 2018, from http://simepar.br/

Simon, M. C., Hudda, N., Naumova, E. N., Levy, J. I., Brugge, D., & Durant, J. L. (2017). Comparisons of traffic-related ultrafine particle number concentrations measured in two urban areas by central, residential, and mobile monitoring. *Atmospheric Environment*, *169*, 113–127. https://doi.org/10.1016/j.atmosenv.2017.09.003

Smith, O. I. (1981). Fundamentals of soot formation in flames with application to diesel engine particulate emissions. *Progress in Energy and Combustion Science*, *7*(4), 275–291.

Snider, G., Weagle, C. L., Murdymootoo, K. K., Ring, A., Ritchie, Y., Stone, E., … Martin, R. V. (2016). Variation in global chemical composition of $PM_{2.5}$: emerging results from SPARTAN. *Atmospheric Chemistry and Physics*, *16*(15), 9629–9653. https://doi.org/10.5194/acp-16-9629-2016

Spinazzè, A., Cattaneo, A., Scocca, D. R., Bonzini, M., & Cavallo, D. M. (2015). Multi-metric measurement of personal exposure to ultrafine particles in selected urban microenvironments. *Atmospheric Environment*, *110*, 8–17. https://doi.org/10.1016/j.atmosenv.2015.03.034

Stone, R. (1992). *Introduction to Internal Combustion* (Second Edition). UK: The MacMillan Press Ltd.

Suárez, L., Mesías, S., Iglesias, V., Silva, C., Cáceres, D. D., & Ruiz-Rudolph, P. (2014). Personal exposure to particulate matter in commuters using different transport modes (bus, bicycle, car and subway) in an assigned route in downtown Santiago, Chile. *Environ. Sci.: Processes Impacts*, *16*(6), 1309–1317. https://doi.org/10.1039/C3EM00648D

Targino, A. C., Gibson, M. D., Krecl, P., Rodrigues, M. V. C., dos Santos, M. M., & de Paula Corrêa, M. (2016). Hotspots of black carbon and PM 2.5 in an urban area and relationships to traffic characteristics. *Environmental Pollution*, *218*, 475–486. https://doi.org/10.1016/j.envpol.2016.07.027

Targino, A. C., & Krecl, P. (2016). Local and Regional Contributions to Black Carbon Aerosols in a Mid-Sized City in Southern Brazil. *Aerosol and Air Quality Research*, *16*(1), 125–137. https://doi.org/10.4209/aaqr.2015.06.0388

Targino, A. C., Machado, B. L. F., & Krecl, P. (2017). Concentrations and personal exposure to black carbon particles at airports and on commercial flights. *Transportation Research Part D: Transport and Environment*, *52*, 128–138. https://doi.org/10.1016/j.trd.2017.03.003

Targino, A. C., Rodrigues, M. V. C., Krecl, P., Cipoli, Y. A., & Ribeiro, J. P. M. (2018). Commuter exposure to black carbon particles on diesel buses, on bicycles and on foot: a case study in a Brazilian city. *Environmental Science and Pollution Research*, *25*(2), 1132–1146. https://doi.org/10.1007/s11356-017-0517-x

Tavares, M., Pinto, J. P., Souza, A. L., Scarmínio, I. S., & Cristina Solci, M. (2004). Emission of polycyclic aromatic hydrocarbons from diesel engine in a bus station, Londrina, Brazil. *Atmospheric Environment*, *38*(30), 5039–5044. https://doi.org/10.1016/j.atmosenv.2004.06.020

Tiwary, A., & Colls, J. (2010). *Air Pollution: Measurement, modelling and mitigation* (Third). New York, NY, USA: Routledge.

Trisotto, F. (2014, July 21). Via Calma é implantada oficialmente na Av. Sete de Setembro. Retrieved February 16, 2018, from http://www.gazetadopovo.com.br/vida-e-cidadania/via-calma-e-implantada-oficialmente-na-av-sete-de-setembro-eb541h6rhcv66l1t18olzb7ta

Uherek, E., Halenka, T., Borken-Kleefeld, J., Balkanski, Y., Berntsen, T., Borrego, C., … Lelieveld, J. (2010). Transport impacts on atmosphere and climate: Land transport. *Atmospheric Environment*, *44*(37), 4772–4816. https://doi.org/10.1016/j.atmosenv.2010.01.002

URBS. (2018). URBS - Urbanização de Curitiba. Retrieved February 20, 2018, from https://www.urbs.curitiba.pr.gov.br/

Vardoulakis, S., Fisher, B. E., Pericleous, K., & Gonzalez-Flesca, N. (2003). Modelling air quality in street canyons: a review. *Atmospheric Environment*, *37*(2), 155–182.

Vouitsis, I., Taimisto, P., Kelessis, A., & Samaras, Z. (2014). Microenvironment particle measurements in Thessaloniki, Greece. *Urban Climate*, *10*, 608–620. https://doi.org/10.1016/j.uclim.2014.03.009

Wallace, L. A., Emmerich, S. J., & Howard-Reed, C. (2004). Effect of central fans and in-duct filters on deposition rates of ultrafine and fine particles in an occupied townhouse. *Atmospheric Environment*, *38*(3), 405–413.

Wallace, L. A., Wheeler, A. J., Kearney, J., Van Ryswyk, K., You, H., Kulka, R. H., … Xu, X. (2011). Validation of continuous particle monitors for personal, indoor, and outdoor exposures. *Journal of Exposure Science and Environmental Epidemiology*, *21*(1), 49.

Wallace, L., & Ott, W. (2011). Personal exposure to ultrafine particles. *Journal of Exposure Science and Environmental Epidemiology*, *21*(1), 20–30. https://doi.org/10.1038/jes.2009.59

Weichenthal, S., Dufresne, A., Infante-Rivard, C., & Joseph, L. (2008). Determinants of ultrafine particle exposures in transportation environments: findings of an 8-month survey conducted in Montreal, Canada. *Journal of Exposure Science and Environmental Epidemiology*, *18*(6), 551–563.

Whitby, K. . (1978). The physical characteristics of sulfur aerosols. *Atmospheric Environment*, *12*, 135–159.

Whitby, K. ., Husar, R. ., & Liu, B. Y. . (1972). The aerosol size distribution of Los Angeles smog. *Journal of Colloid and Interface Science*, *39*(1), 177–204. https://doi.org/10.1016/0021-9797(72)90153-1

WHO. (2016). Ambient air pollution: A global assessment of exposure and burden of disease. Retrieved from http://www.who.int/phe/publications/air-pollution-global-assessment/en/

Wijnand, H. P., & van de Velde, R. (2000). Mann–Whitney/Wilcoxon's nonparametric cumulative probability distribution. *Computer Methods and Programs in Biomedicine*, *63*(1), 21–28.

Wilson, W. E., & Brauer, M. (2006). Estimation of ambient and non-ambient components of particulate matter exposure from a personal monitoring panel study. *Journal of Exposure Science and Environmental Epidemiology*, *16*(3), 264.

Wilson, W. E., & Suh, H. H. (1997). Fine Particles and Coarse Particles: Concentration Relationships Relevant to Epidemiologic Studies. *Journal of the Air & Waste Management Association*, *47*(12), 1238–1249. https://doi.org/10.1080/10473289.1997.10464074

Xu, B., Liu, S., Liu, J., & Zhu, Y. (2011). Effects of Vehicle Cabin Filter Efficiency on Ultrafine Particle Concentration Ratios Measured In-Cabin and On-Roadway. *Aerosol Science and Technology*, *45*(2), 234–243. https://doi.org/10.1080/02786826.2010.531792

Xu, B., & Zhu, Y. (2013). Investigation on lowering commuters' in-cabin exposure to ultrafine particles. *Transportation Research Part D: Transport and Environment*, *18*, 122–130. https://doi.org/10.1016/j.trd.2012.10.005

Xu, J., Wang, A., & Hatzopoulou, M. (2016). Investigating near-road particle number concentrations along a busy urban corridor with varying built environment characteristics. *Atmospheric Environment*, *142*, 171–180. https://doi.org/10.1016/j.atmosenv.2016.07.041

Yan, C., Zheng, M., Yang, Q., Zhang, Q., Qiu, X., Zhang, Y., … Zhu, Y. (2015). Commuter exposure to particulate matter and particle-bound PAHs in three transportation modes in Beijing, China. *Environmental Pollution*, *204*, 199–206. https://doi.org/10.1016/j.envpol.2015.05.001

Yang, F., Kaul, D., Wong, K. C., Westerdahl, D., Sun, L., Ho, K., … Ning, Z. (2015). Heterogeneity of passenger exposure to air pollutants in public transport microenvironments. *Atmospheric Environment*, *109*, 42–51. https://doi.org/10.1016/j.atmosenv.2015.03.009

Yin, Z., Ye, X., Jiang, S., Tao, Y., Shi, Y., Yang, X., & Chen, J. (2015). Size-resolved effective density of urban aerosols in Shanghai. *Atmospheric Environment*, *100*, 133–140. https://doi.org/10.1016/j.atmosenv.2014.10.055

Zhang, Q., & Zhu, Y. (2010). Measurements of ultrafine particles and other vehicular pollutants inside school buses in South Texas. *Atmospheric Environment*, *44*(2), 253–261.

Zhang, R., Khalizov, A. F., Pagels, J., Zhang, D., Xue, H., & McMurry, P. H. (2008). Variability in morphology, hygroscopicity, and optical properties of soot aerosols during atmospheric processing. *Proceedings of the National Academy of Sciences*, *105*(30), 10291–10296.

Zhao, S. X., Guo, N. S., Li, C. L. K., & Smith, C. (2017). Megacities, the World's Largest Cities Unleashed: Major Trends and Dynamics in Contemporary Global Urban Development. *World Development*, *98*, 257–289. https://doi.org/10.1016/j.worlddev.2017.04.038

Zuurbier, M., Hoek, G., Oldenwening, M., Lenters, V., Meliefste, K., van den Hazel, P., & Brunekreef, B. (2010). Commuters' Exposure to Particulate Matter Air Pollution Is Affected by Mode of Transport, Fuel Type, and Route. *Environmental Health Perspectives*, *118*(6), 783–789. https://doi.org/10.1289/ehp.0901622

Appendix A Bus Records

June 20th, 2016

Ellen and Julian

Londrina

Overcast

Bus route #113, Bus #4174, License #AUX-4245

-regular full/not overly

-at front, right next to front door

-9:49am-10:09am

Bus Stop: 9:50,51,51,53,55,56,58,59

10:00,02,04,06

Stop Light:

9:52

10:03,03,05,06

Front Door Open: 9:50,51,56,59,

10:00,06

Back Door Open: 9:51,53,55,56,58,

10:00,06

Slope

Downhill: 9:56,10:08

Uphill: 10:01,10:03

Street Type:

Roundabout: 10:01,

Other:

Wheelchair boarded, idled with doors open 9:56

Bus route #217, Bus 4179, License #AUR-4357

-bus mostly full

-Ellen

-windows open

-10:12-11:19

Bus stop: 10:15,16,17,19,20,20,21,23,24,25,29,34,37,56,57,58

11:01,05,06,11,13,15,15

Stop Light: 10:16,18,23,25,39

11:04,05,07,08,09,12,14

Front Door: 10:15,16,54

11:05,06,13,15,15

Back Door: 10:17,19,20,20,21,23,24,25,29,34,37,57,58

11:01,05,06,11

Slope

Downhill: 10:19,10;25,11;02,11;09,11;18

Uphill: 10:15,10;38,11:08,11:10,11:15

Street Type:

Highway 10:35,10:51

Roundabout: 10:26,10:31,11:02

Other:

10:40-10:48 Acapulco Terminal

Bus Route #113, Bus #4174, License #AUX-4245

-windows open

-very full

-2 rows in front back door

-11:39-12:00

Bus Stops: 11:42,46,47,50,51,52,53,53,54,55,56,57,57,58,59

Stop Light: 11:41,43,45,49

Front Door Open: 11:42,50,56,57,57,59

Back Door Open: 11:42,46,47,50,51,52,53,53,54,55,56,57,57,58

Slope:

Uphill: 11:48

Downhill:11:45

Roundabout: 11:45,11:57

Other: 11:59 smell smoke

June 21st , 2016

Ellen and Julian

Londrina

Sunny, cloudy, windy, little colder

Bus route #113, Bus #3350, License #AYS-6218

-3 behind middle door

-windows open

-9:51am-10:06am

Bus Stop: 9:51,53,54,54,56,57,58

10:04

Stop Light:

10:001,02,05

Front Door Open: 9:51,53,57,58b,

10:04

Back Door Open: 9:51,54,54,56,57,58,58

10:04

Slope

Downhill: 9:56,10:05,

Uphill: 10:00,10:03

Street Type:

Roundabout: 9:51,10:00

Other:

Bus route #217, Bus 4163, License #ASQ-8244

-3 behind mid

-Ellen

-some windows open

-10:13-11:20

Bus stop: 10:17,19,22,22,24,24,25,26,29,29,30,32,33,34,36,37,39,56,58

11:04,04,06,07,09,10

Stop Light: 10:18,20,21,40

11:02,05,06,08,12,14,16,18,19

Front Door: 10:17,19,24,24,30,

11:04,06,07,10

Back Door: 10:22,22,24,24,25,26,29,29,30,32,33,34,36,37,39,56,58

11:04,04,09,10

Slope

Downhill: 10:21,26,55

11:14,17

Uphill: 10:16,28,35,

11:03,10,15

Street Type:

Highway 10:35,10:51

Roundabout: 10:27,33,57

11:02

Other:

10:41-10:48 Acapulco Terminal

10:24 smoke smell

lots of trucks along highway

Bus Route #113, Bus #3350, License #AYS-6218

-windows open

-in front of back door

-11:40-12:02

Bus Stops: 11:42,45,47,48,51,51,52,53,54,56,57,58,59,12:00

Stop Light: 11:43,44,46,50,55

Front Door Open: 11:42,45,47,51,51,52,58,59

Back Door Open: 11:47,48,52,53,54,56,57,58,59,12:00

Slope:

Uphill: 11:46,58

Downhill:11:49

Roundabout: 11:46

Other

June 22nd , 2016

Ellen and Julian

Londrina

Sunny, cloudy, windy, little cold

Bus route #113, Bus #4179, License #AUR-4357

-2 seats behind mid door

-windows open

-9:49am-10:04am

Bus Stop: 9:50,51,54,57

10:01

Stop Light:

9:59,59

10:00,01,02,03

Front Door Open: 9:51,56

10:01

Back Door Open: 9:50,54,56,57

10:01

Slope

Downhill: 9:54,10:03

Uphill: 9:58

Street Type:

Roundabout: 9:49,9:58

Other:

9:54 idle with doors open to let wheelchair board bus

Bus route #217, Bus 4162, License #ASQ-8343

-2 behind mid

-Ellen

-some windows open

-10:15-11:18

Bus stop: 10:18,20,22,24,27,28,30,32,34,35,36,36,54,56,59

11:00,00,04,06,09,11,13,15,15

Stop Light: 10:16,17,19,21,24,25,41,

11:03,05,06,09,10,12

Front Door: 10:18,20,27,32,36b,54,56

11:00a,04,06,13,15a,15b

Back Door: 10:22,24,27,28,30,32,34,35,36a,59

11:00b,09,11,13,15b

Slope

Downhill: 10:23,3955

11:12,17

Uphill: 10:54

11:14

Street Type:

Roundabout: 10:29,34,58,11:02

Other:

10:42-10:47 Acapulco Terminal

10:50,11:08 smoke smell

10:38 cross highway

Bus Route #113, Bus #4179, License #AUR-4357

-windows open

-2 seats behind mid door

-11:40-12:00

Bus Stops: 11:42,44,46,47,51,52,53,54,54,55,56,57,57,59

Stop Light: 11:41,43,44,49

Front Door Open: 11:42,44,47,54b,55,56,57,57,59

Back Door Open: 11:46,47,51,52,53,54,54,55,56,57

Slope:

Uphill: 11:49

Downhill:11:45

Roundabout: 11:45,11:56

Other

June 23rd , 2016

Ellen and Julian

Londrina

Sunny, very foggy at university

Bus route #113, Bus #4169, License #ASQ-8387

-3 seats behind mid door

-windows open

-9:51am-10:06am

Bus Stop: 9:52,54,55,56,58,59,

10:00,04

Stop Light:

10:01,02,03

Front Door Open: 9:52,54,55

10:00,04

Back Door Open: 9:54,56,58,59

10:00,04

Slope

Downhill: 9:57,10:05

Uphill: 10:00

Street Type:

Roundabout: 9:52,10:00

Other:

Bus route #217, Bus 4163, License #ASQ-8244

-4 behind mid

-Ellen

-some windows open

-became full back close to the terminal

-10:15-11:19

Bus stop: 10:20,24,25,27,28,31,33,35,36,40,55,56,57

11:03,04,06,07,09,10,10,13,17

Stop Light: 10:21,25,33,55,

11:05,06,08,12,14,17

Front Door: 10:20,25,33,55

11:04,07,09,10,10

Back Door: 10:24,25,27,28,31,33,35,36,40,55,56,57

11:03,04,06,10,10,13,17

Slope

Downhill: 10:29,11:13,11:19

Uphill: 10:22,31,38,53

11:03,08,12,16

Street Type:

Roundabout: 10:30,35,58,11:02

Other:

10:42-10:47 Acapulco Terminal

Bus Route #113, Bus #4179, License #AUR-4357

-windows open

-2+3 rows (split) behind mid door

-11:41-12:02

Bus Stops: 11:43,46,47,48,51,53,55,56,57,58

Stop Light: 11:43,44,54,

Front Door Open: 11:43,46,47,51,56,57,57,58

Back Door Open: 11:43,47,48,53,55,57,57,58

Slope:

Uphill: 11:49

Downhill:11:46

Roundabout: 11:46

Other

June 24th , 2016

Ellen and Julian

Londrina

Sunny and cold

Bus route #113, Bus #4168, License #ASQ-8351

-3 seats behind mid door

-windows some open

-9:49am-10:06am

Bus Stop: 9:51,53,56,58

10:03

Stop Light:

10:00,01,02,03,05

Front Door Open: 9:51,53,56,58

10:03

Back Door Open: 9:53,56,58

10:03

Slope

Downhill: 9:55,10:05

Uphill: 10:00

Street Type:

Roundabout: 10:00

Other:

9:56 wheelchair boarded, bus idled with doors open

Bus route #217, Bus 4163, License #ASQ-8244

-3 behind mid

-Ellen

-windows open

-bus not too full

-10:13-11:18

Bus stop: 10:17,19,20,22,24,25,26,27,30,31,33,35,39,54,56

11:00,01,06,07,08,09,13,15,16

Stop Light: 10:16,19,21,26

11:02,05,07,11,12,14,15

Front Door: 10:17,19,25,27

11:00,01,09,13,15,16

Back Door: 10:20,22,24,26,27,30,30,31,33,35,39,54,56

11:06,07,08,15,16

Slope

Downhill: 10:27,11:11,11:17

Uphill: 10:36,

11:03,10,16

Street Type:

Roundabout: 10:28,34,57,11:01

Other:

10:41-10:48 Acapulco Terminal

Bus Route #113, Bus #4179, License #AUR-4357

-windows open

-3 rows behind middle

-11:40-11:58

Bus Stops: 11:42,43,45,45,46,48,50,51,52,53,54,55,55

Stop Light: 11:41,47

Front Door Open: 11:42,43,48,54,55,55

Back Door Open: 11:42,45,45,46,50,51,52,53,54,55

Slope:

Uphill: 11:46

Downhill:11:44

Roundabout: 11:44,11:54

Other

June 27th , 2016

Ellen and Julian

SP

Sunny with clouds

*Ellen's watch 2 minutes fast, affects all records with Ellen

Bus route #8707-10, Bus #8 1061

-seated at very front behind driver

-windows open

-bus full

-2:08pm-2:28pm

Bus Stop: 2:09,11,12,15,17,18,21

Stop Light:

2:10,13,14,19,22,25

Front Door Open: 2:15,21

Back Door Open: 2:09,11,15,21

Slope

Downhill:

Uphill:

Street Type:

Roundabout:

Street Type:

2:08 –Sky scrapers, 6 lanes, somewhat open

2:23 – Smaller/narrower street

Other:

Bus route #805L-10, Bus 3 9905, License #ELQ-7397

-a little behind middle

-Ellen

-windows open

-bus not full, became full along avenida paulista

-2:44-3:46

Bus stop: 2:50, 55,57,59

3:03,06,08,09,12,14,15,17,22,24,25,28,33,35,41,42

Stop Light: 2:47 (long), 51,54,56

3:00,01,04,06,10,11,15,16,20,21,22,25,30,35,36,37,39

Front Door: 2:55, 57,59

3:03,06,08,09,12,14,17,22,24,25,28,33,35,41,42

Back Door: 2:50,

3:12, 15, 22, 24, 25, 42

Slope

Downhill: 3:04, 13

Uphill: 3:01, 10, 16, 19

Street Type:

2:52 – park on right

3:01 – very busy intersection

3:05 – overpass above highway

3:08 – narrow/street canyon

3:22 – over highway again

3:30 – avenida paulista

Other:

3:18 idle

3:30 lots of traffic

June 28th , 2016

Ellen and Julian

SP

Sunny and warm

*Ellen's watch 2 minutes fast, affects all records with Ellen

Bus route #778R-10, Bus #8 1041, License # EZL-5851

-seated middle next to door

-windows open

-2:09pm-2:24pm

Bus Stop: 2:11, 13, 14, 16, 18, 20, 22

Stop Light:

2:13, 15, 15, 17, 18, 21, 22

Front Door Open: 2:16, 18, 20, 22

Back Door Open: 2:11, 13, 14, 20, 22

Slope

Downhill:

Uphill:

Street Type:

Roundabout:

Street Type:

Other:

Bus route #805L-10, Bus 3 9876, License #DTD-0575

-a little behind middle

-Ellen

-windows open

-mostly empty

-2:43-3:44

Bus stop: 2:44,48,50,52,57,59

3:00,01,03,05,08,10,11,12,14,17,18,20,22,23,28,32,40,42

Stop Light: 2:45,49,51,53,55,58

3:03,06,06,15,21,25(long),34,35,37,39

Front Door: 2:50,52,57,59,

3:00,01,03,05,08,10,11,17,18,20,22,23,28,32,38,40

Back Door: 2:44, 48,57

3:05,10,11,12,14,17,23,28,32,40,42

Slope

Downhill: 2:58,3:07

Uphill: 2:55,3:05,3:09,3:13

Street Type:

Other:

3:25 lots of traffic, bus lane very slow

June 29th , 2016

Ellen and Julian

SP

Sunny, cloudy, hot

*Ellen's watch 2 minutes fast, affects all records with Ellen

Bus route #8707-10, Bus #8 1003, License # DTC-8174

-near middle

-windows open

-medium full

-2:10-2:34pm

Bus Stop: 2:12,14,15,18,22,26,30

Stop Light:

2:13,21,24,27,28,29,31,33

Front Door Open: 2:18,22,26,30

Back Door Open: 2:12,14,15,18,22,26,30

Slope

Downhill:

Uphill:

Street Type:

Roundabout:

Street Type:

Other:

2:22 lots of traffic

Bus route #805L-10, Bus 3 9903, License #ELQ-7398

-behind middle

-Ellen

-windows open

-mostly empty

-2:40-3:42

Bus stop: 2:46,49,50,52,57,58

3:00,02,03,06,07,09,10,12,15,16,17,20,27,30,36,37

Stop Light: 2:41,43,47,50,54,55,59

3:01,03,05,06,07,09,13,18,24,25,30,32

Front Door: 2:49,50,52,57,58

3:00,02,03,06,07,09,10,15,16,17,20,27,30,36,37

Back Door: 2:46,50,

3:02,03,0612,15,20,27,38

Slope

Downhill: 2:57,3:07

Uphill: 2:54,3:03,3:09

Street Type:

2:59 cross highway

3:17 avenida paulista (traffic)

Other:

June 30th , 2016

Ellen and Julian

SP

Cloudy and warm

*Ellen's watch 2 minutes fast, affects all records with Ellen

Bus route #8707-10, Bus #8 1018, License # DTC-8180

-front of middle

-windows open

-very full

-1:39-2:00pm

Bus Stop: 1:40,42,43,45,48,51,55,58

Stop Light:

1;41,43,44,45,47,50,52,53,55,57,59

Front Door Open: 1:48

Back Door Open: 1:40,42,43,45,48,51,55,58

Slope

Downhill:

Uphill:

Street Type:

Roundabout:

Street Type:

Other:

Bus route #805L-10, Bus 3 9876, License #DTD-0575

-behind middle

-Ellen

-some windows open

-mostly empty

-2:08-2:13

Bus stop: 2:12,15,18,19,21,24,27,28,29,30,31,35,57,42,45,49,50,52

3:00,05,07,10

Stop Light: 2:10,13,22,29,33,34,38,44,55,57

3:11

Front Door: 2:18,19,24,27,28,30,31,45,59,50

3:00,05,07

Back Door: 2:12,15,18,21,28,29,31,35,37,42,45,52

3:00,10

Slope

Downhill: 2:28,33,36,41

Uphill: 2:22,38

Street Type:

2:29 cross highway

3:43 traffic

Other:

July 25th , 2016

Ellen and Thiago

Curitiba

Sunny, warm, blue sky

Bus route #002, Bus #DN023, License # DTC-8180

-small bus

-at back

-windows open, no AC

-very full

-left hotel 1:50pm

-2:02pm-2:48ish

Bus Stop: 2:03,06,09,11,12,20,22,33,34,35,36,42,45,46

Stop Light:

2:05,07,08,10,13,15,16,18,31,38,39,41,43

Front Door Open: 2:03,06,09,12,33,34,36,45,46

Back Door Open: 2:09,11,20,22,33,35,42(hotel stop),45

Slope

Downhill: 2:06,35

Uphill: 2:22,34

Street Type:

Roundabout:

Street Type:

Other:

2:16 behind truck, lots of traffic

2:22-2:30 bus turned off

Bus route #001, Bus BN997, License #

-middle

-Ellen

-windows open

-2:53-3:18

Bus stop: 2:57,59

3:01,04,05,07,12,13

Stop Light: 2:55,56,

3:03,09,11,13

Front Door: 2:59

3:01,05,07

Back Door: 2:57,59

3:04,05,07,12,13

Slope

Downhill:

Uphill:

Street Type:

Other:

3:07-3:08 long stop, bus idling

July 26th , 2016

Ellen and Thiago

Curitiba

Sunny and clear

Bus route #002, Bus #DN024, License # AKQ-2248

-small bus

-at back

-windows open, no AC

-more full today

-left hotel 1:40pm

-1:53pm-2:37ish

Bus Stop: 1:55,59 (thiago off),

2:01,03,06,08,09,11,13,16,20,22,23,24,25,28,30,32,33

Stop Light: 1:58,59

2:01,02,05,07,10,12,13,14,15,18,24,26,27,35

Front Door Open: 1:55

2:01,06,08,09,20,24,28,32,33

Back Door Open: 1:55,59

2:01,03,06,11,13,20,22,23,24,25,(hotel stop),30,32,33

Slope

Downhill: 2:22

Uphill:

Street Type:

Roundabout:

Street Type:

Other:

2:16-2:18 driver change

Bus route #001, Bus BN997, License #

-front

-Ellen

-windows open

-2:46-3:08

Bus stop: 2:51,52,55,57,58,

3:00,01

Stop Light: 2:49,51,55,59,

3:02,03,04,05(first stop),07

Front Door: 2:51,52,55

3:01

Back Door: 2:52,57,58

3:00,01

Slope

Downhill:

Uphill:

Street Type:

Other:

Lots of traffic

July 27th , 2016

Ellen and Thiago

Curitiba

Sunny and warm

Bus route #002, Bus #DN029, License # AQU-2215

-near front

-windows open, no AC

-more full today

-left hotel 1:48pm

-1:56pm-2:55pm

Bus Stop: 1:57,

2:01,04(thiago off),05,09,14,17,21,24,30,32,35,37,42,45,48,51

Stop Light: 1:57,59,

2:00,07,08,10,11,12,13,15,16,22,23,27,28,34,36,37,39,40,43,45,47,50,52

Front Door Open: 1:57

2:09,14,21,24,30,32,35,37,42,45,48,51

Back Door Open: 1:57

2:01,04,05,09,17,24,30,37,45,48,51

Slope

Downhill: 2:33

Uphill: 2:31

Street Type:

Roundabout:

Street Type:

Other:

2:15 traffic

2:39-43 traffic

2:47-50 traffic

Bus route #001, Bus BN998, License #

-middle

-Ellen

-windows open

-very empty

-3:05-3:34

Bus stop: 3:10,12,16,18,20,24,25

Stop Light: 3:07,08,11,14,22,23,26,28,29

Front Door: 3:10,12,18,20

Back Door: 3:12,16,18,20,24,25

Slope:

Downhill:

Uphill:

Street Type:

Other:

July 28th , 2016

Ellen and Thiago

Curitiba

Cloudy and chilly

Bus route #002, Bus #DN027, License # AKQ 2250

-front

-windows open, no AC

-2:05-2:48

Bus Stop: 2:07,11(thiago),14,16,20,21,26,32,34,35,36,38,43

Stop Light: 2:07,10,12,13,15,17,18,19,22,23,24,35,39,42,43,44,46

Front Door Open: 2:07,16,21,26,32,35,36,43

Back Door Open: 2:11,14,16,20,21,26,34,35,38

Slope

Downhill: 2:34

Uphill:

Street Type:

Roundabout:

Street Type:

Other:

2:26-2:30 bus turned off for driver change

Bus route #001, Bus BN997, License #ALJ 8237

-middle-back

-Ellen

-windows mostly closed

-2:54-3:24

Bus stop: 2:58

3:02,06,07,11,12,13,15

Stop Light: 2:54,55,57,59

3:01,02,05,10,17,18,19,20

Front Door: 2:58

3:06,07,12,13

Back Door: 2:58

3:02,06,07,11,15

Slope

Downhill:

Uphill:

Street Type:

Other:

3:07 idle at stop

3:09 heavy traffic until 3:20

July 29th , 2016

Ellen and Thiago

Curitiba

Cloudy and chilly and windy

Bus route #002, Bus #DN028, License #

-front + middle

-windows open, no AC

-instruments on at 1:31

-reporters off bus 2:25

-route start on sete de setembro 2:28-3:15

Bus Stop: 2:28,30,32,35,37,40,42,45,48,53,55,55,56,58,

3:02,03,05(hotel),07,10,12

Stop Light: 2:30,31,33,34,36,39,41,44,46,48,51,59

3:01,03,08

Front Door Open: 2:32,37,40,42,48,53,55a,56,58

3:02,05,10,12

Back Door Open: 2:28,30,32,35,37,45,48,53,55b,56,58

3:03,05,07,10

Slope

Downhill:

Uphill: 2:54

Street Type:

Roundabout:

Street Type:

Other:

2:48-50 driver change

2:42 traffic

Bus route #001, Bus BN999, License #ALJ 8231

-front middle

-Ellen

-windows a little open

-3:19-3:48

Bus stop: 3:24,26,32,33,37

Stop Light: 3:20,21,23,25,27,29,30,34,37,39,40,42,44,45

Front Door: 3:24,26

Back Door: 3:24,26,32,33,37

Slope

Downhill:

Uphill: 3:28

Street Type:

Other:

Traffic 3:40-45

Appendix B Daily Pollution Maps

Pollution maps for each pollutant on each day of measurement are included below.

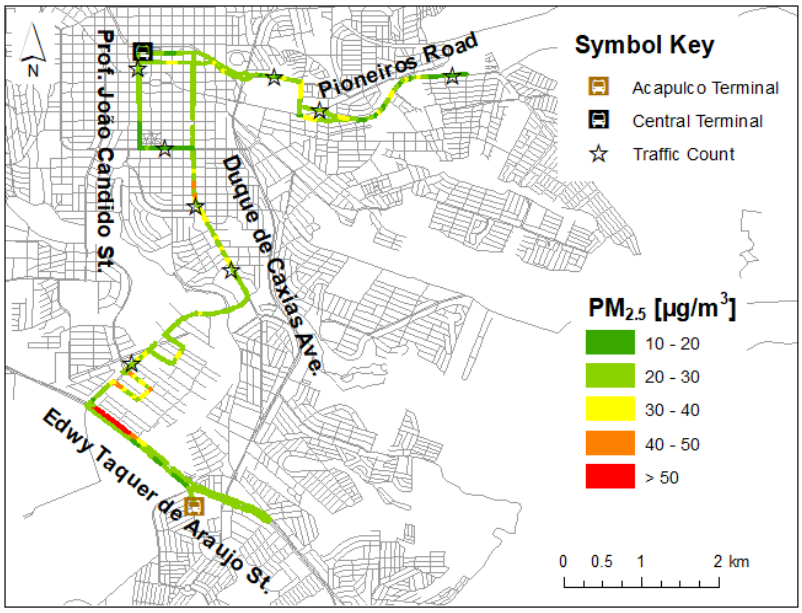

Figure B-1: Map of $PM_{2.5}$ concentrations in Londrina on June 20, 2016.

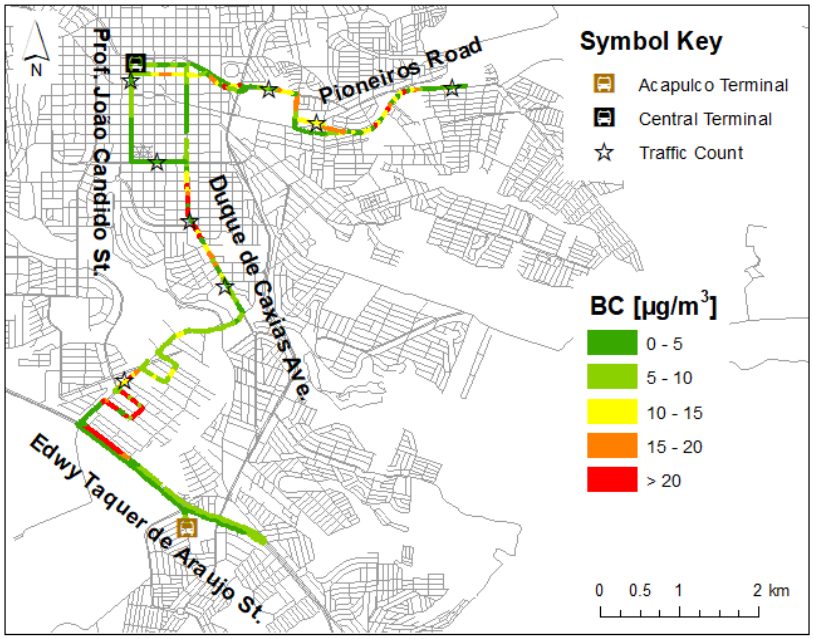

Figure B-2: Map of BC concentrations in Londrina on June 20, 2016.

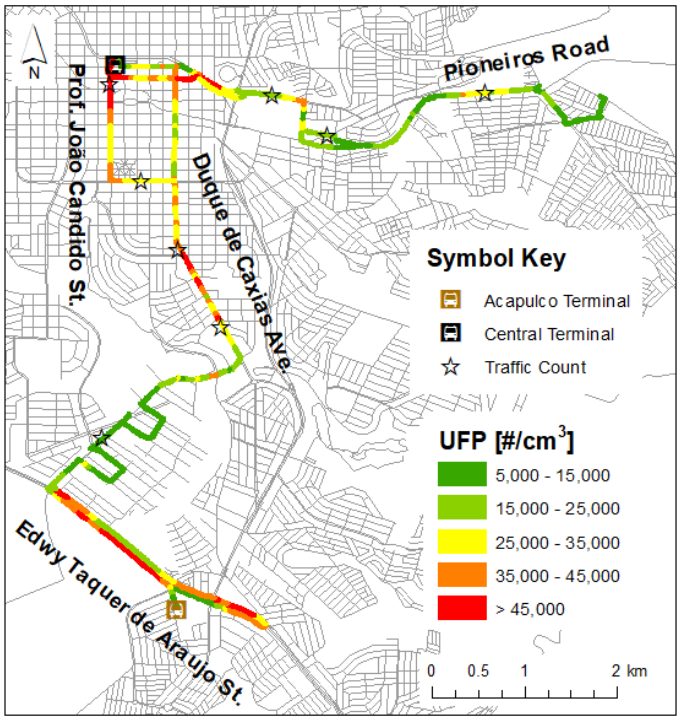

Figure B-3: Map of UFP concentrations in Londrina on June 20, 2016.

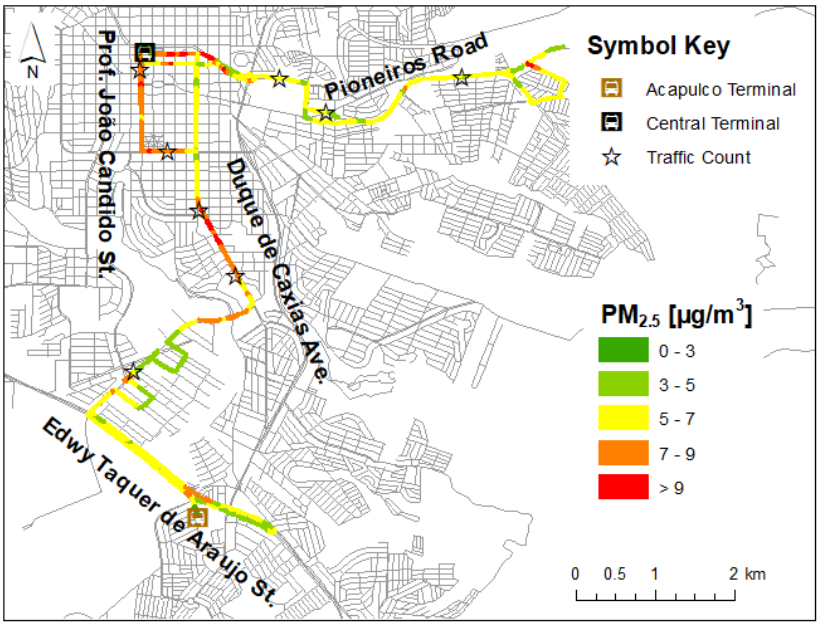

Figure B-4: Map of $PM_{2.5}$ concentrations in Londrina on June 21, 2016.

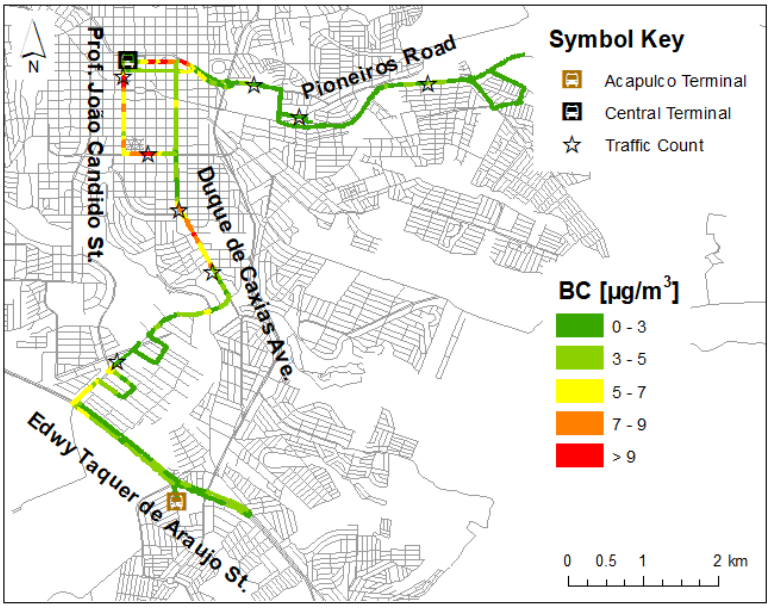

Figure B-5: Map of BC concentrations in Londrina on June 21, 2016.

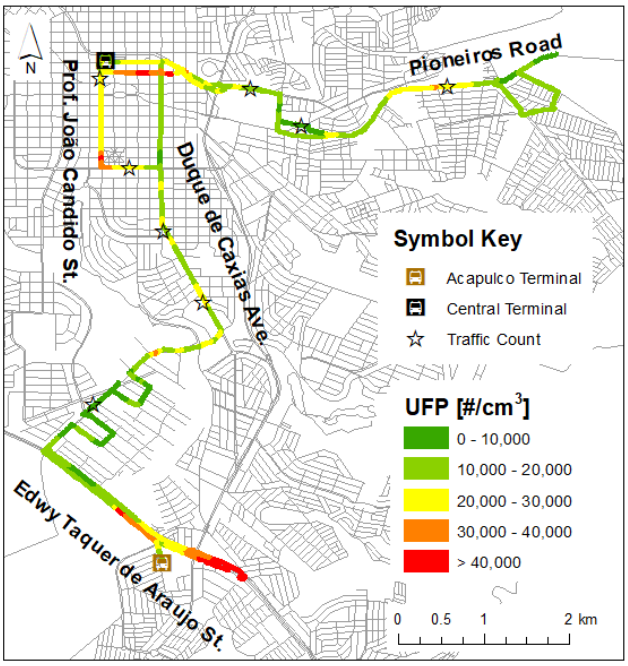

Figure B-6: Map of UFP concentrations in Londrina on June 21, 2016.

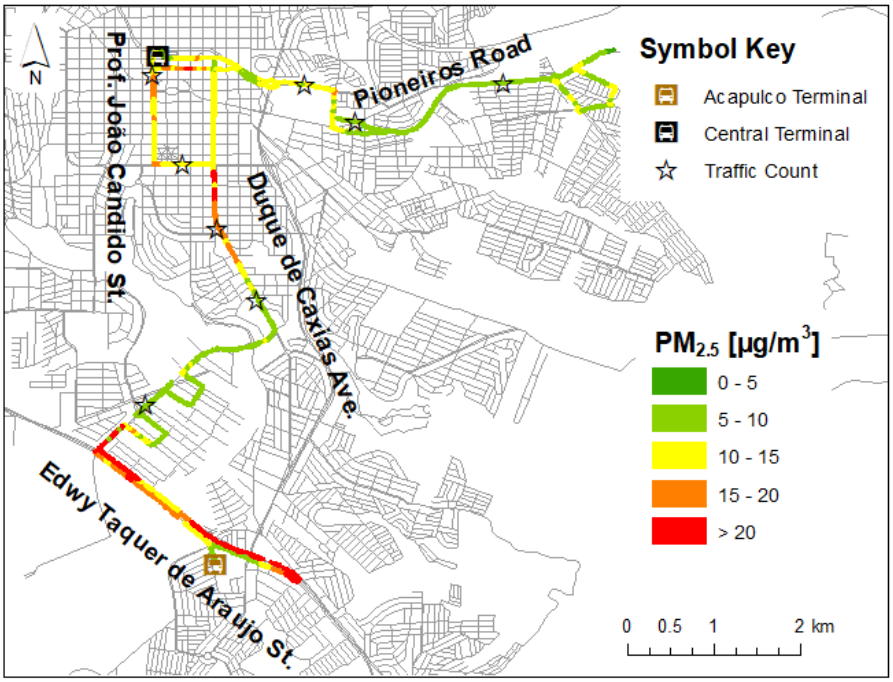

Figure B-7: Map of $PM_{2.5}$ concentrations in Londrina on June 22, 2016.

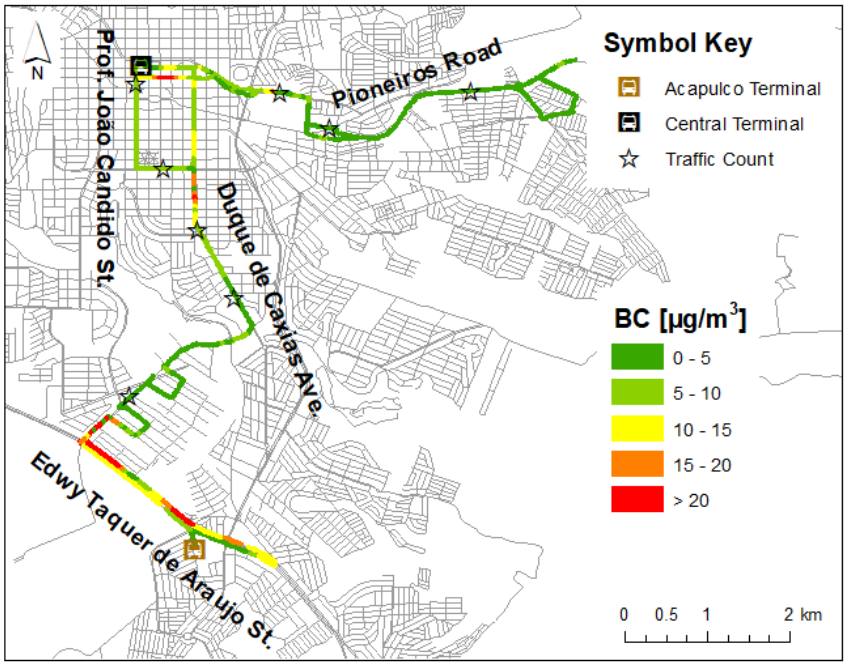

Figure B-8: Map of BC concentrations in Londrina on June 22, 2016.

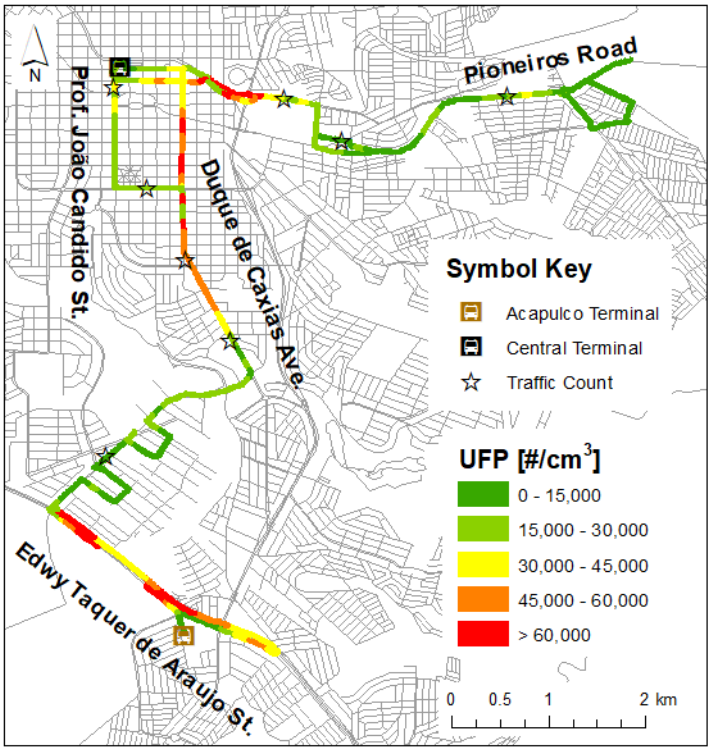

Figure B-9: Map of UFP concentrations in Londrina on June 22, 2016.

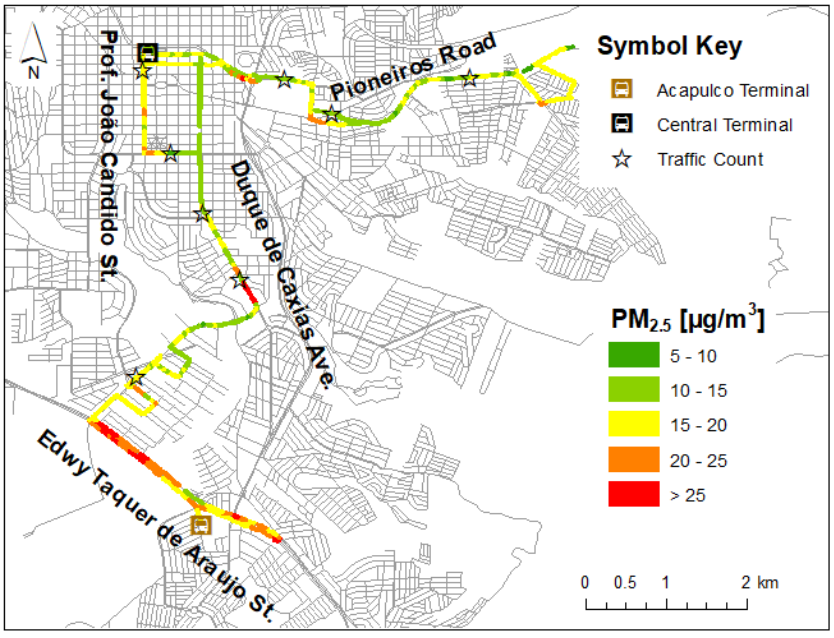

Figure B-10: Map of $PM_{2.5}$ concentrations in Londrina on June 23, 2016.

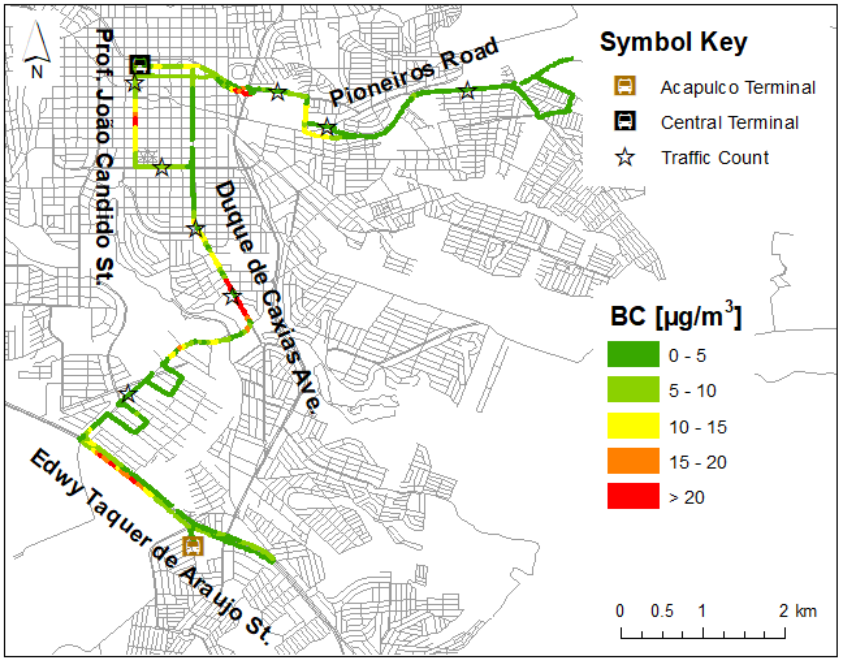

Figure B-11: Map of BC concentrations in Londrina on June 23, 2016.

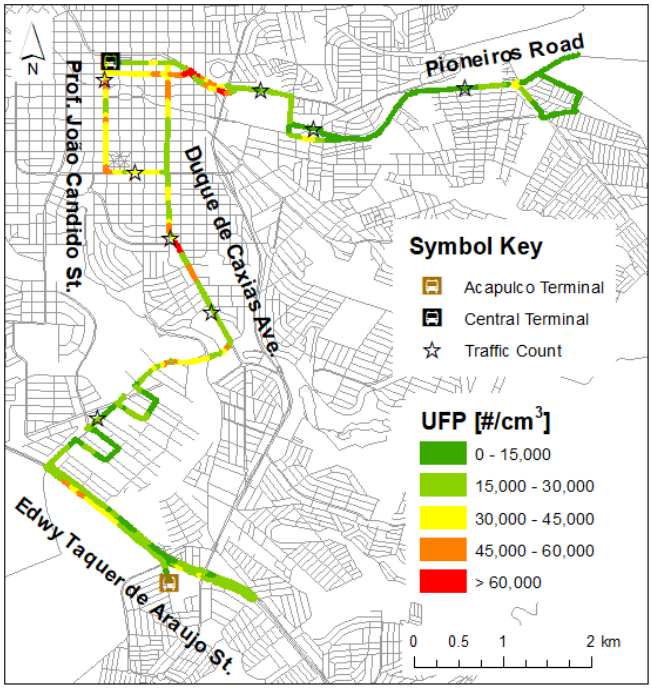

Figure B-12: Map of UFP concentrations in Londrina on June 23, 2016.

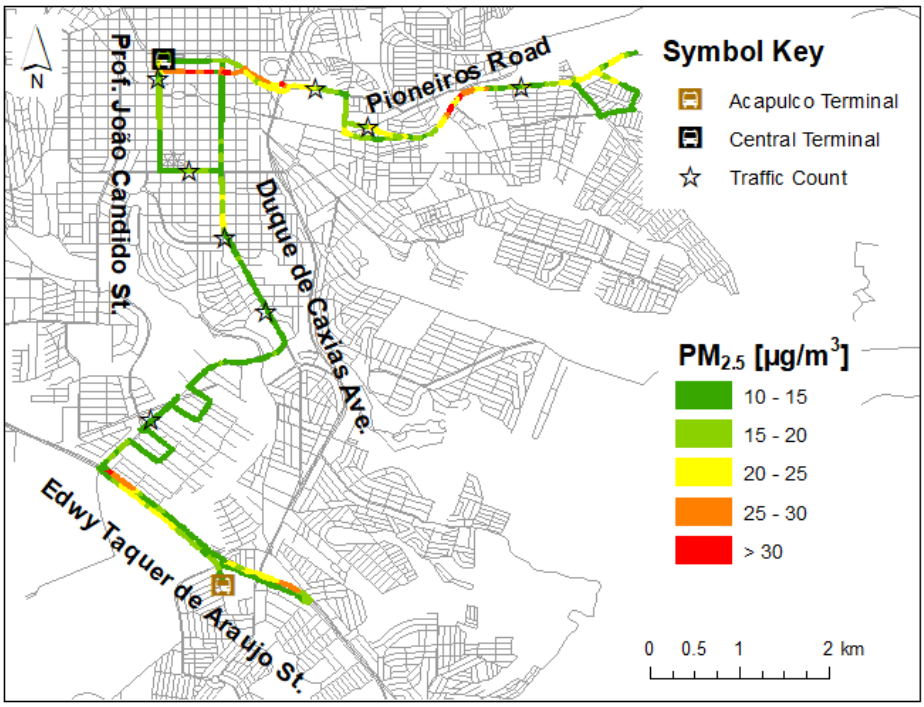

Figure B-13: Map of $PM_{2.5}$ concentrations in Londrina on June 24, 2016.

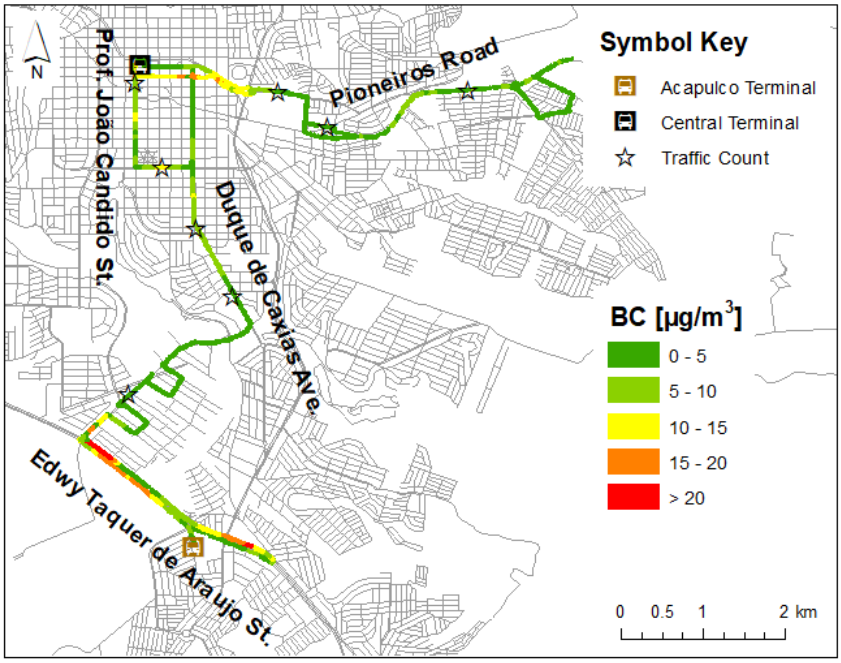

Figure B-14: Map of BC concentrations in Londrina on June 24, 2016.

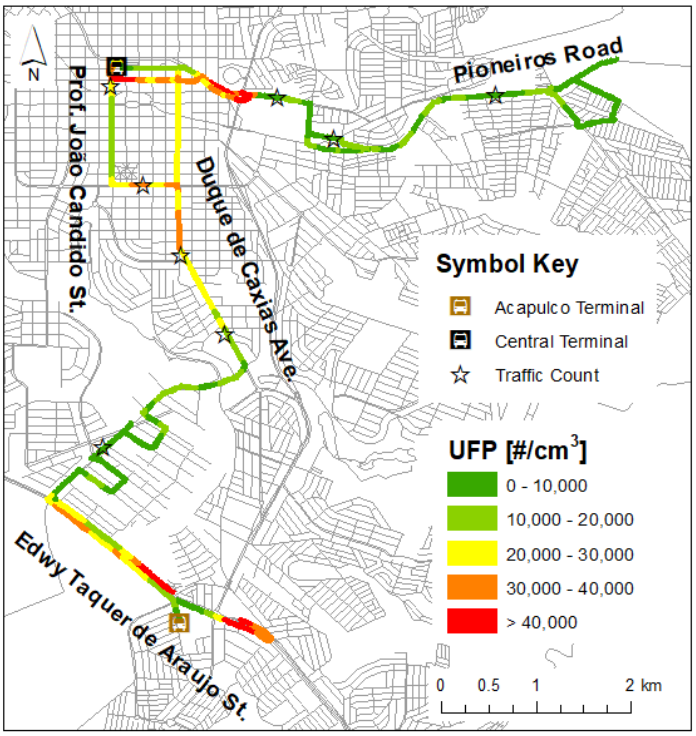

Figure B-15: Map of UFP concentrations in Londrina on June 24, 2016.

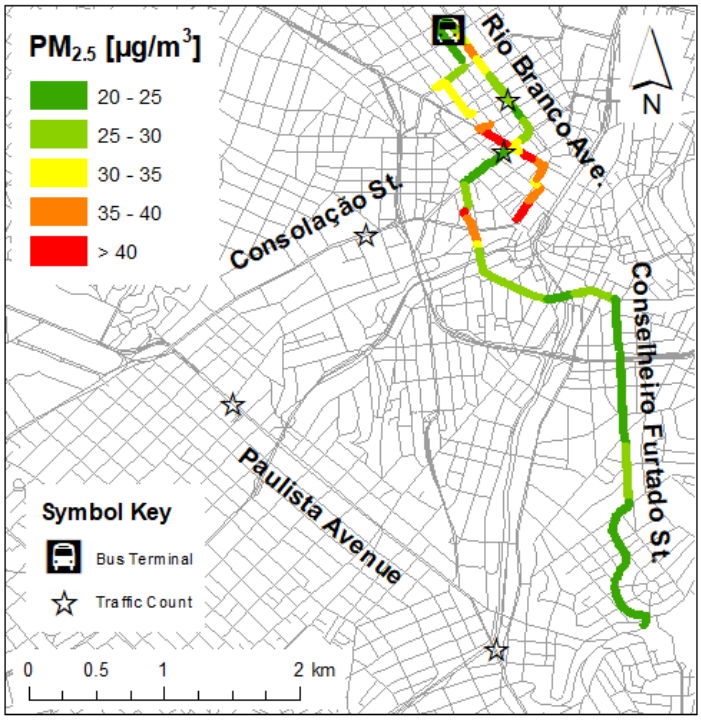

Figure B-16: Map of $PM_{2.5}$ concentrations in São Paulo on June 27, 2016.

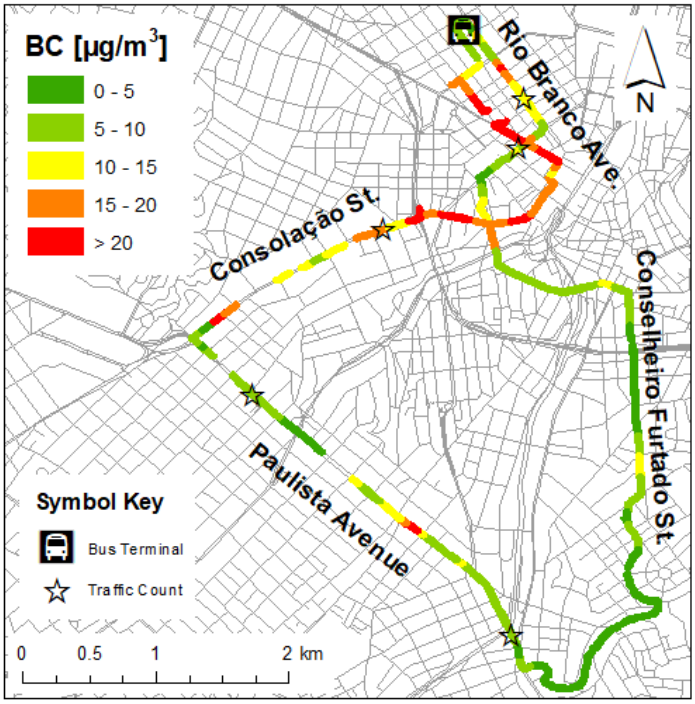

Figure B-17: Map of BC concentrations in São Paulo on June 27, 2016.

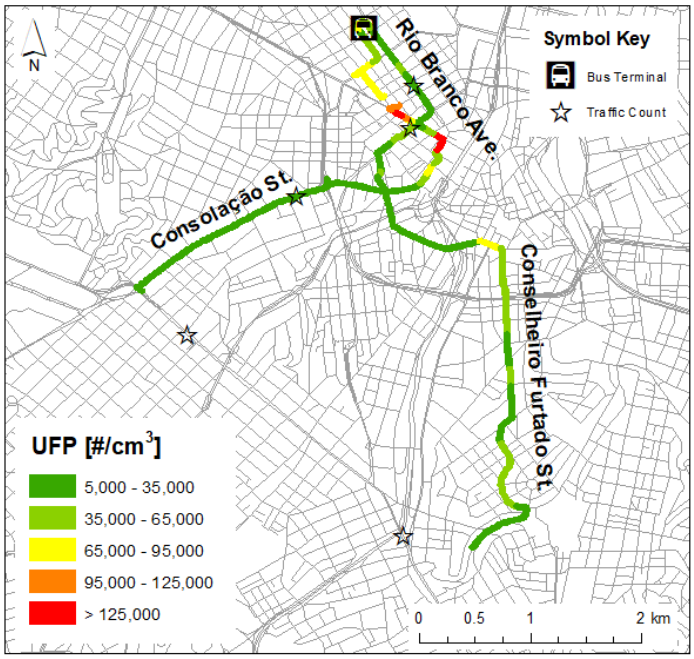

Figure B-18: Map of UFP concentrations in São Paulo on June 27, 2016.

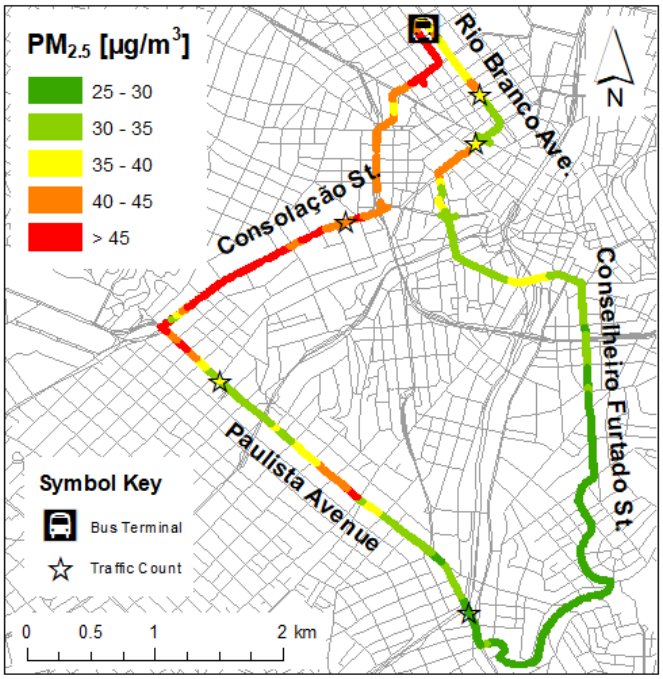

Figure B-19: Map of $PM_{2.5}$ concentrations in São Paulo on June 28, 2016.

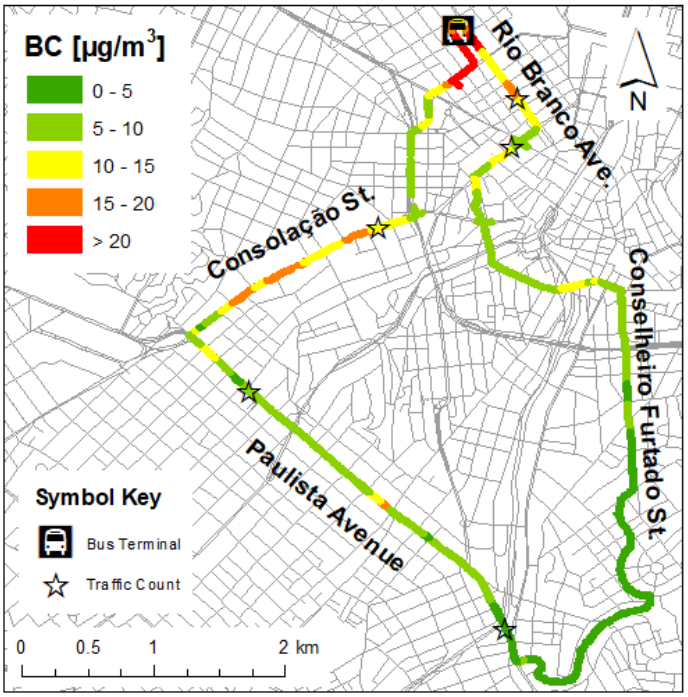

Figure B-20: Map of BC concentrations in São Paulo on June 28, 2016.

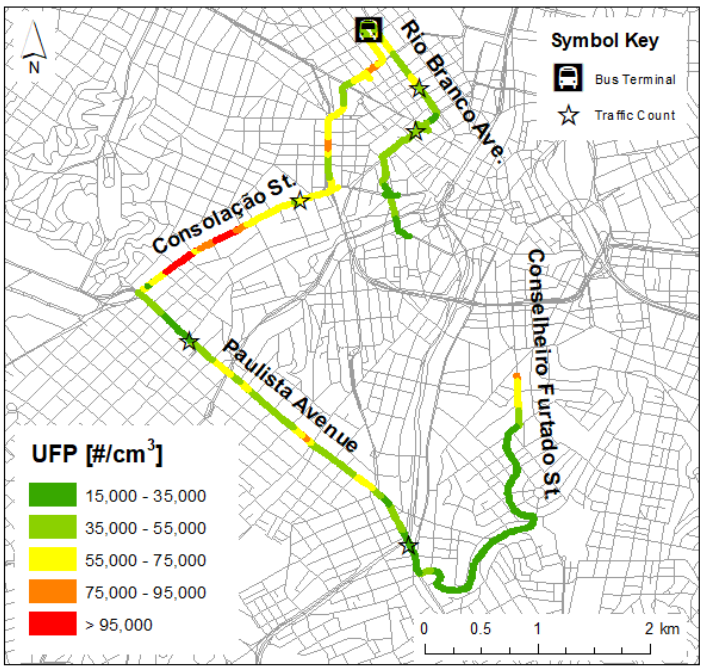

Figure B-21: Map of UFP concentrations in São Paulo on June 28, 2016.

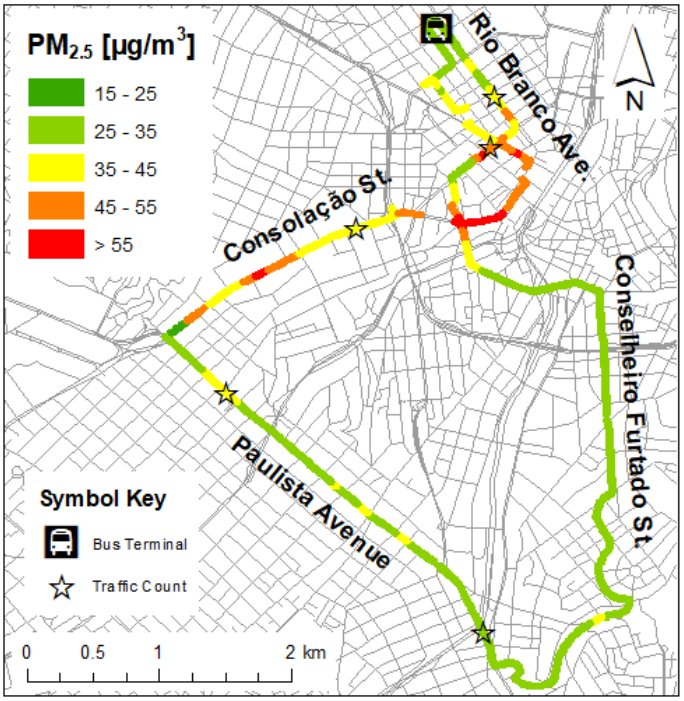

Figure B-22: Map of $PM_{2.5}$ concentrations in São Paulo on June 29, 2016.

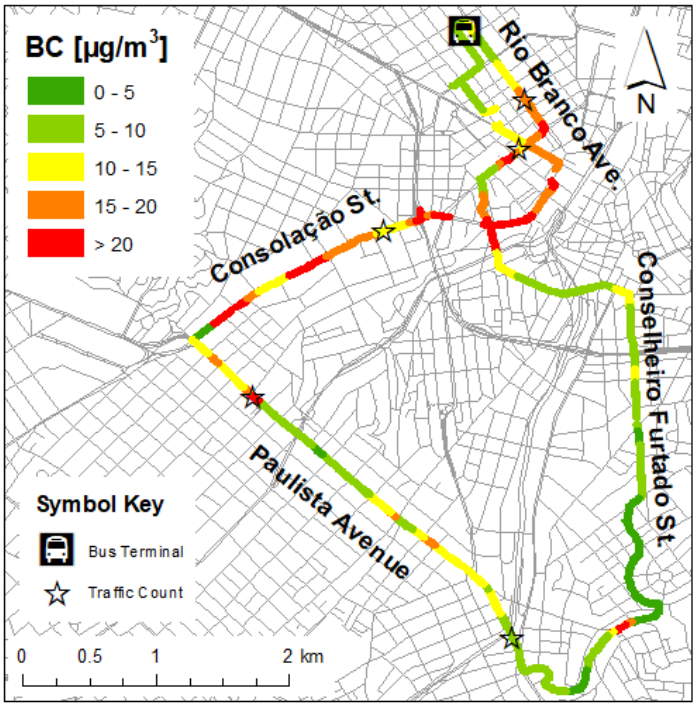

Figure B-23: Map of BC concentrations in São Paulo on June 29, 2016.

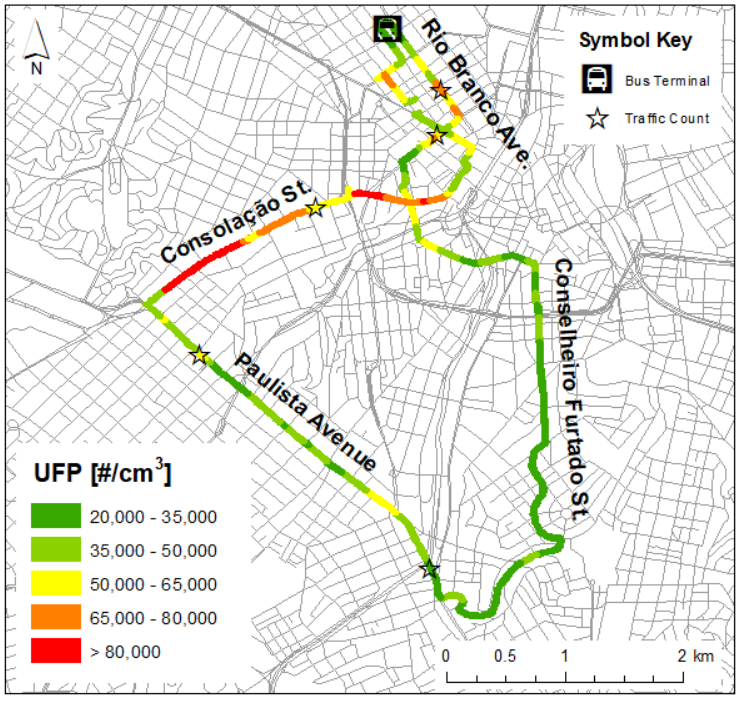

Figure B-24: Map of UFP concentrations in São Paulo on June 29, 2016.

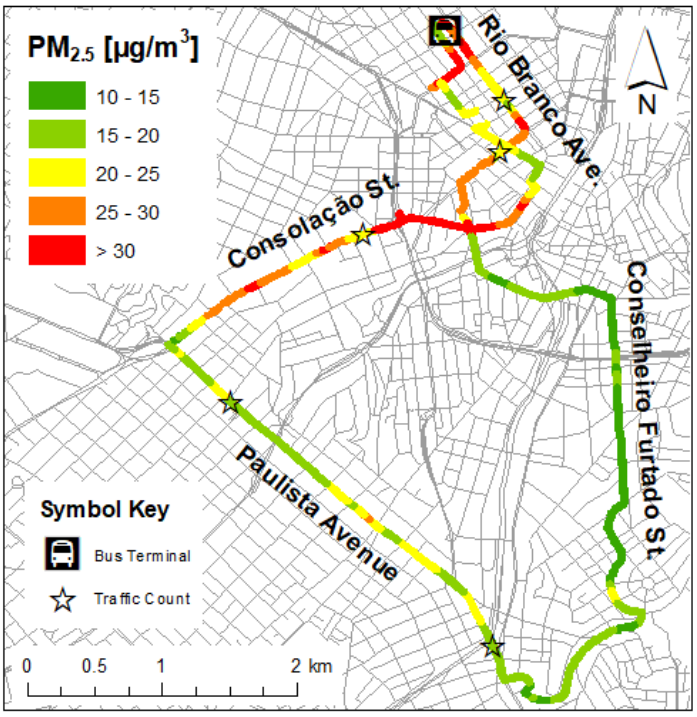

Figure B-25: Map of $PM_{2.5}$ concentrations in São Paulo on June 30, 2016.

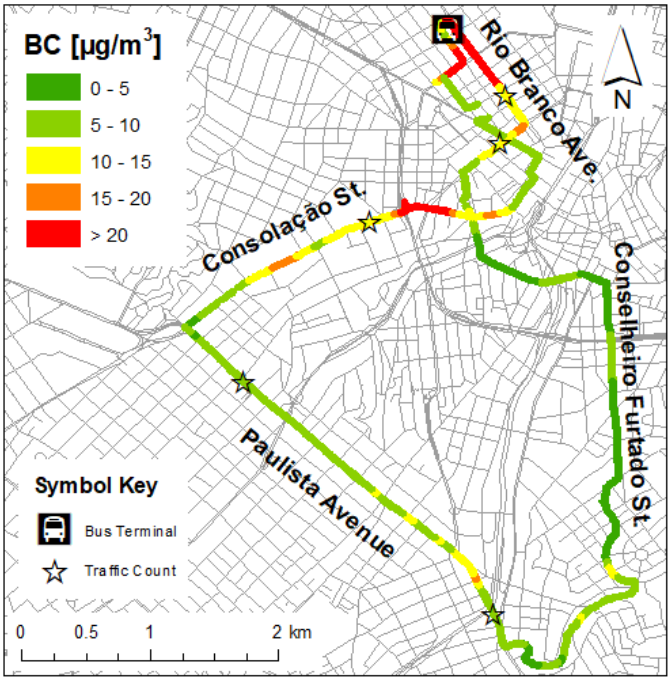

Figure B-26: Map of BC concentrations in São Paulo on June 30, 2016.

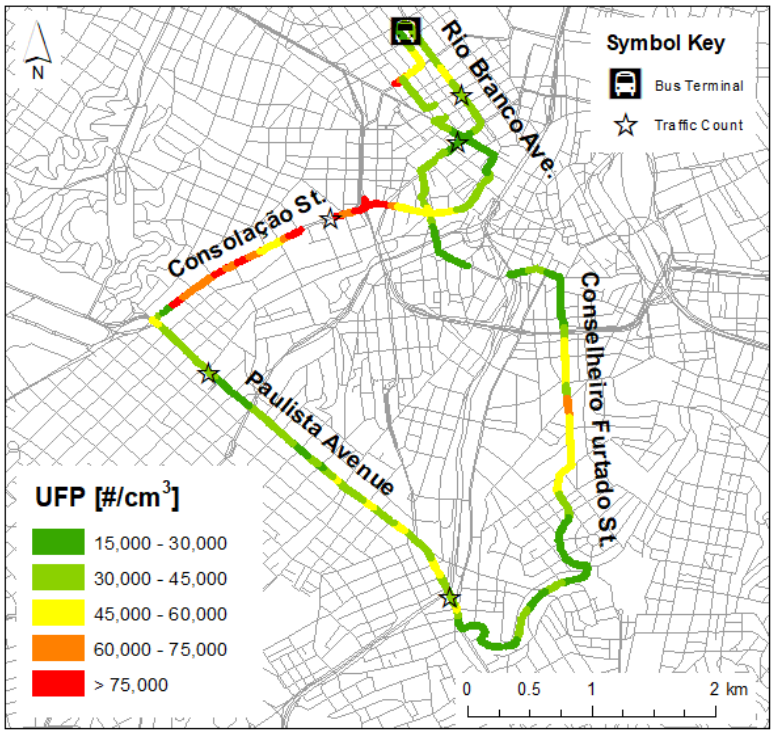

Figure B-27: Map of UFP concentrations in São Paulo on June 30, 2016.

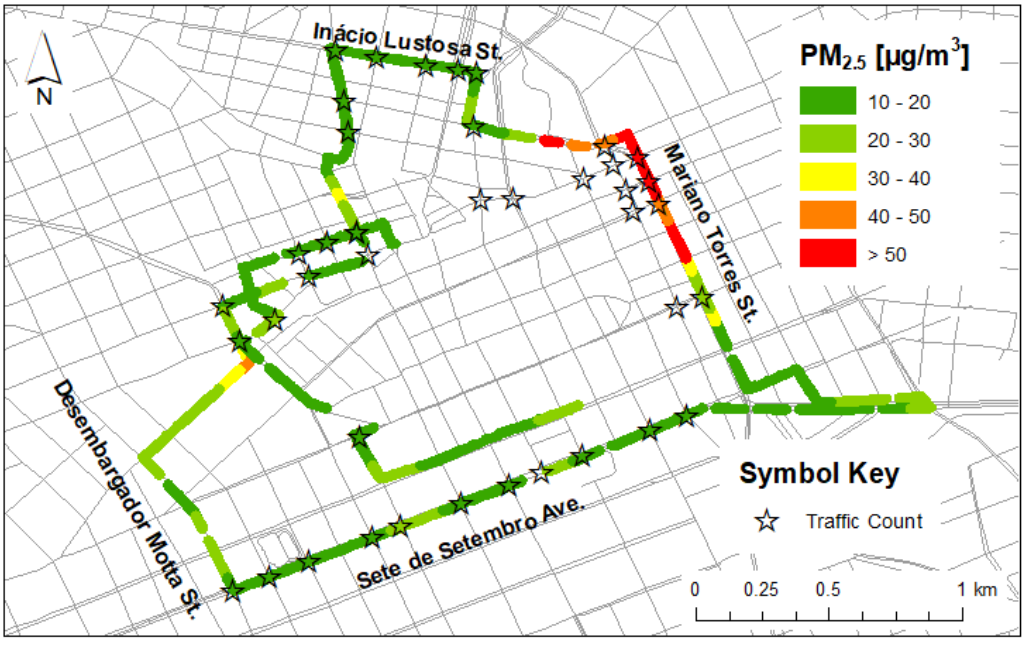

Figure B-28: Map of $PM_{2.5}$ concentrations in Curitiba on July 25, 2016.

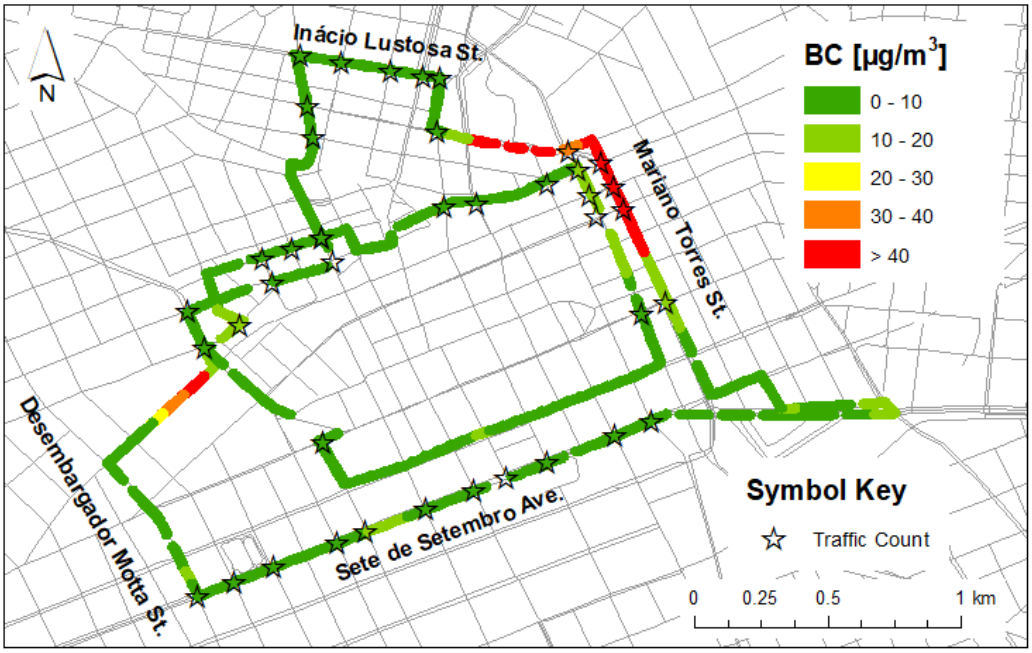

Figure B-29: Map of BC concentrations in Curitiba on July 25, 2016.

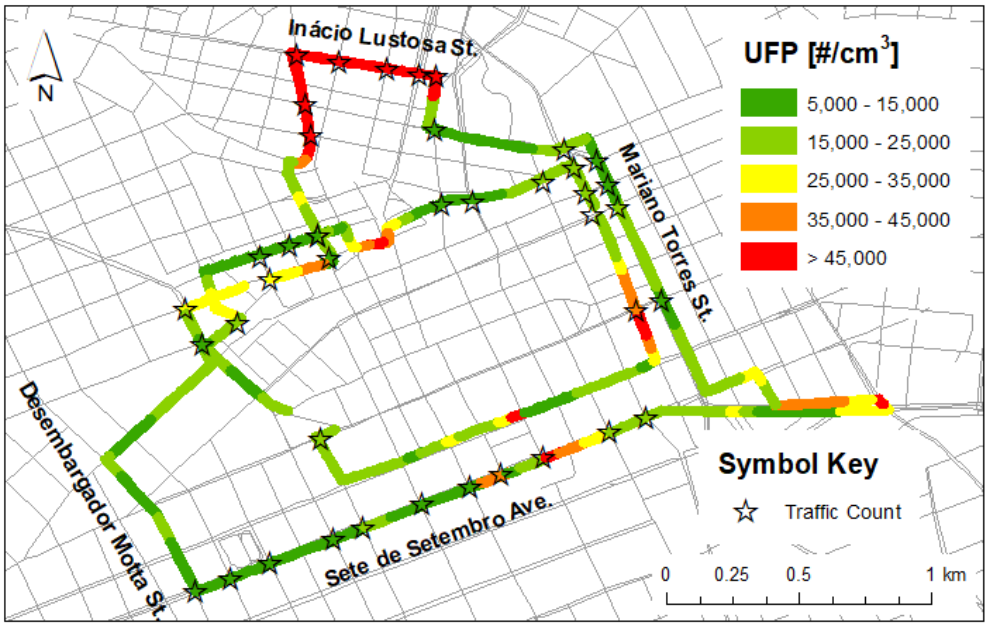

Figure B-30: Map of UFP concentrations in Curitiba on July 25, 2016.

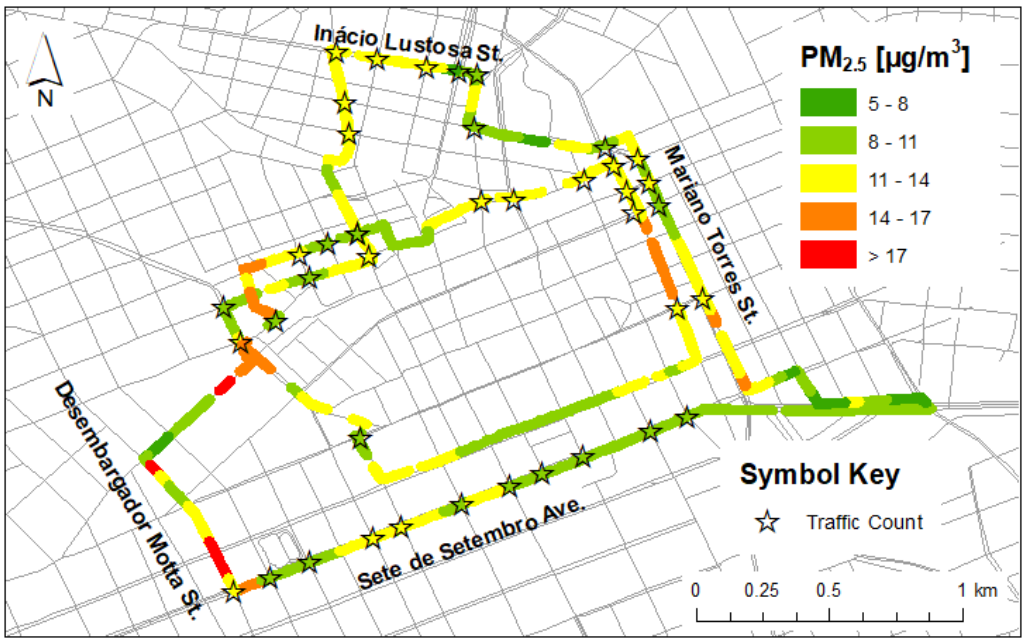

Figure B-31: Map of $PM_{2.5}$ concentrations in Curitiba on July 26, 2016.

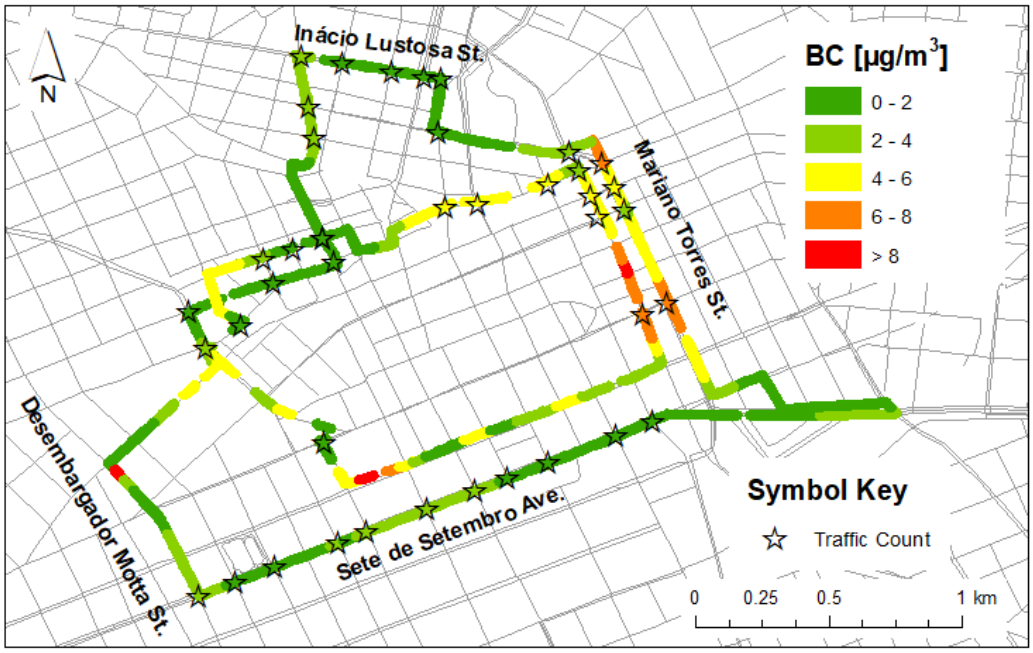

Figure B-32: Map of BC concentrations in Curitiba on July 26, 2016.

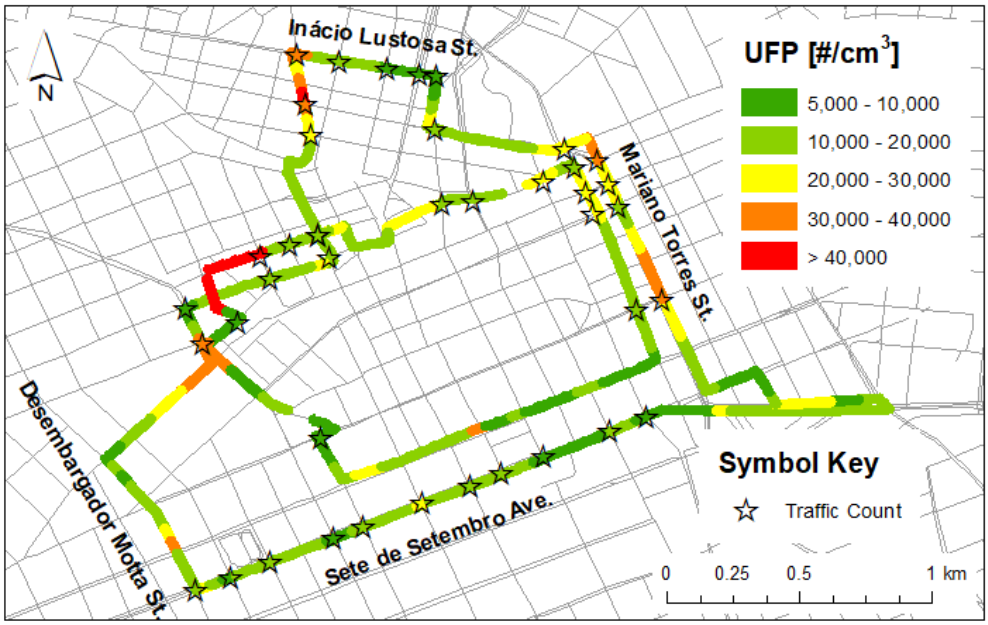

Figure B-33: Map of UFP concentrations in Curitiba on July 26, 2016.

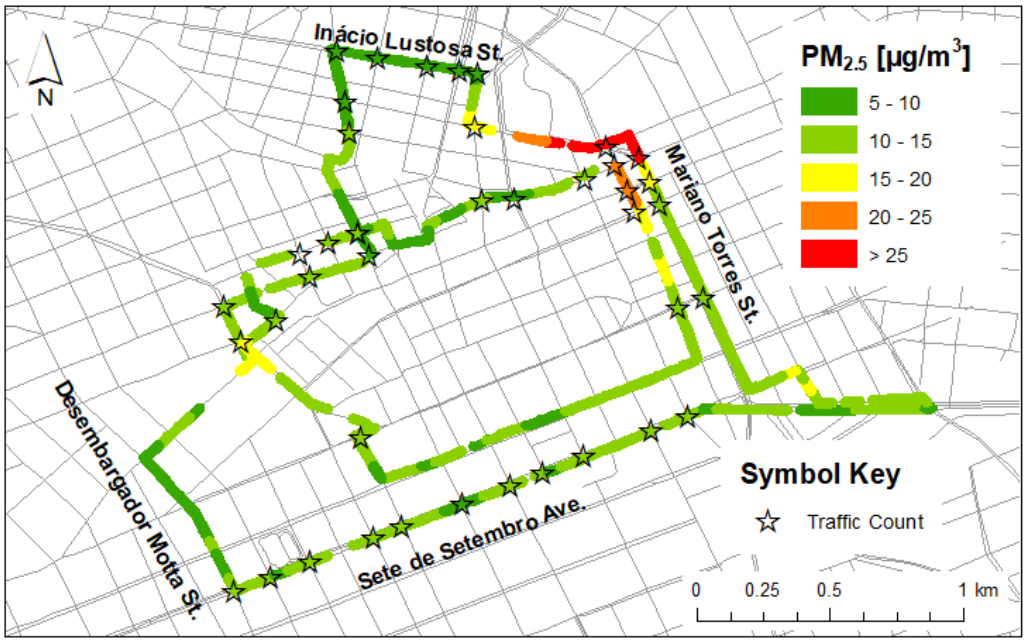

Figure B-34: Map of $PM_{2.5}$ concentrations in Curitiba on July 27, 2016.

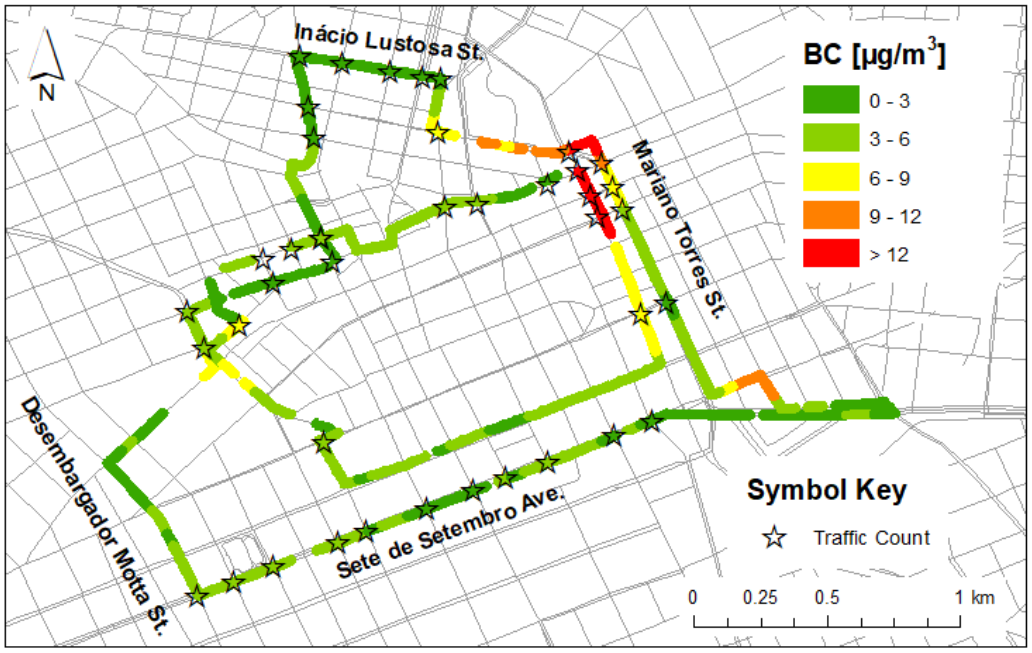

Figure B-35: Map of BC concentrations in Curitiba on July 27, 2016.

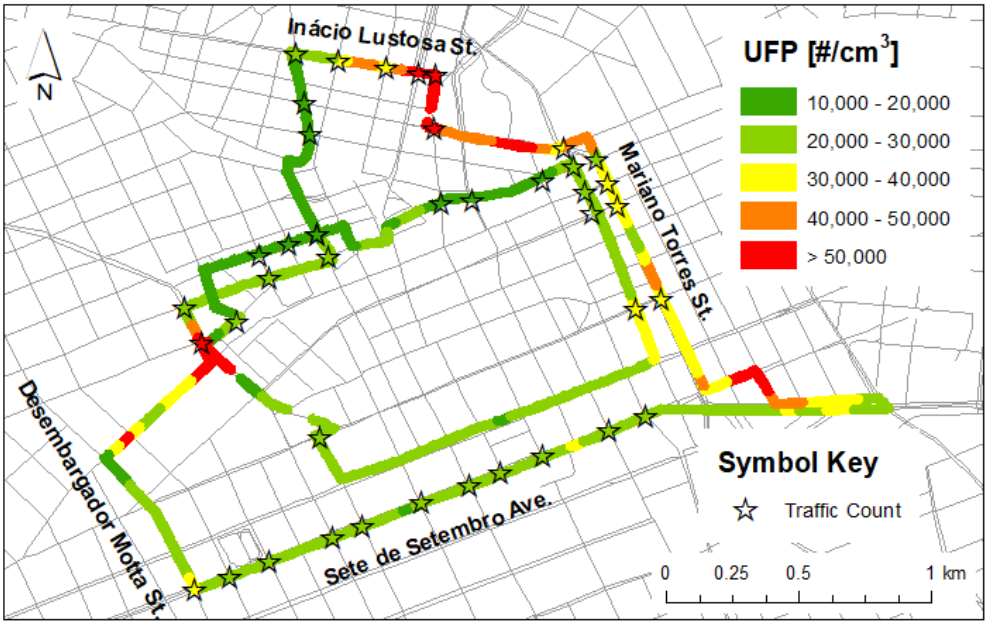

Figure B-36: Map of UFP concentrations in Curitiba on July 27, 2016.

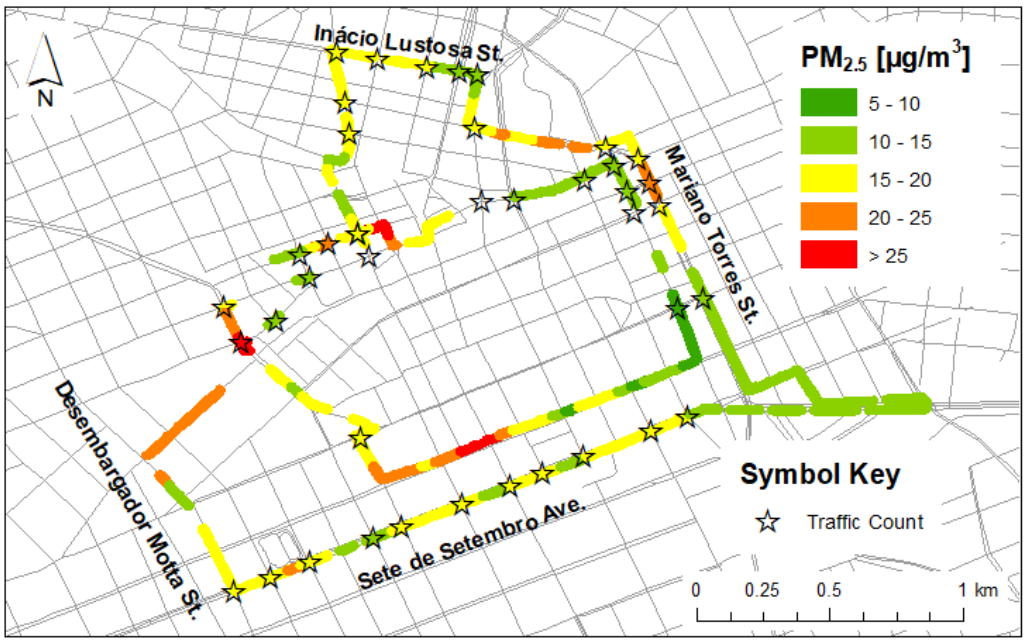

Figure B-37: Map of $PM_{2.5}$ concentrations in Curitiba on July 28, 2016.

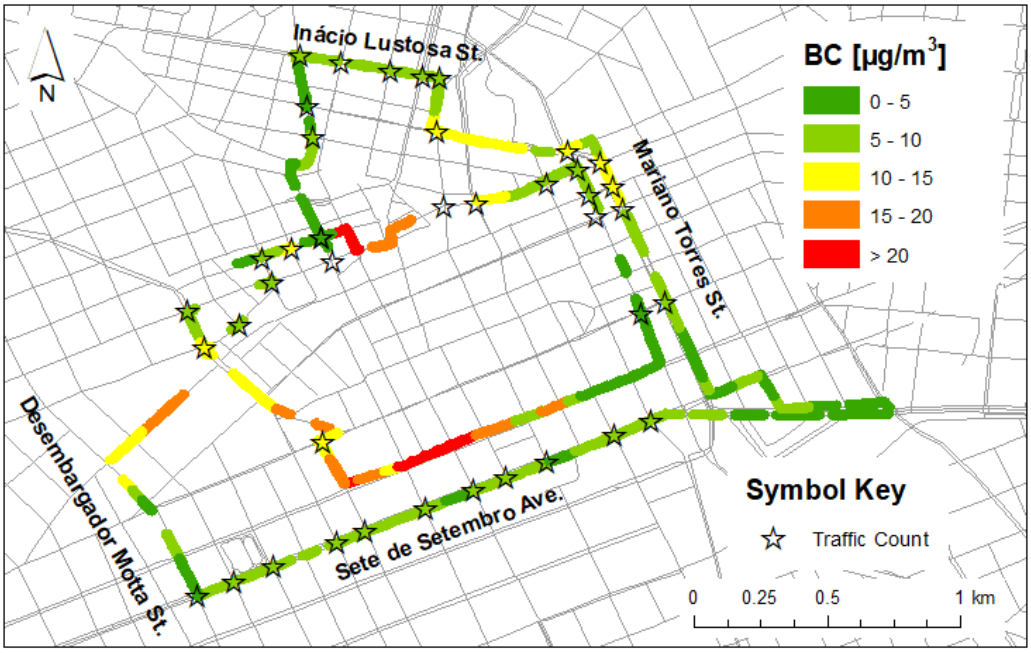

Figure B-38: Map of BC concentrations in Curitiba on July 28, 2016.

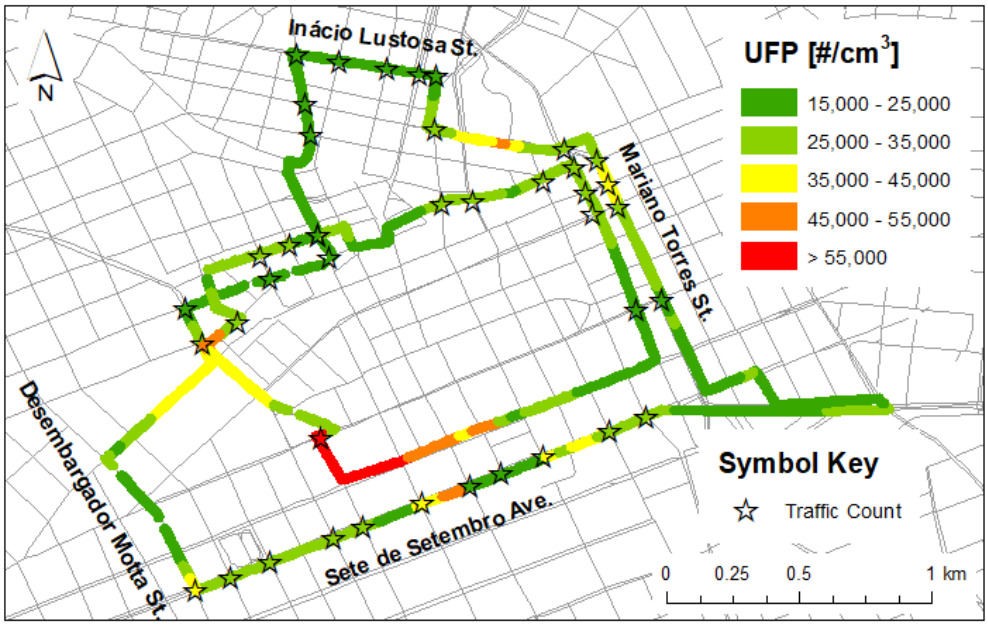

Figure B-39: Map of UFP concentrations in Curitiba on July 28, 2016.

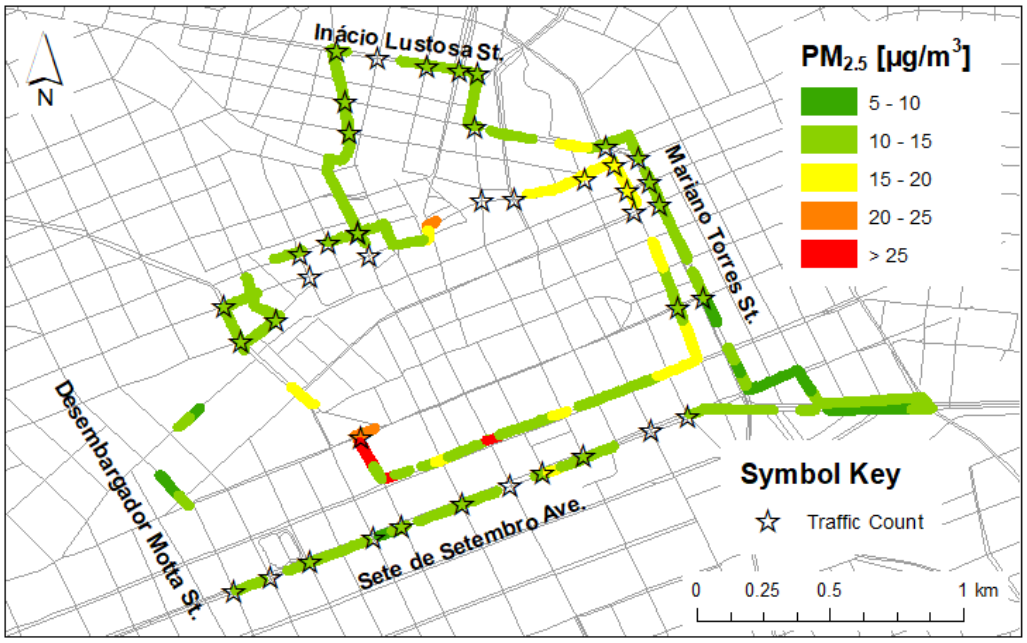

Figure B-40: Map of $PM_{2.5}$ concentrations in Curitiba on July 29, 2016.

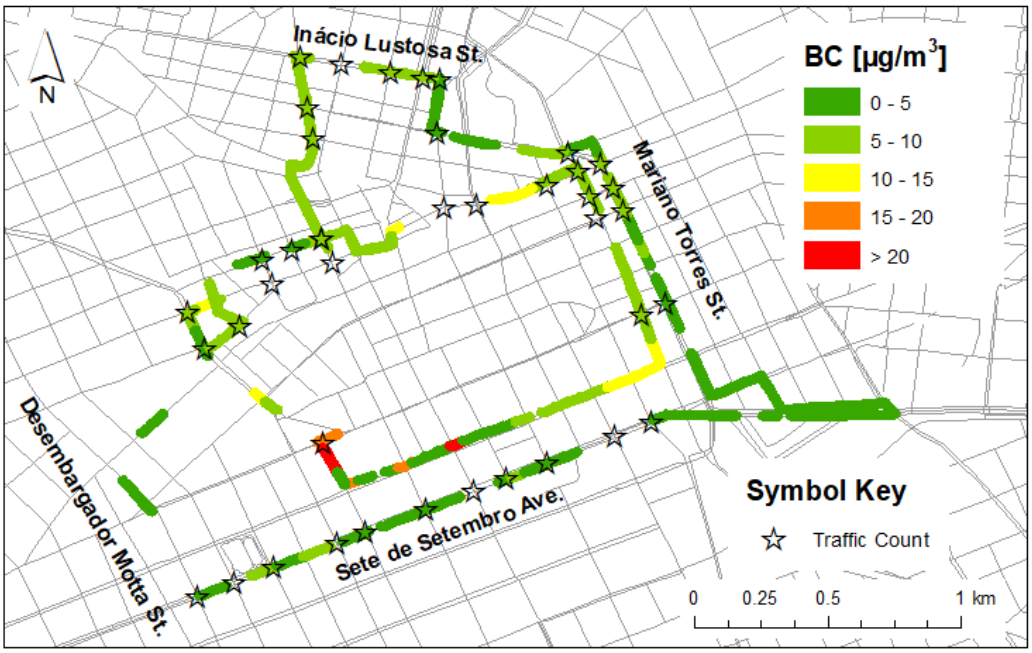

Figure B-41: Map of BC concentrations in Curitiba on July 29, 2016.

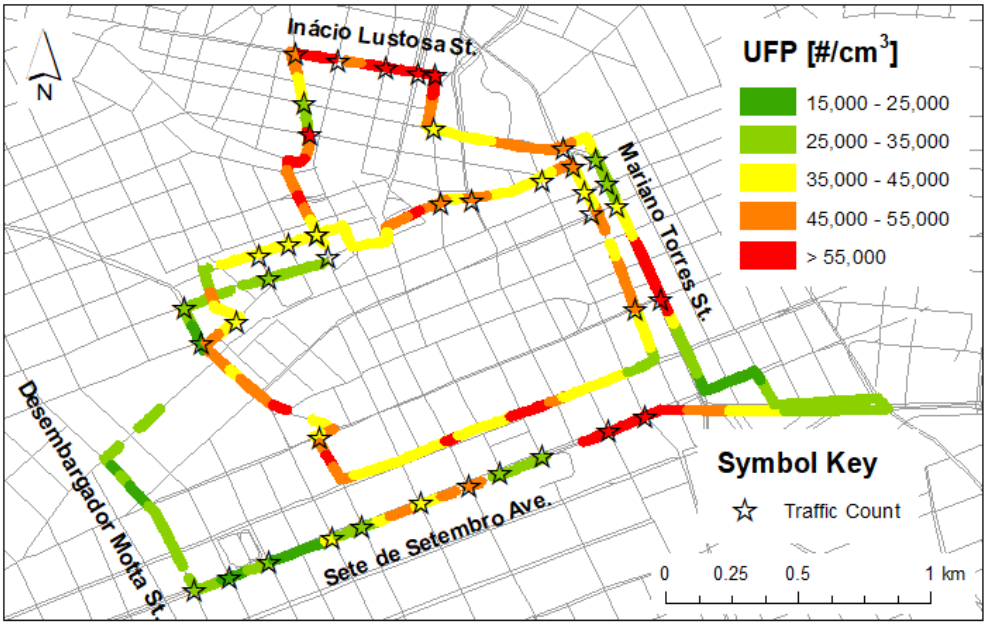

Figure B-42: Map of UFP concentrations in Curitiba on July 29, 2016.

Appendix C Copyright Agreements

Copyright agreements for figures used in this thesis from other publications are included below.

This Agreement between Ms. Ellen Patrick ("You") and Elsevier ("Elsevier") consists of your license details and the terms and conditions provided by Elsevier and Copyright Clearance Center.

License Number	4276000626629
License date	Jan 25, 2018
Licensed Content Publisher	Elsevier
Licensed Content Publication	Atmospheric Environment
Licensed Content Title	Transport impacts on atmosphere and climate: Land transport
Licensed Content Author	Elmar Uherek,Tomas Halenka,Jens Borken-Kleefeld,Yves Balkanski,Terje Berntsen,Carlos Borrego,Michael Gauss,Peter Hoor,Katarzyna Juda-Rezler,Jos Lelieveld,Dimitrios Melas,Kristin Rypdal,Stephan Schmid
Licensed Content Date	Dec 1, 2010
Licensed Content Volume	44
Licensed Content Issue	37
Licensed Content Pages	45
Start Page	4772
End Page	4816
Type of Use	reuse in a thesis/dissertation
Portion	figures/tables/illustrations
Number of figures/tables/illustrations	1
Format	both print and electronic
Are you the author of this Elsevier article?	No
Will you be translating?	No
Original figure numbers	Figure 3
Title of your thesis/dissertation	Quantifying the Spatiotemporal PM2.5, Black Carbon, and Ultrafine Particle Concentrations Aboard Public Buses in Brazil: A Comparison of Three Cities
Expected completion date	Mar 2018
Estimated size (number of pages)	180

This Agreement between Ms. Ellen Patrick ("You") and Elsevier ("Elsevier") consists of your license details and the terms and conditions provided by Elsevier and Copyright Clearance Center.

License Number	4276041060875
License date	Jan 25, 2018
Licensed Content Publisher	Elsevier
Licensed Content Publication	Biochimica et Biophysica Acta (BBA) - General Subjects
Licensed Content Title	Beyond PM2.5: The role of ultrafine particles on adverse health effects of air pollution
Licensed Content Author	Rui Chen,Bin Hu,Ying Liu,Jianxun Xu,Guosheng Yang,Diandou Xu,Chunying Chen
Licensed Content Date	Dec 1, 2016
Licensed Content Volume	1860
Licensed Content Issue	12
Licensed Content Pages	12
Start Page	2844
End Page	2855
Type of Use	reuse in a thesis/dissertation
Intended publisher of new work	other
Portion	figures/tables/illustrations
Number of figures/tables/illustrations	1
Format	both print and electronic
Are you the author of this Elsevier article?	No
Will you be translating?	No
Original figure numbers	Figure 2
Title of your thesis/dissertation	Quantifying the Spatiotemporal PM2.5, Black Carbon, and Ultrafine Particle Concentrations Aboard Public Buses in Brazil: A Comparison of Three Cities
Expected completion date	Mar 2018
Estimated size (number of pages)	180